64-12

REPORT NO. RF-TR-64-6

COPY NO. 20

INVESTIGATION OF FIN GAP EFFECTS ON STATIC STABILITY CHARACTERISTICS OF FIN STABILIZED MISSILES

10 April 1964

U S ARMY MISSILE COMMAND
REDSTONE ARSENAL, ALABAMA

DDC AVAILABILITY NOTICE

Qualified requesters may obtain copies of this report from the Defense Documentaion Center for Scientific and Technical Information, Cameron Station, Alexandria, Virginia, 22314.

DESTRUCTION NOTICE

Destroy; do not return.

10 April 1964

Report No. RF-TR-64-6

INVESTIGATION OF FIN GAP EFFECTS ON STATIC STABILITY CHARACTERISTICS OF FIN STABILIZED MISSILES

by

T. L. Killough

Aerodynamics Branch
Future Missile Systems Division
Directorate of Research and Development
U. S. Army Missile Command
Redstone Arsenal, Alabama

TABLE OF CONTENTS

LIST OF ILLUSTRATIONS

LIST OF ILLUSTRATIONS (Continued)

LIST OF ILLUSTRATIONS (Continued)

LIST OF ILLUSTRATIONS (Continued)

LIST OF ILLUSTRATIONS (Concluded)

LIST OF COEFFICIENTS AND SYMBOLS

I. COEFFICIENTS AND SYMBOLS

A	Aspect ratio, $\frac{(\text{exposed fin span at zero gap})^2}{(\text{exposed fin area})}$
$C_{A,b}$	Base axial-force coefficient, $(P_\infty - pb)/q_\infty$
$C_{A,F}$	Forebody axial-force coefficient, $C_{A,T} - C_{A,b}$
$C_{A,T}$	Total axial-force coefficient, axial force/$q_\infty S$
C_m	Pitching-moment coefficient referenced to a point at the model nose, pitching moment/q_∞ DS
$C_{m\alpha}$	Rate of change of pitching-moment coefficient with angle of attack, dC_m/d_α, at $C_m = 0$
C_N	Normal-force coefficient, normal force/q_∞ S
C_{N_α}	Rate of change of normal-force coefficient with angle of attack, dC_N/d_α, at $C_N = 0$
D	Model reference diameter, 1.000 in.
g	Gap width, calibers
M_∞	Free stream Mach number
p_b	Static pressure at model base, psi
p_t	Tunnel total pressure, psi
p_∞	Free stream static pressure, psi
q_∞	Free stream dynamic pressure, psi
r_o	Body radius, calibers
S	Model reference area, $\pi D^2/4$, 0.7854 in^2
S_o^*	Maximum semi-span of fin from body center-line, when gap is zero, calibers
V_∞	Free stream velocity, ft/sec
X_{np}	Neutral point location measured in calibers from the model nose, dC_m/dC_N at $C_m = 0$, positive forward

α Angle of attack corrected for sting and balance deflections, positive nose-up, degree

II. CONFIGURATIONS

B Body alone

BF_{4A} Body plus low aspect ratio fin, A = 1.0, no gap

BF_{4B} Body plus low aspect ratio fin, 0.08-caliber gap

BF_{4C} Body plus low aspect ratio fin, 0.16-caliber gap

BF_{4D} Body plus low aspect ratio fin, 0.25-caliber gap

BF_{5A} Body plus intermediate aspect ratio fin, A = 2.0, no gap

BF_{5B} Body plus intermediate aspect ratio fin, 0.08-caliber gap

BF_{5C} Body plus intermediate aspect ratio fin, 0.16-caliber gap

BF_{5D} Body plus intermediate aspect ratio fin, 0.25-caliber gap

BF_{6A} Body plus high aspect ratio fin, A = 3.0, no gap

BF_{6B} Body plus high aspect ratio fin, 0.08-caliber gap

BF_{6C} Body plus high aspect ratio fin, 0.16-caliber gap

BF_{6D} Body plus high aspect ratio fin, 0.25-caliber gap

F_{4A} Low aspect ratio fin plus carry-over, no gap

F_{4B} Low aspect ratio fin plus carry-over, 0.08-caliber gap

F_{4C} Low aspect ratio fin plus carry-over, 0.16-caliber gap

F_{4D} Low aspect ratio fin plus carry-over, 0.25-caliber gap

F_{5A} Intermediate aspect ratio fin plus carry-over, no gap

F_{5B} Intermediate aspect ratio fin plus carry-over, 0.08-caliber gap

F_{5C} Intermediate aspect ratio fin plus carry-over, 0.16-caliber gap

F_{5D} Intermediate aspect ratio fin plus carry-over, 0.25-caliber gap

II. CONFIGURATIONS (Continued)

F_{6A} High aspect ratio fin plus carry-over, no gap

F_{6B} High aspect ratio fin plus carry-over, 0.08-caliber gap

F_{6C} High aspect ratio fin plus carry-over, 0.16-caliber gap

F_{6D} High aspect ratio fin plus carry-over, 0.25-caliber gap

INVESTIGATION OF FIN GAP EFFECTS ON STATIC STABILITY CHARACTERISTICS OF FIN STABILIZED MISSILES

I. INTRODUCTION

A simply guided or unguided missile operating throughout its speed envelope with a particular or closely controlled static stability margin offers improved accuracy over a missile with a varying stability margin. Since the static stability margin is a function of the location of the center-of-gravity with respect to the center-of-pressure, a constant or linear shift of the center-of-pressure is desirable. A finned body of revolution of high fineness ratio usually exhibits a center-of-pressure shift which varies considerably with Mach number. As M_∞ increases, X_{np} moves progressively aft until $M_\infty \approx 1$. As speed increases further, X_{np} reverses its travel and moves forward. This effect makes programming a center-of-gravity shift with X_{np} for a constant static stability margin difficult to accomplish by simple means, such as fuel burning. The forces acting on the missile to affect X_{np} are C_N and X_{np} of the body alone, C_N and X_{np} of the fin alone, the body crossflow effect on the fin, and the fin carry-over effect on the body. The fin carry-over effect change with Mach number is quite pronounced. Theoretically this fin carry-over effect could be minimized or eliminated by varying the distance between the body and the fins.

To confirm this theory, wind tunnel static stability tests were conducted on typical missile configurations with variable fin gaps. Rectangular fin planforms with aspect ratios of 1, 2, and 3, and similar but not exact areas, arranged in cruciform were used to determine the effect on the neutral point by varying the fin gap. Tests were conducted in two facilities to cover a Mach number range from 0.80 to 4.50. The transonic portion of the test was conducted in the 1-Foot Transonic Model Tunnel of the Propulsion Wind Tunnel Facility, Arnold Engineering Development Center, Arnold Air Force Station, Tennessee, through Mach number 1.50 during the period of 4-11 June 1962. The supersonic portion of the test was conducted in the Supersonic Tunnel No. 1, Ballistic Research Laboratories, Aberdeen, Maryland, through a Mach number range of 1.75 to 4.50 during the period of 17-27 September 1962.

II. APPARATUS

The 1-Foot Transonic Model Tunnel is a continuous-flow nonreturn system operating over a Mach range from 0.80 to 1.50. The test section

is 12 inches square in cross section and 35.7 inches long with all four walls preforated. See Reference 1 for a complete test facility description. A photograph of the test article in the test section is shown in Figure 1.

The BRL Supersonic Tunnel No. 1 is a continuously operated, variable density, closed circuit tunnel having a test section 15 inches high by 13 inches wide. A two-dimensional flexible nozzle is variable for test section Mach number of 1.50 to 5.00. A complete test facility description is contained in Reference 2. A photograph of the test article installed in the test section is shown in Figure 2.

III. TEST ARTICLE

The model is an ogive-cylinder body with provisions for mounting the various fin configurations of interest and was utilized for tests at both tunnel facilities. The model body is 12 calibers in length, including a 4-caliber tangent ogive nose, and is physically one inch in diameter. A photograph of the model with a representative fin for each configuration is shown in Figure 3. Model details and dimensions, and fin details and dimensions are shown in Figures 4 and 5 respectively. The three fin designs have rectangular planforms of different aspect ratio, (A = 1, 2, and 3) two having wedge-plate sections and one a wedge section. The fin gap distances varied from zero to 0.25 caliber. The fins were spaced 90 degrees apart, two positioned horizontally and two vertically.

IV. INSTRUMENTATION

For tests in the 1-Foot Transonic Model Tunnel, the model was mounted on a three-component internal strain-gage balance with loading limits of $\pm$20 lb. normal force, $\pm$60 in. lb. pitching moment, and $\pm$7 lb. axial force. The normal force, pitching moment and axial force outputs were received into an analog-to-digital converter equipped with visual and tape outputs. Base pressure was obtained from two static pressure orifices located at the base of the model. Data were reduced to aerodynamic coefficients and corrected angle of attack by the facility's Computing Laboratory.

Model instrumentation for testing in the BRL Supersonic Tunnel No. 1 was similar and the three-component balance outputs and the base pressure outputs were also recorded on tape. These data were reduced to aerodynamic coefficients and corrected angle of attack by the facility's Computing Laboratory.

V. TEST PROCEDURE

Data were taken through an angle-of-attack range of -4 to +10 degrees and a Mach number range of 0.80 to 1.50 for each model configuration with the model installed in the 1-Foot Transonic Model Tunnel. A Reynolds number of approximately 0.40×10^6 per inch was maintained through the test. Testing was terminated prior to running configurations BF_{6C} and BF_{6D}.

Data taken in the BRL Supersonic Tunnel No. 1 were over a Mach number range of 1.75 to 4.50 at a constant Reynolds number of 0.49 X 10^6 per inch and through an angle-of-attack range of $\pm$8 degrees for each model configuration.

VI. ACCURACY OF RESULTS

The uncertainties in the data as determined by statistical methods using a normal error distribution curve and a 95 percent confidence level for the 1-Foot Transonic Model Tunnel are as follows:

Symbol	M_∞ = 0.80	M_∞ = 1.0	M_∞ = 1.50
C_m	$\pm$0.23	$\pm$0.23	$\pm$0.17
C_N	$\pm$0.026	$\pm$0.022	$\pm$0.018
X_{np}	$\pm$0.10 Cal.	$\pm$0.10 Cal.	$\pm$0.08 Cal.
α	$\pm$0.10 Deg.	$\pm$0.10 Deg.	$\pm$0.10 Deg.

The uncertainties in the data as determined in a like manner for the BRL Supersonic Tunnel No. 1 are as follows:

$$C_{A,F} = \pm 0.003$$

$$C_m = \pm 0.095$$

$$C_N = \pm 0.010$$

$$X_{np} = \pm 0.050 \text{ Cal.}$$

$$\alpha = \pm 0.100 \text{ Deg.}$$

While the $C_{A,F}$ value presented is the computed accuracy, the axial force data presented should be used only for approximations rather than absolute values. The model-balance-tunnel combination was such that tunnel mechanical vibrations induced a large amount of scatter in the data, indicating that a balance with less axial sensitivity to dynamic response was required. The same balance was utilized for the tests conducted in the 1-Foot Transonic Model Tunnel, and similar effects were experienced. The scatter in the axial force data was of such magnitude as to make the data unsuitable for presenting herein.

VII. CORRECTIONS

The data which were taken in the 1-Foot Transonic Model Tunnel and presented herein have angle of attack corrections for sting and balance deflections. No correction has been made for test section flow inclinations or tunnel wall effect. Deviations from the tunnel mean values in the test region are included in the accuracy of results presented in the previous section.

The data obtained in the BRL Supersonic Tunnel No. 1 also have angle of attack corrected for balance and sting deflections. In addition, corrections have been made for tare effects and flow angularity. No corrections were applied for tunnel blockage effects.

VIII. RESULTS AND DISCUSSION

Reduced data for all configurations are presented in Figures 6 through 44. The variations of C_N with α, C_m with C_N, and α with $C_{A,F}$ are presented in Figures 6 through 18, Figures 19 through 31, and Figures 32 through 44 respectively.

Slopes were measured from the basic plots and the variations of C_N and X_{np} with Mach number are presented in Figures 45 and 46. As expected, the neutral point of the complete missile rapidly shifts aft until $M \approx 1$, then reverses and gradually moves forward as M_∞ increases for the closed gap configurations. Of the three aspect ratios tested with closed gap, the lowest aspect ratio (A = 1) configuration exhibited the smallest X_{np} shift, which was approximately 2.80 calibers, over the Mach range. With gap introduced, the major reduction in C_{N_α} occurs in the transonic region and the neutral point total shift over the Mach range decreases. For all aspect ratios, the greatest rate of change in neutral point occurs between the zero and 0.08-caliber gap setting. The X_{np} rate of change diminishes as the gap is increased to the 0.16-caliber setting, with only a slight change noticeable between the 0.16 and 0.25-caliber gap setting. The low aspect ratio configuration which shows the smallest X_{np} shift with no gap also has the greatest percentage X_{np} shift reduction with gap introduced. For configuration BF_{4D} (A = 1, gap = 0.25-caliber) the total X_{np} shift is 2.20 calibers which results in a 20 percent improvement over no gap.

The variations of body alone C_{N_α}, X_{np}, and C_{m_α} with Mach number are shown in Figures 45, 46, and 47 respectively. A pronounced X_{np} shift for the body is apparent, rising to a peak at $M_\infty \approx 1$ and decreasing rapidly to a low at $M_\infty \approx 2.0$, where it again rises gradually to $M_\infty \approx 4.5$, the upper limit of the investigation. This effect in the transonic Mach range aggravates the missile X_{np} shift caused by fin carry-over. Investigation into other body alone configurations, to determine if more suitable X_{np} characteristics are possible, would be desirable for X_{np} shift improvement of a complete missile configuration.

Fin plus carry-over results are given in Figures 48 through 51. The variations of C_{N_α} and C_{m_α} for fin plus carry-over with Mach number for all fin gap settings are presented in Figures 48 and 49, and variations of C_{N_α} and C_{m_α} for fin plus carry-over with fin gap for representative Mach numbers and presented in Figures 50 and 51. Carry-over effects are apparent in the closed gap condition for all aspect ratios. With gap introduced, a considerable decrease in fin plus carry-over C_{N_α} and C_{m_α} is apparent for all aspect ratios, particularly in the transonic speed region. The greatest rate of decrease is in the 0.08-caliber gap setting with some additional decrease at the 0.16-caliber gap. Only a small reduction is noticeable between the 0.16 and the 0.25-caliber gap settings. The low

aspect ratio fin has the smallest C_{N_α} and C_{m_α} variation over the Mach number range with no gap, and also shows the largest percentage change with gap introduced. C_{N_α} for the A = 1 fin without gap (F_{4A}) varies from a maximum of 0.076 to a minimum of 0.024, whereas the 0.16-caliber gap position (F_{4C}) reduces the C_{N_α} variation from 0.043 to 0.022 which results in a 40 percent reduction of the C_{N_α} variation through the Mach number range tested. Tests with an instrumented fin with variable gap will be necessary for accurate determination of the X_{np} variation with gap of the fin plus carry-over. Additional gains in X_{np} shift reduction may be realized by testing fin configurations with aspect ratios lower than those selected for these tests.

Figure 52 presents the lift ratios of fin plus carry-over lift to lift for zero gap for each of the aspect ratios investigated at several Mach numbers. A comparison of the experimental results with the slender-body theory predictions of Reference 3 is shown in Figure 52(a). The theoretical lift ratio is predicted for a $r_o/S_{o*} = 0.50$ value, whereas the experimental configuration has a $r_o/S_{o*} = 0.538$ value; therefore, the comparison is approximate. The point of interest is that a pronounced Mach number effect on lift ratio is shown which is not predicted by slender-body theory.

An unresolved effect of fin gap on experimental lift ratio values is apparent in Figure 52(c) (A = 3 configuration) where increasing fin gaps show lift greater than the closed gap lift for Mach number 3.5 and higher. This is contrary both to theory and the results obtained on the two lower aspect ratios investigated. It was noted, however, that gap settings in excess of 0.08 calibers did produce lift ratios that increased with aspect ratio. It was noted also that the fin support posts have a progressively larger percentage of the fin area with increasing aspect ratio. For the 0.25-caliber fin extension, the post to fin area ratio is 5.1 percent for A = 1, 6.5 percent for A = 2, and 8.5 percent for A = 3. It is possible that these posts act as lifting surfaces. If so, their C_N contribution would increase the $C_{N_\alpha} / C_{N_{\alpha g = 0}}$ value as a function of post to fin area ratio. This contribution apparently becomes greater than the lift reductions due to the fin gap effect on the A = 3 configuration at Mach numbers greater than 3.5.

IX. CONCLUSIONS

From the results of the experimental investigation of the effects of fin gap on a typical finned, ogive-cylinder model, the following conclusions can be made:

1. Introduction of gap between the fin and body does reduce the total neutral point migration through the Mach number range tested for each configuration. The low aspect ratio fin (A = 1) gives the best results, reducing the model neutral point total shift by 20 percent at the 0.25-caliber gap setting.

2. Favorable results in reduction of the neutral point migration in this study indicate that additional investigation of fin planform and thickness, and body alone configuration would be warranted.

REFERENCES

1. Test Facilities Handbook, (4th Edition), AEDC, July, 1962.

2. Wind Tunnel Testing Facilities At The Ballistic Research Laboratories, McMillen, J. C., Memorandum Report No. 1292, July, 1960.

3. Theoretical Investigation of the Effects Upon Lift of a Gap Between Wing and Body of a Slender Wing-Body Combination, Dugan, D. W. and Hikido, K., NACA TN3224, August, 1954.

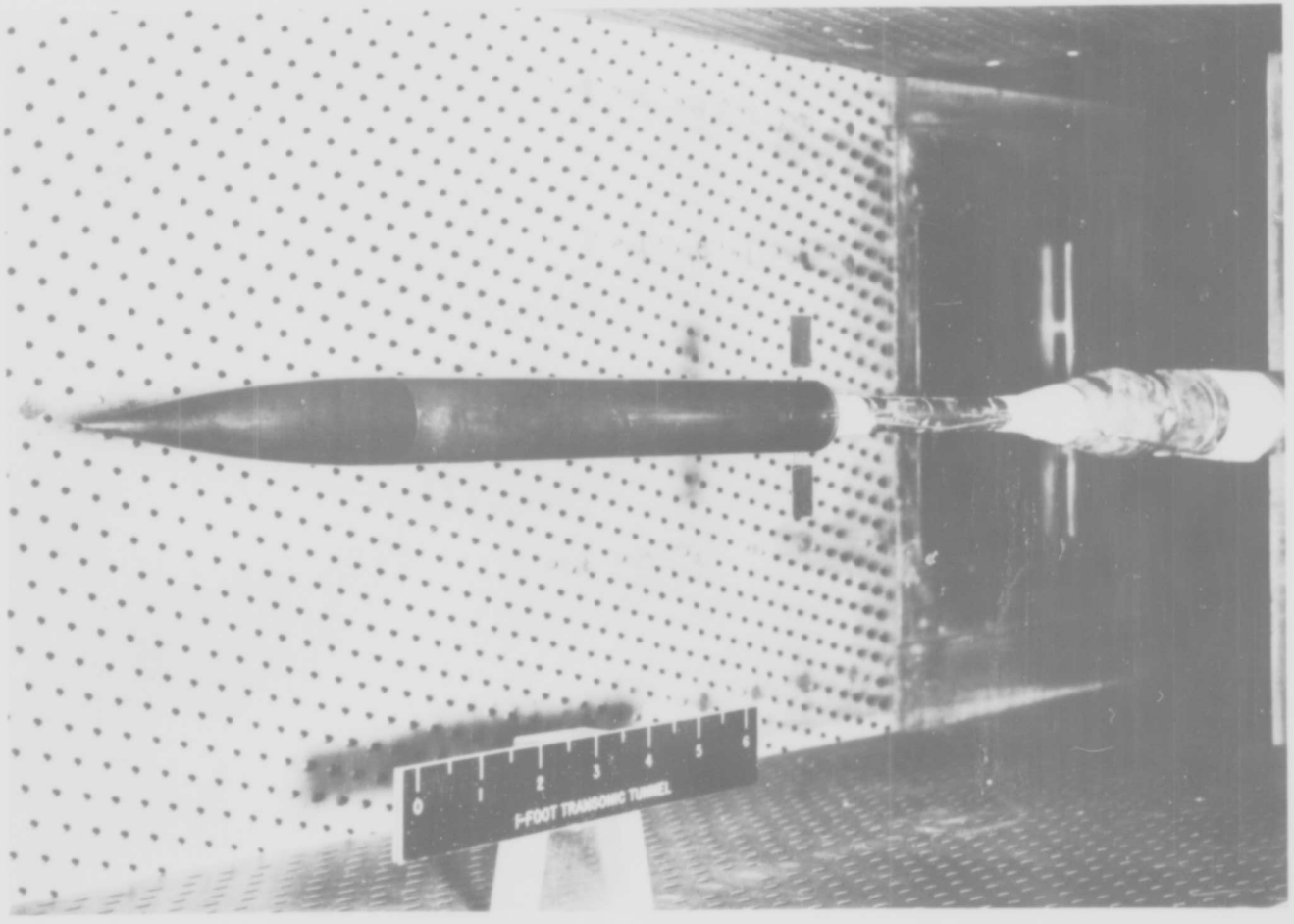

FIGURE 1 PHOTOGRAPH OF MODEL INSTALLED IN TEST SECTION OF 1-FT. TRANSONIC MODEL TUNNEL

FIGURE 2 PHOTOGRAPH OF MODEL INSTALLED IN TEST SECTION OF BALLISTIC RESEARCH LABORATORIES SUPERSONIC TUNNEL NO. 1

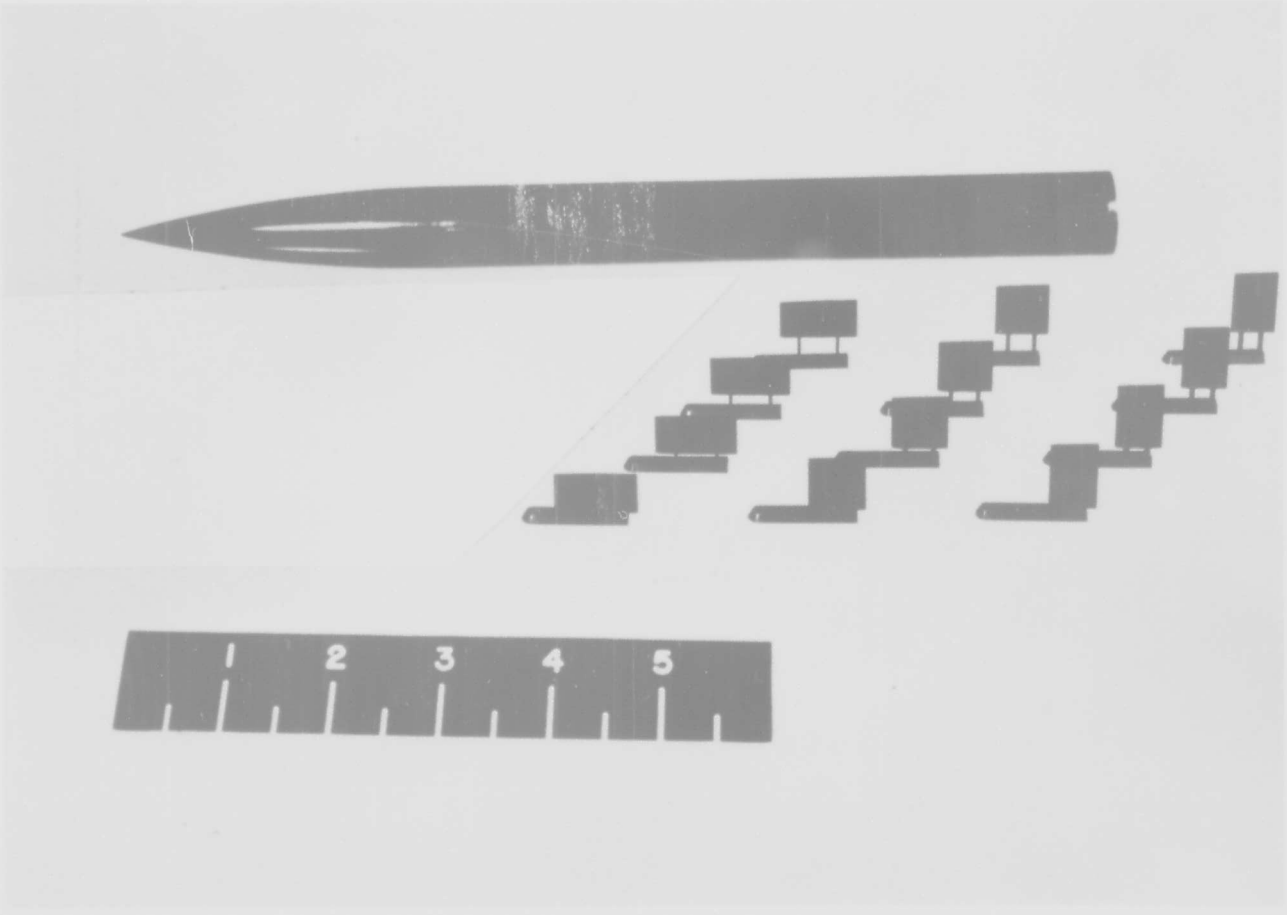

FIGURE 3 PHOTOGRAPH OF TEST MODEL

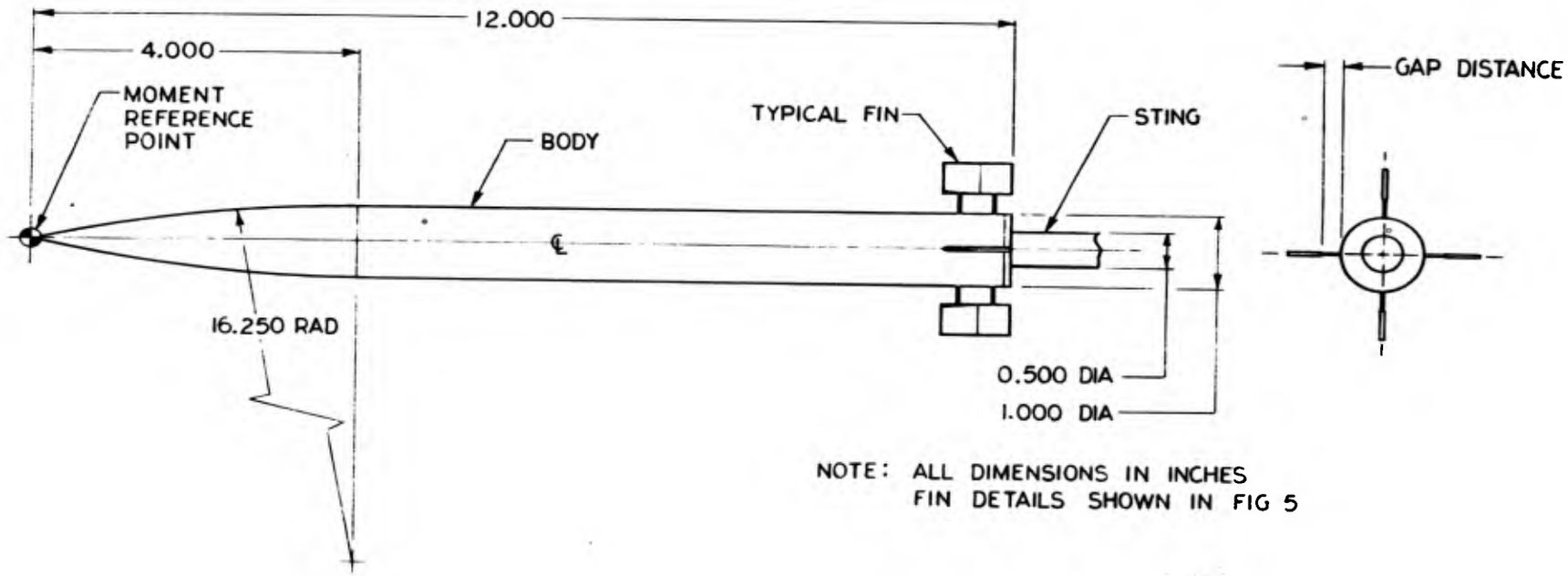

FIGURE 4 MODEL DETAILS AND DIMENSIONS

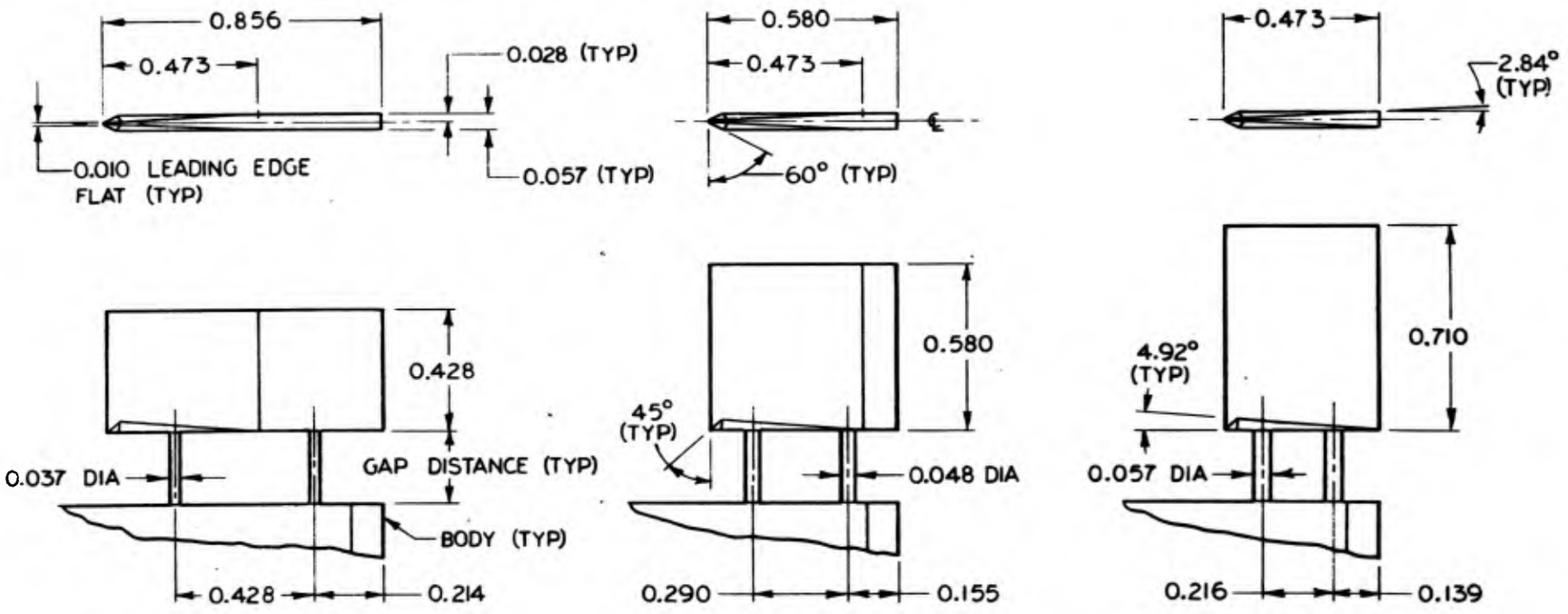

CONFIG	GAP DISTANCE
BF_{4A}	0.000
BF_{4B}	0.080
BF_{4C}	0.160
BF_{4D}	0.250

CONFIG	GAP DISTANCE
BF_{5A}	0.000
BF_{5B}	0.080
BF_{5C}	0.160
BF_{5D}	0.250

CONFIG	GAP DISTANCE
BF_{6A}	0.000
BF_{6B}	0.080
BF_{6C}	0.160
BF_{6D}	0.250

NOTE: ALL DIMENSIONS IN INCHES

FIGURE 5 FIN DETAILS AND DIMENSIONS

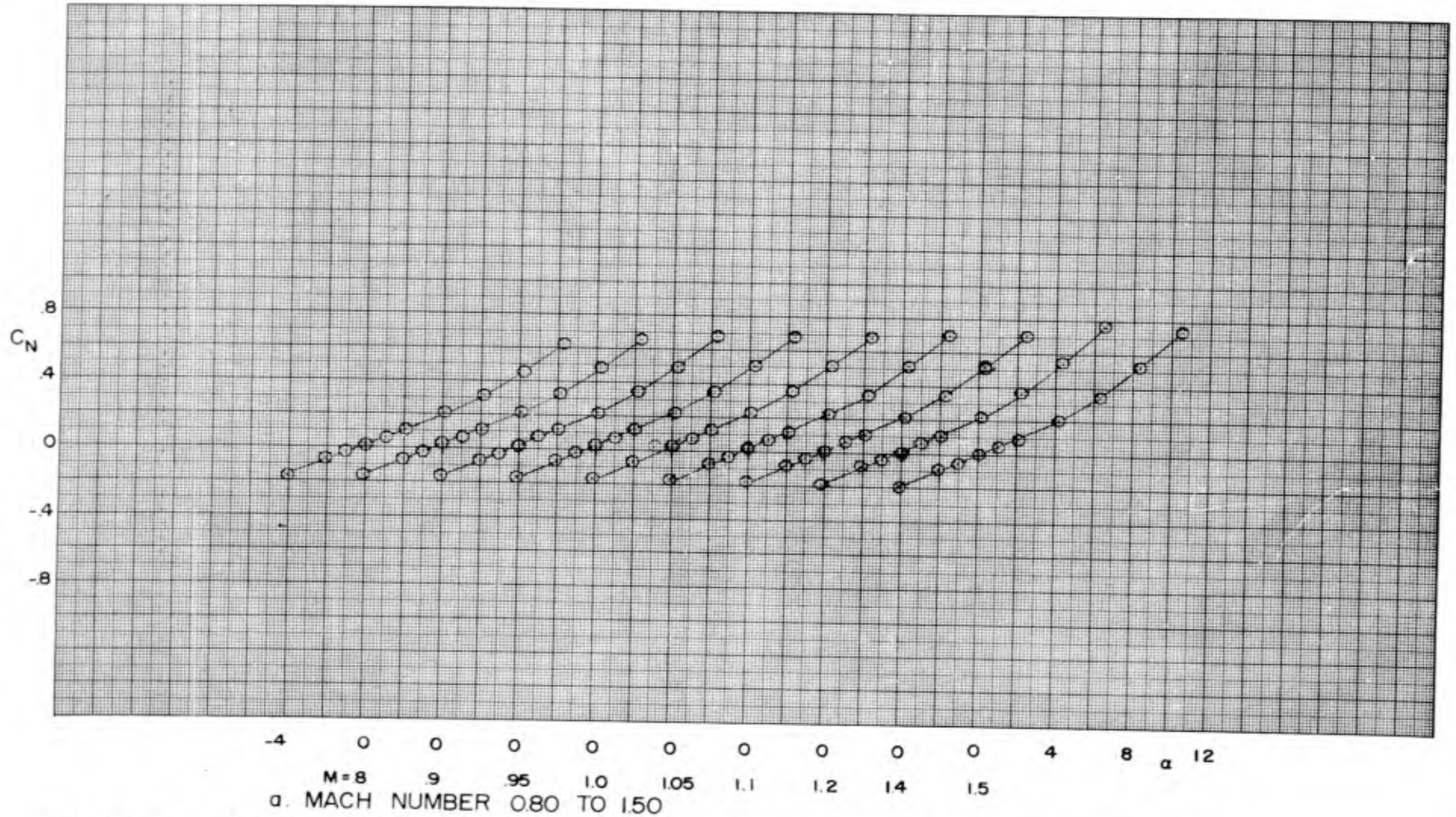

FIGURE 6 NORMAL-FORCE COEFFICIENT VERSUS ANGLE OF ATTACK FOR CONFIGURATION B

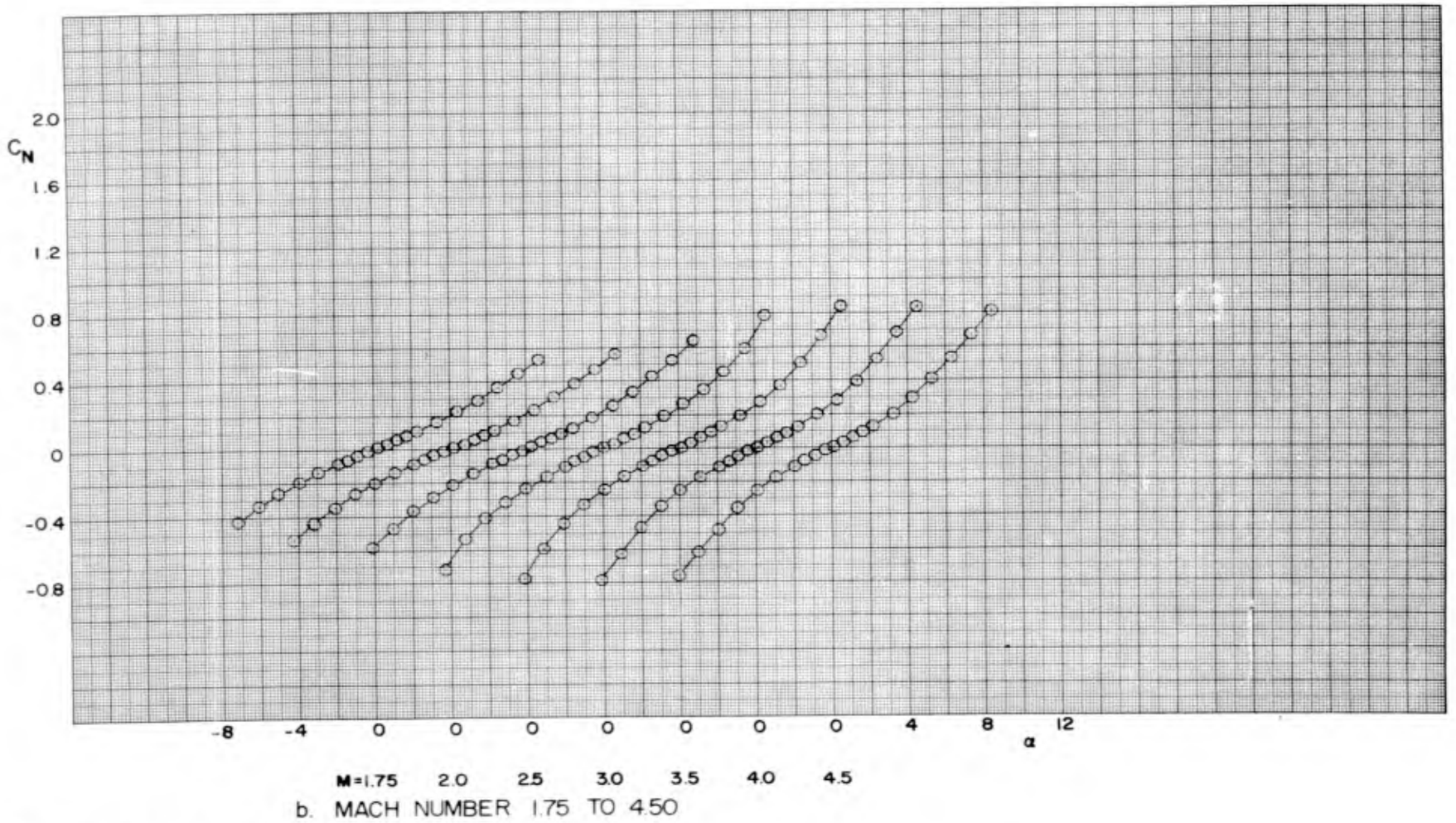

b. MACH NUMBER 1.75 TO 4.50

FIGURE 6 CONCLUDED

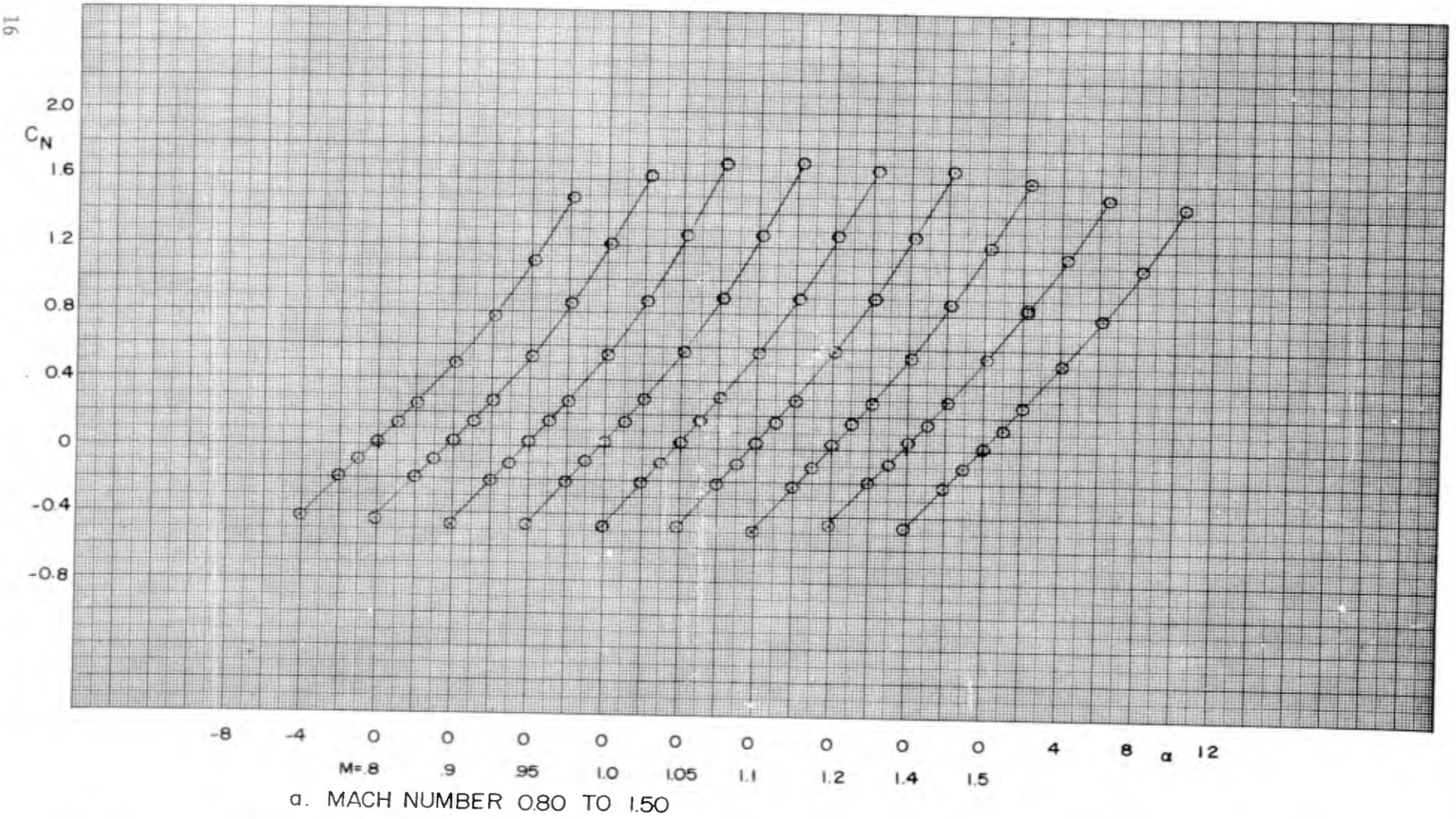

a. MACH NUMBER 0.80 TO 1.50

FIGURE 7 NORMAL-FORCE COEFFICIENT VERSUS ANGLE OF ATTACK FOR CONFIGURATION BF_{4A}

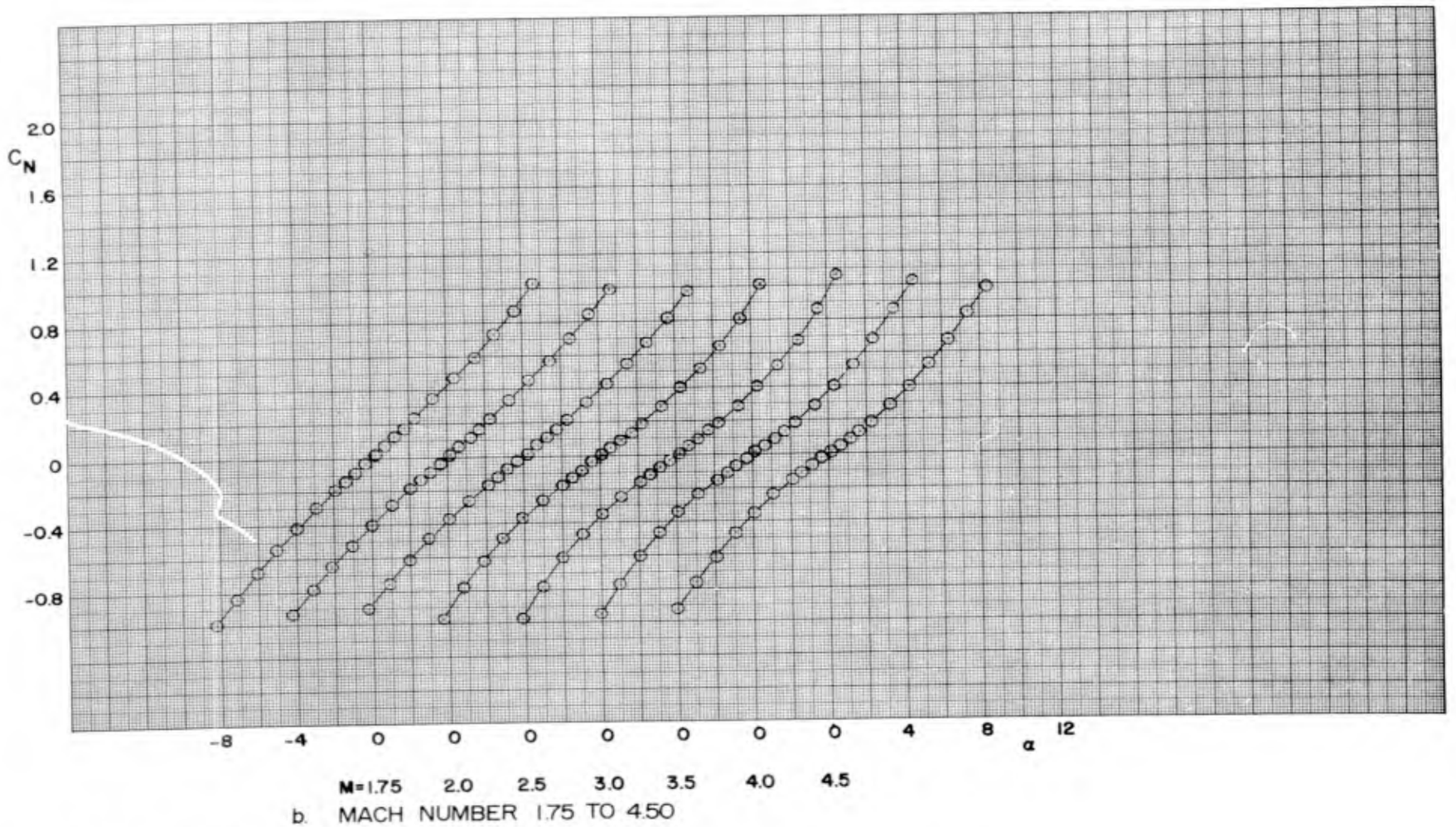

b. MACH NUMBER 1.75 TO 4.50

FIGURE 7 CONCLUDED

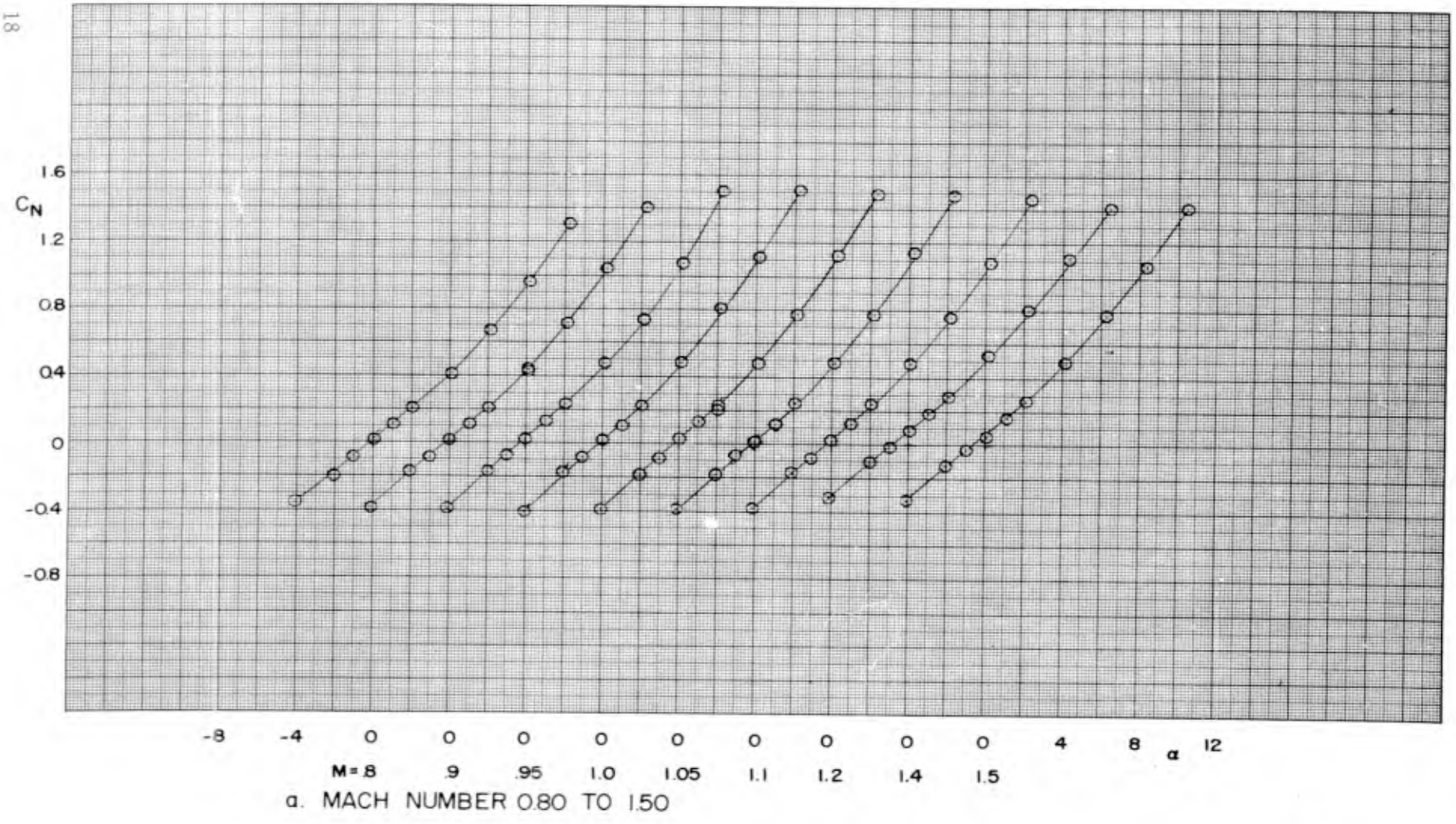

a. MACH NUMBER 0.80 TO 1.50

FIGURE 8 NORMAL-FORCE COEFFICIENT VERSUS ANGLE OF ATTACK FOR CONFIGURATION BF_{4B}

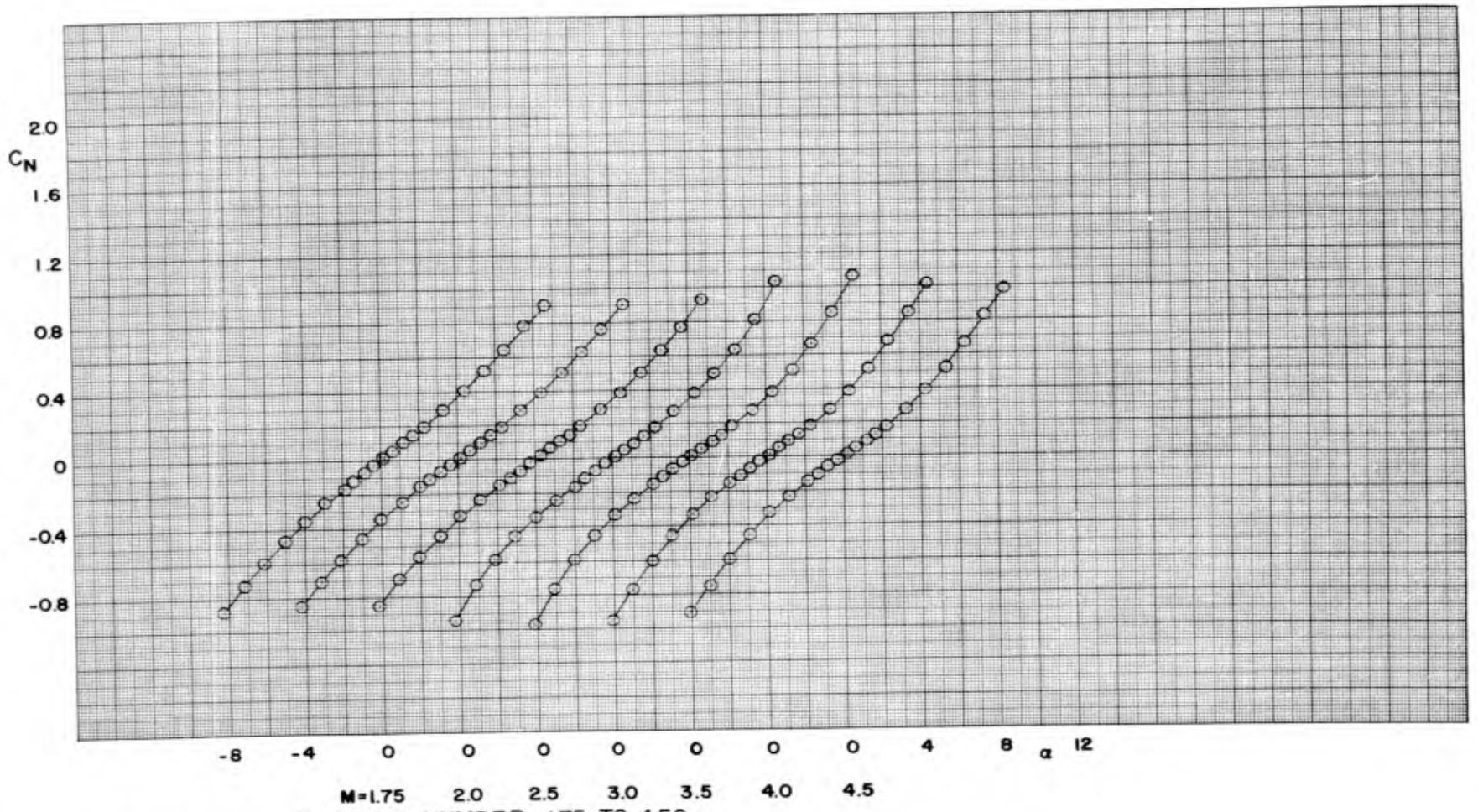

b. MACH NUMBER 1.75 TO 4.50

FIGURE 8 CONCLUDED

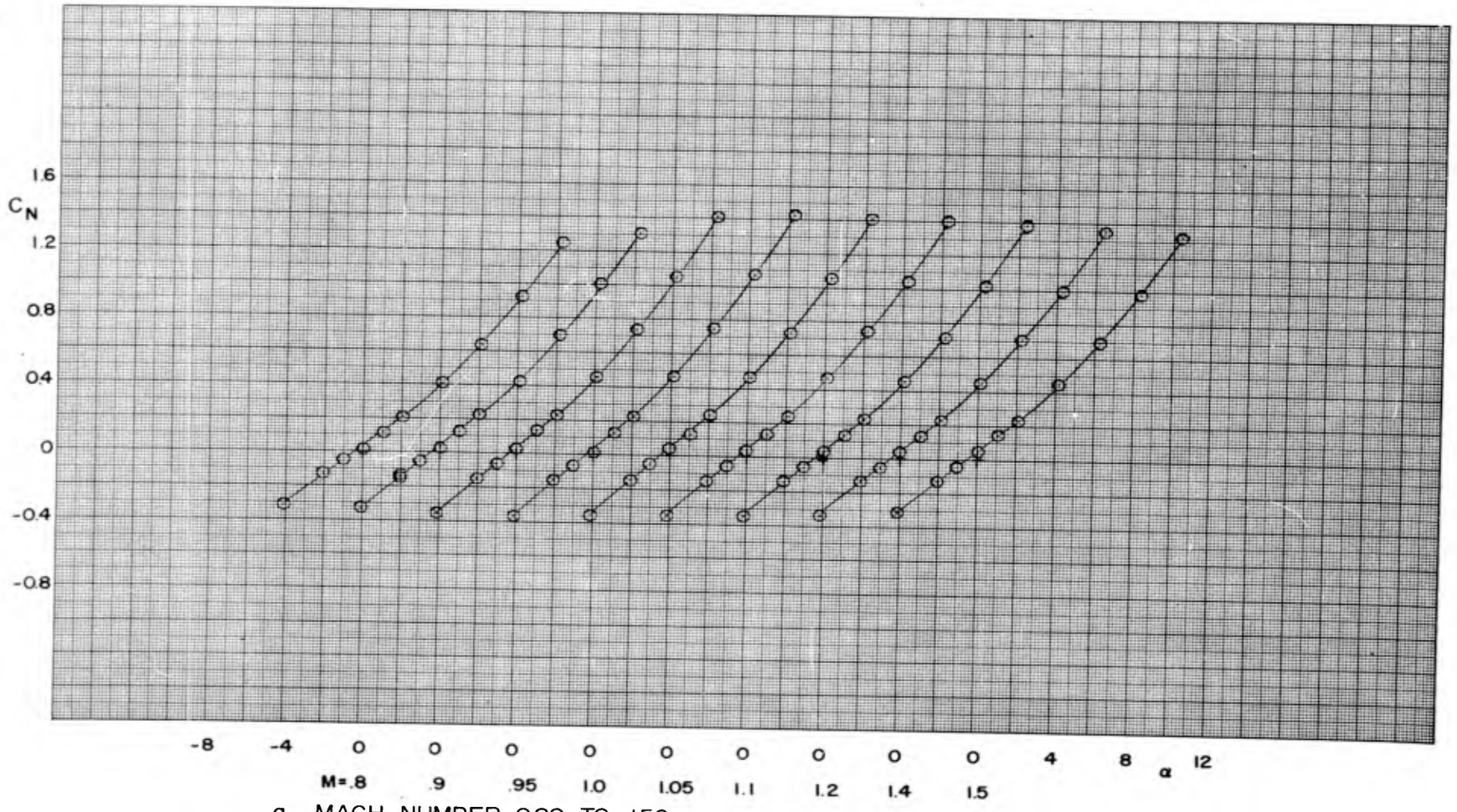

a. MACH NUMBER 0.80 TO 1.50

FIGURE 9 NORMAL-FORCE COEFFICIENT VERSUS ANGLE OF ATTACK FOR CONFIGURATION BF_{4C}

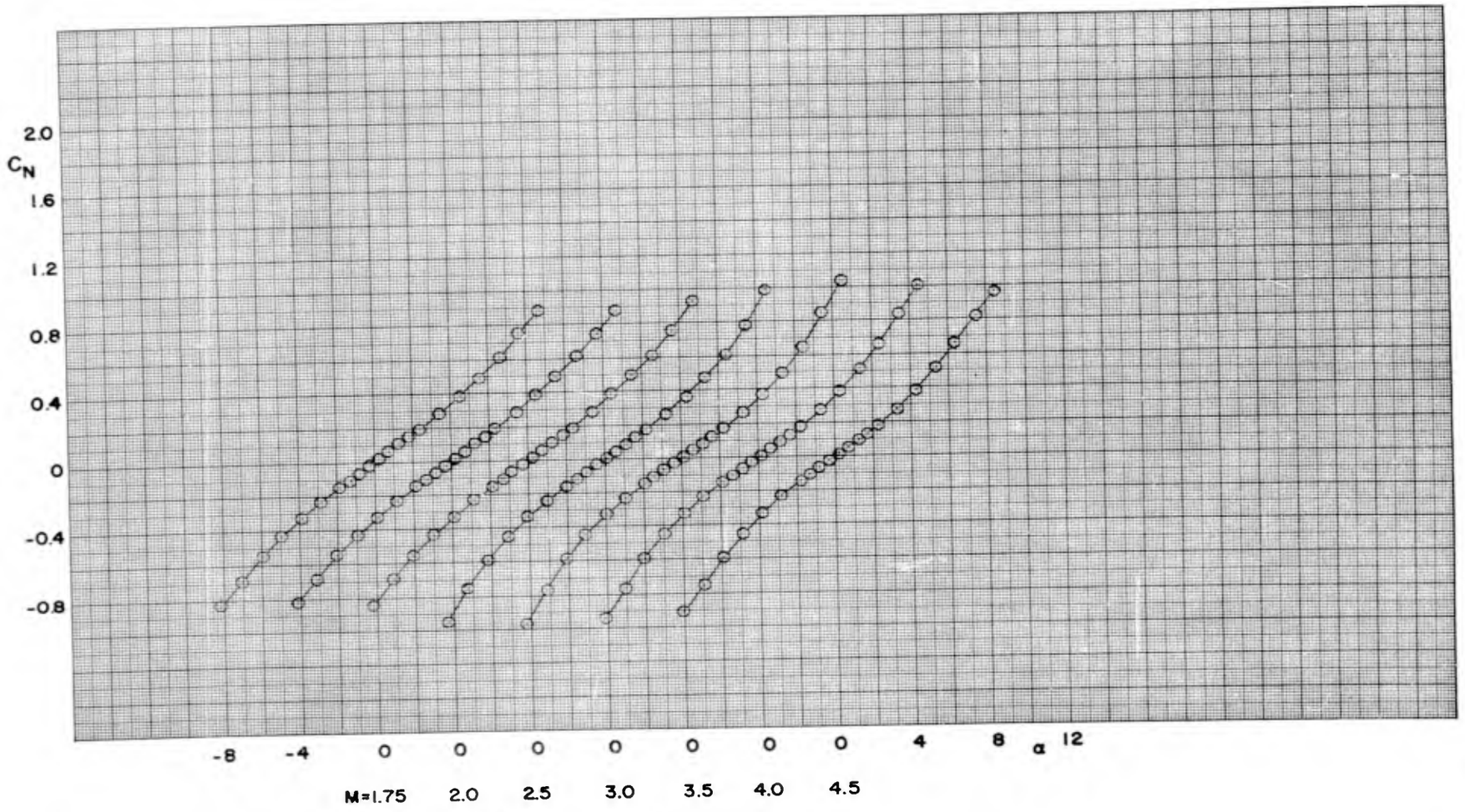

b. MACH NUMBER 1.75 TO 4.50

FIGURE 9 CONCLUDED

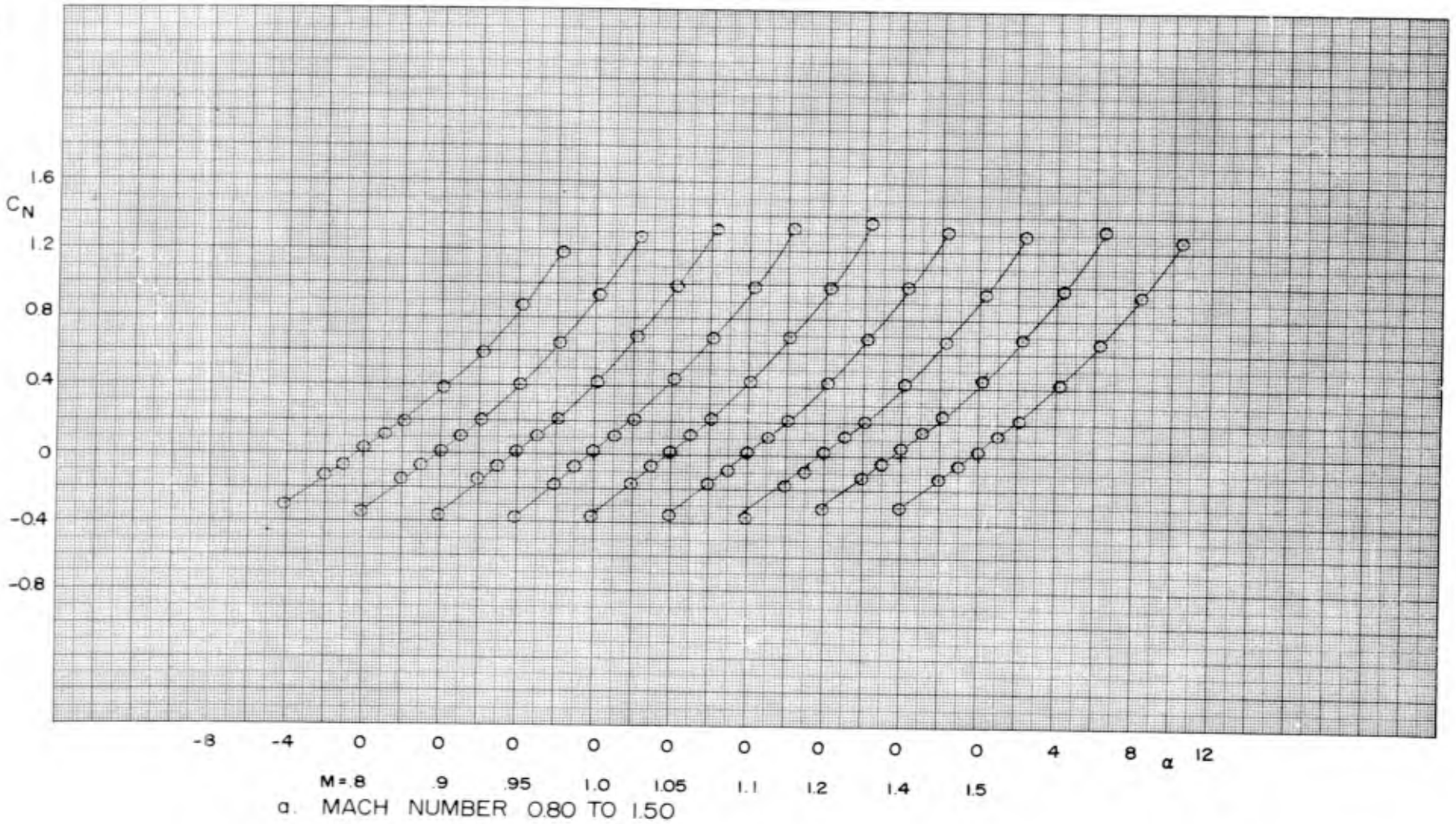

FIGURE 10 NORMAL-FORCE COEFFICIENT VERSUS ANGLE OF ATTACK FOR CONFIGURATION BF_{4D}

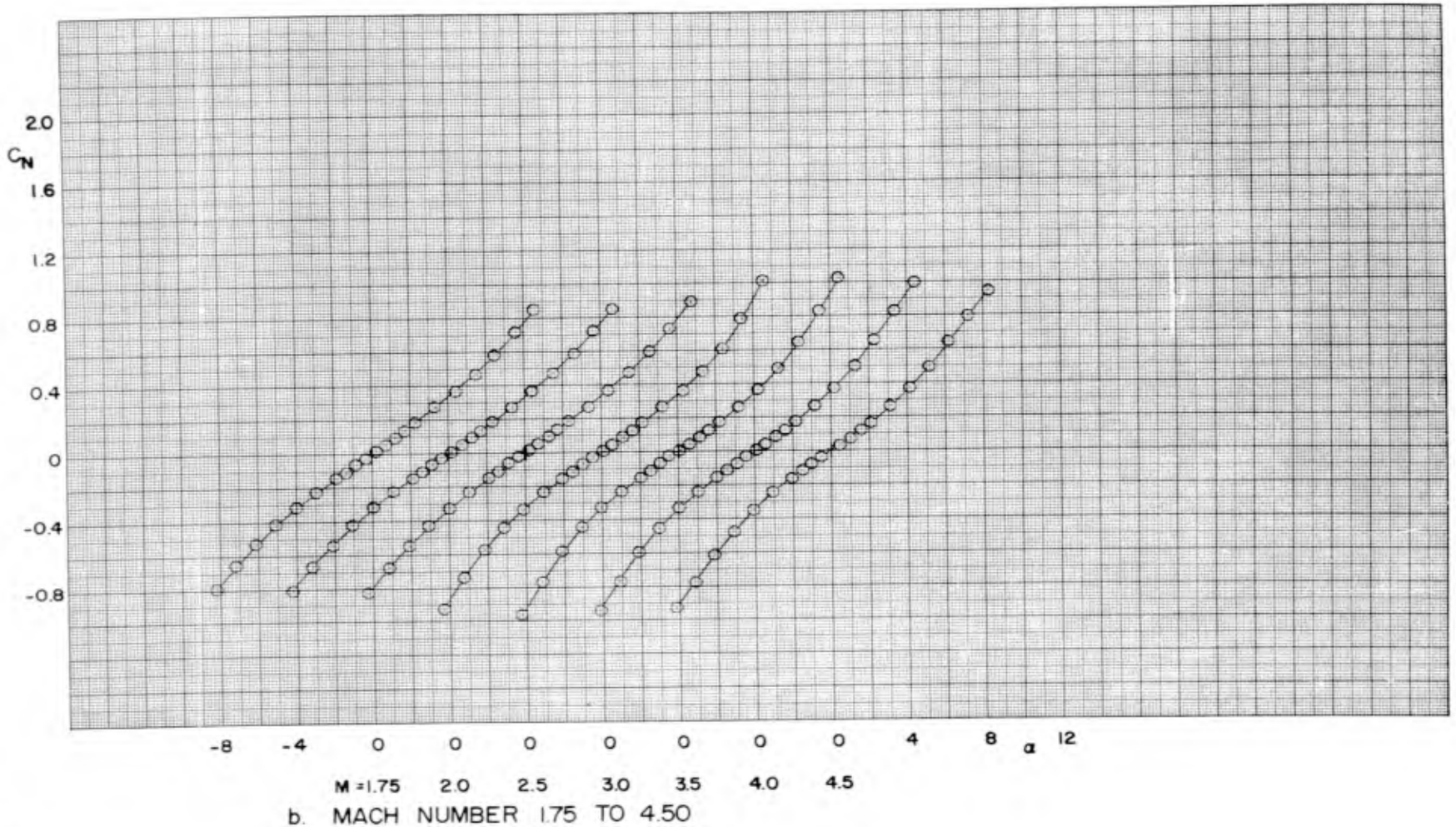

b. MACH NUMBER 1.75 TO 4.50

FIGURE 10 CONCLUDED

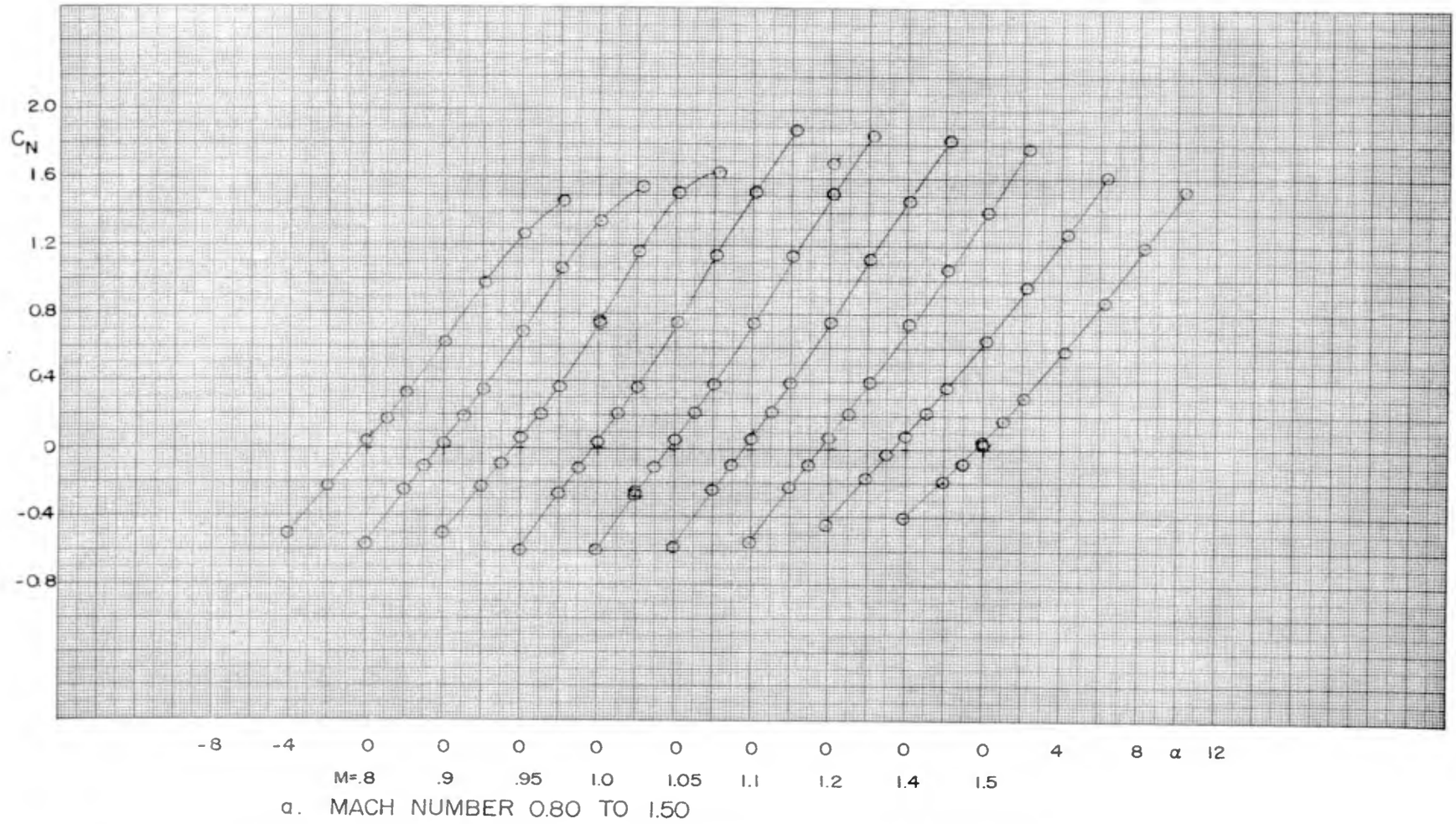

a. MACH NUMBER 0.80 TO 1.50

FIGURE 11 NORMAL-FORCE COEFFICIENT VERSUS ANGLE OF ATTACK FOR CONFIGURATION BF_5A

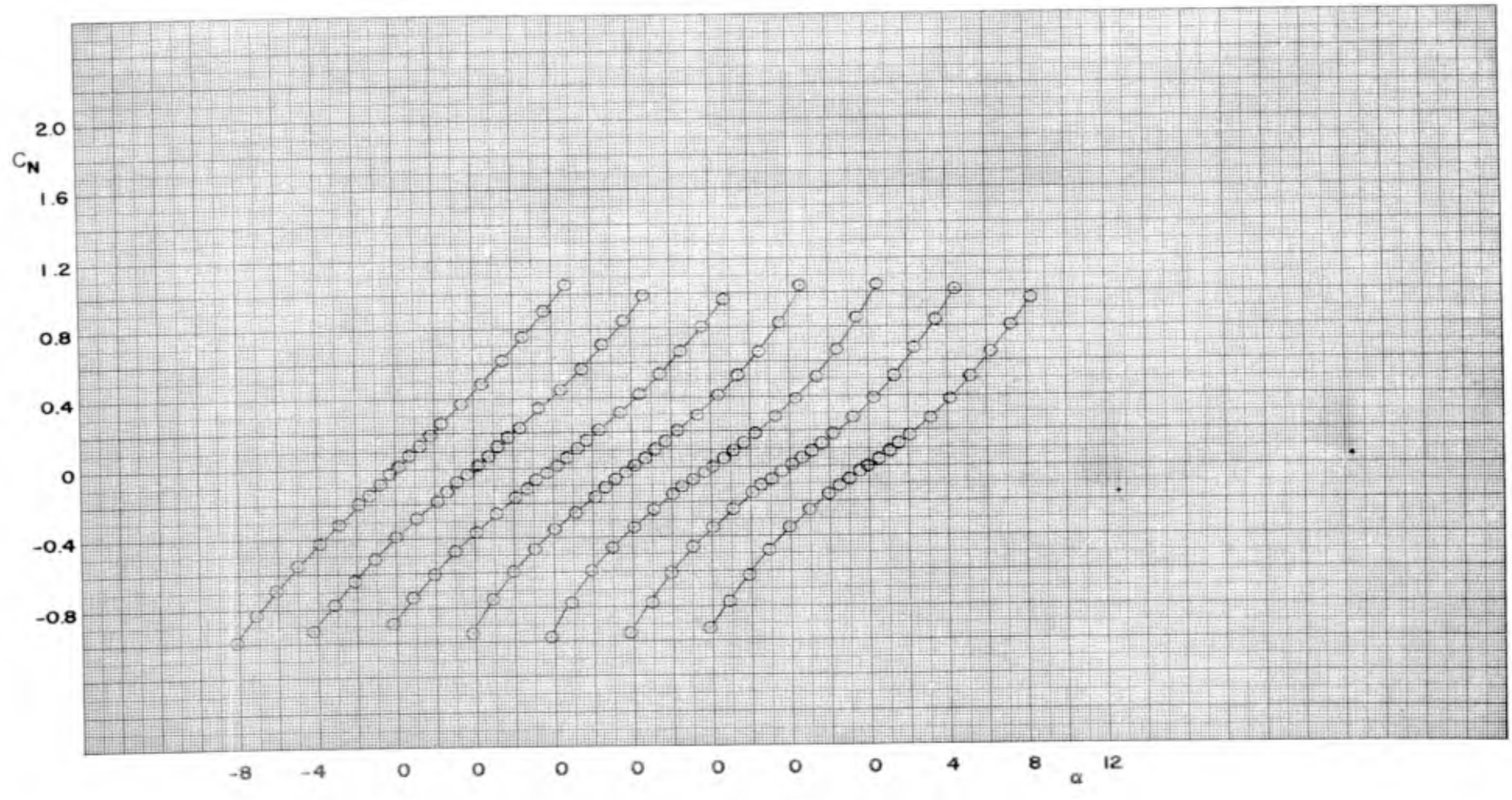

b. MACH NUMBER 1.75 TO 4.50

FIGURE 11 CONCLUDED

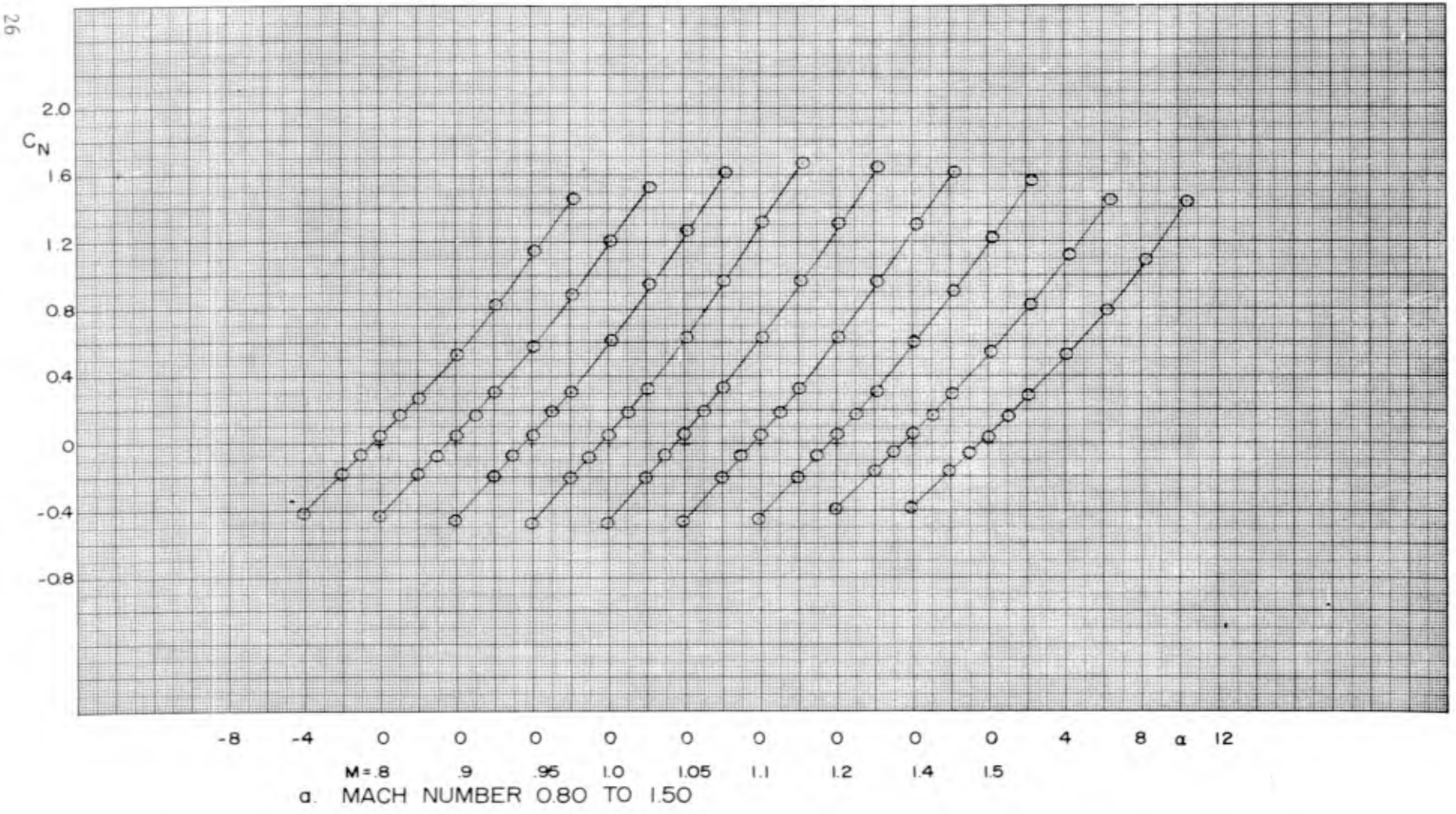

a. MACH NUMBER 0.80 TO 1.50

FIGURE 12 NORMAL-FORCE COEFFICIENT VERSUS ANGLE OF ATTACK FOR CONFIGURATION BF_{5B}

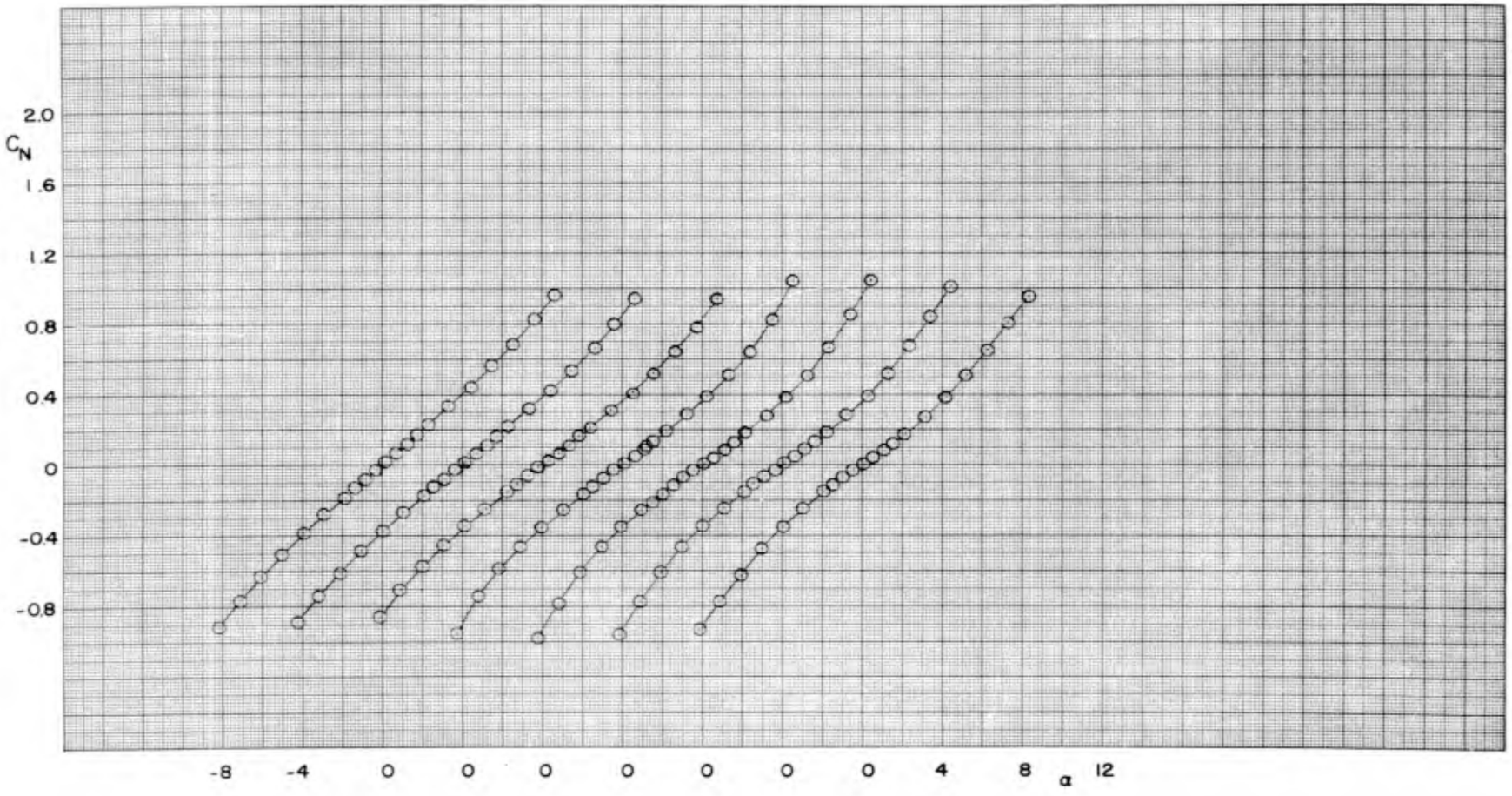

b. MACH NUMBER 1.75 TO 4.50

FIGURE 12. CONCLUDED.

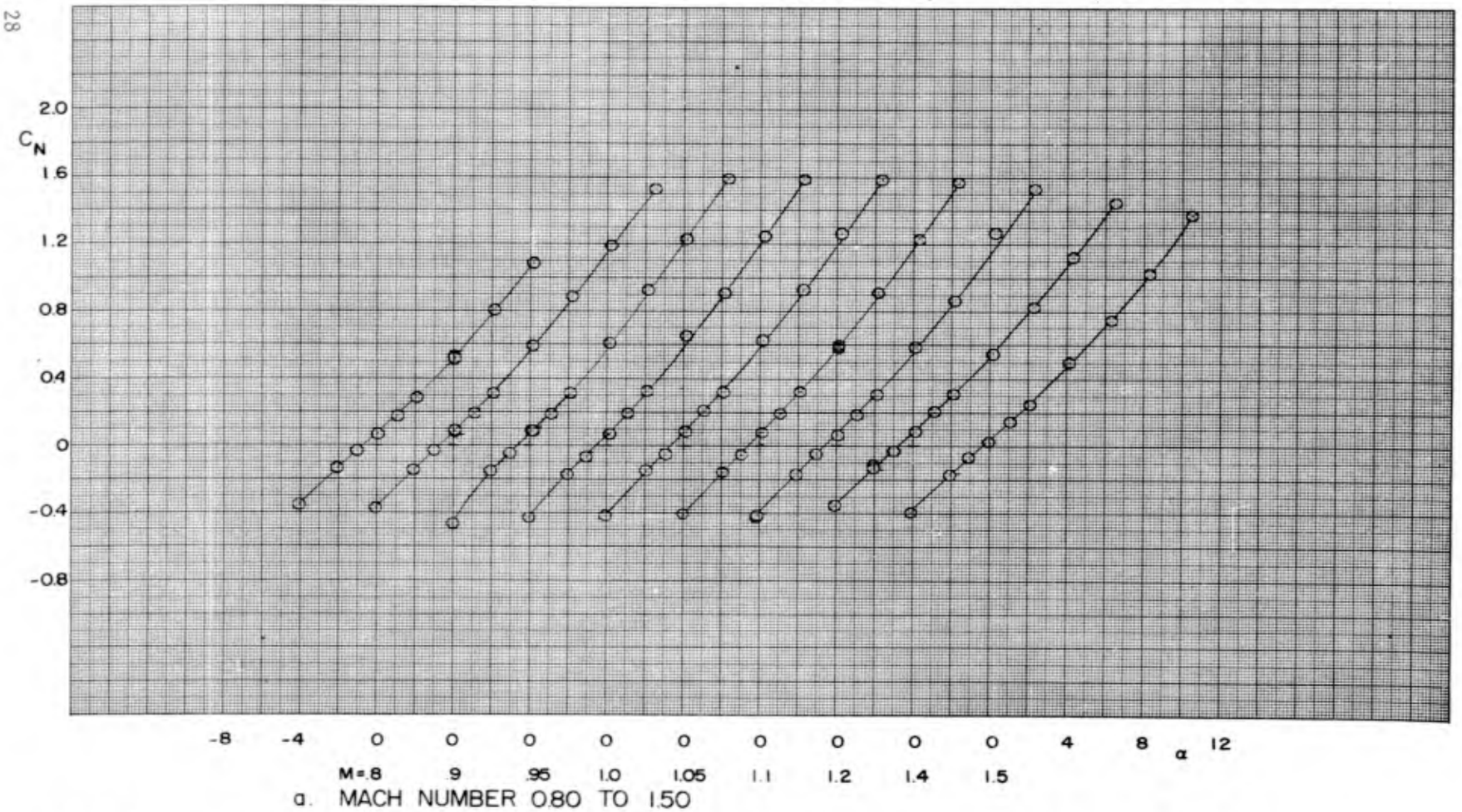

a. MACH NUMBER 0.80 TO 1.50

FIGURE 13 NORMAL-FORCE COEFFICIENT VERSUS ANGLE OF ATTACK FOR CONFIGURATION BF_{5C}

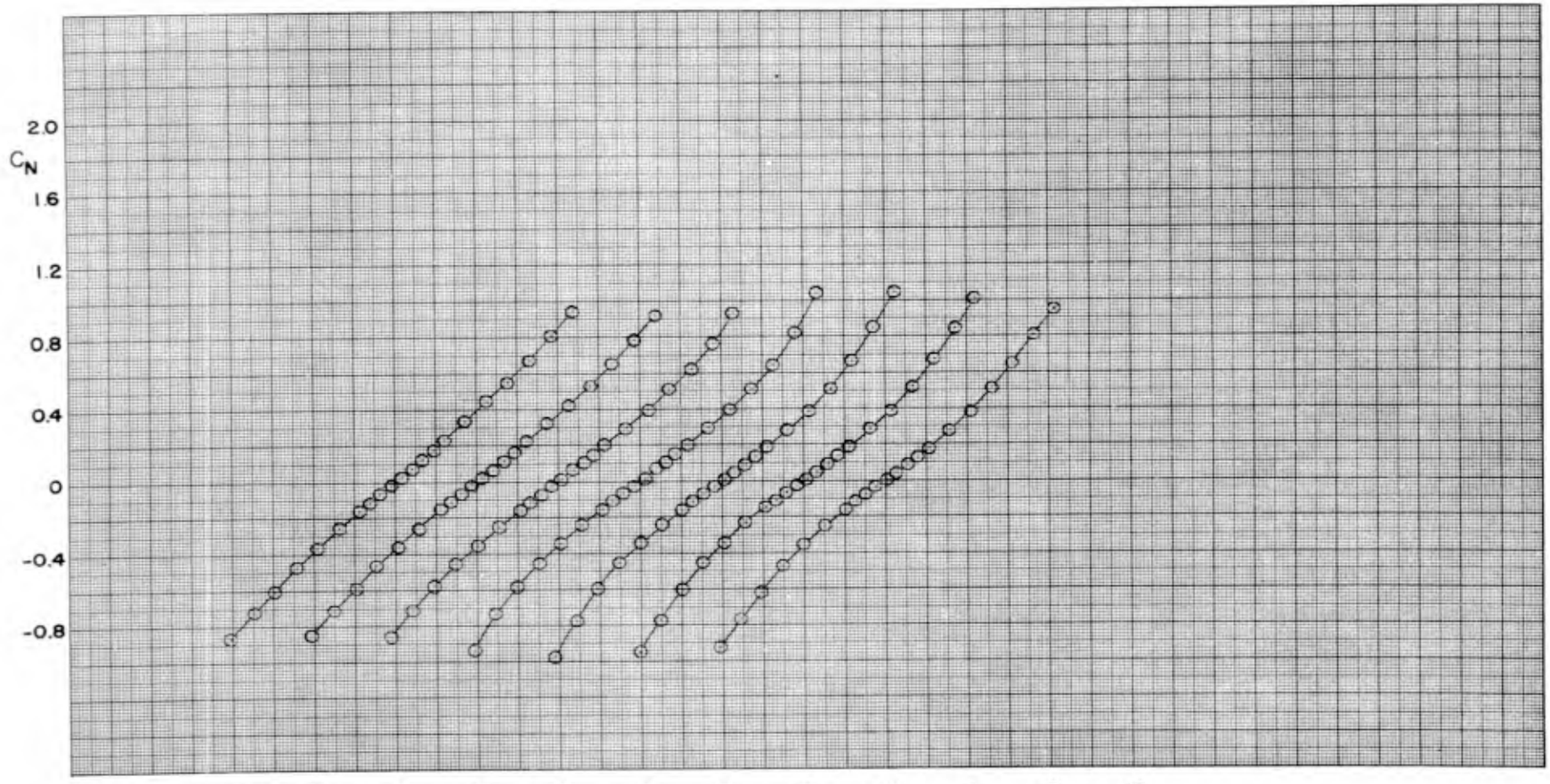

b. MACH NUMBER 1.75 TO 4.50

FIGURE 13 CONCLUDED

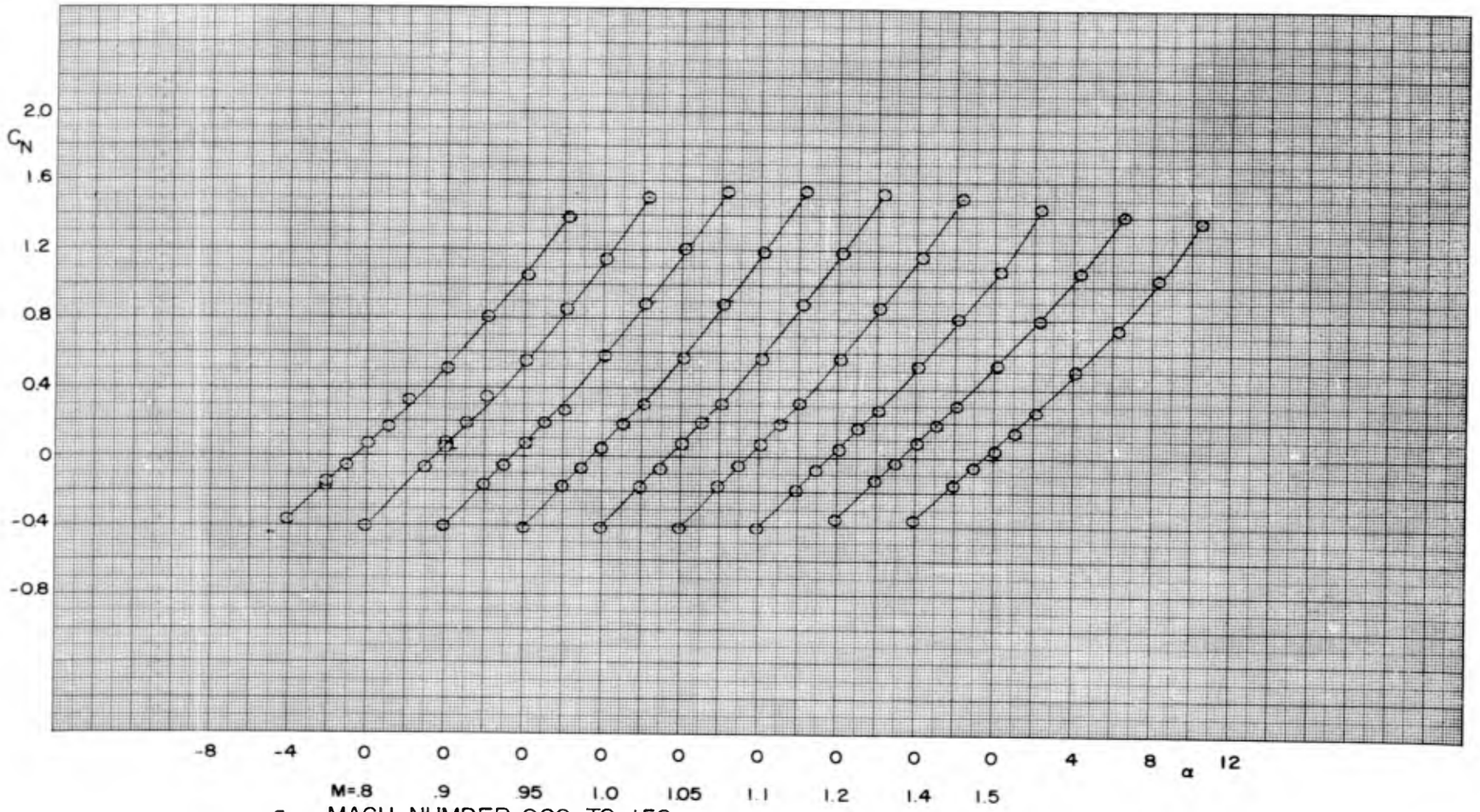

a. MACH NUMBER 0.80 TO 1.50

FIGURE 14 NORMAL-FORCE COEFFICIENT VERSUS ANGLE OF ATTACK FOR CONFIGURATION BF_{5D}

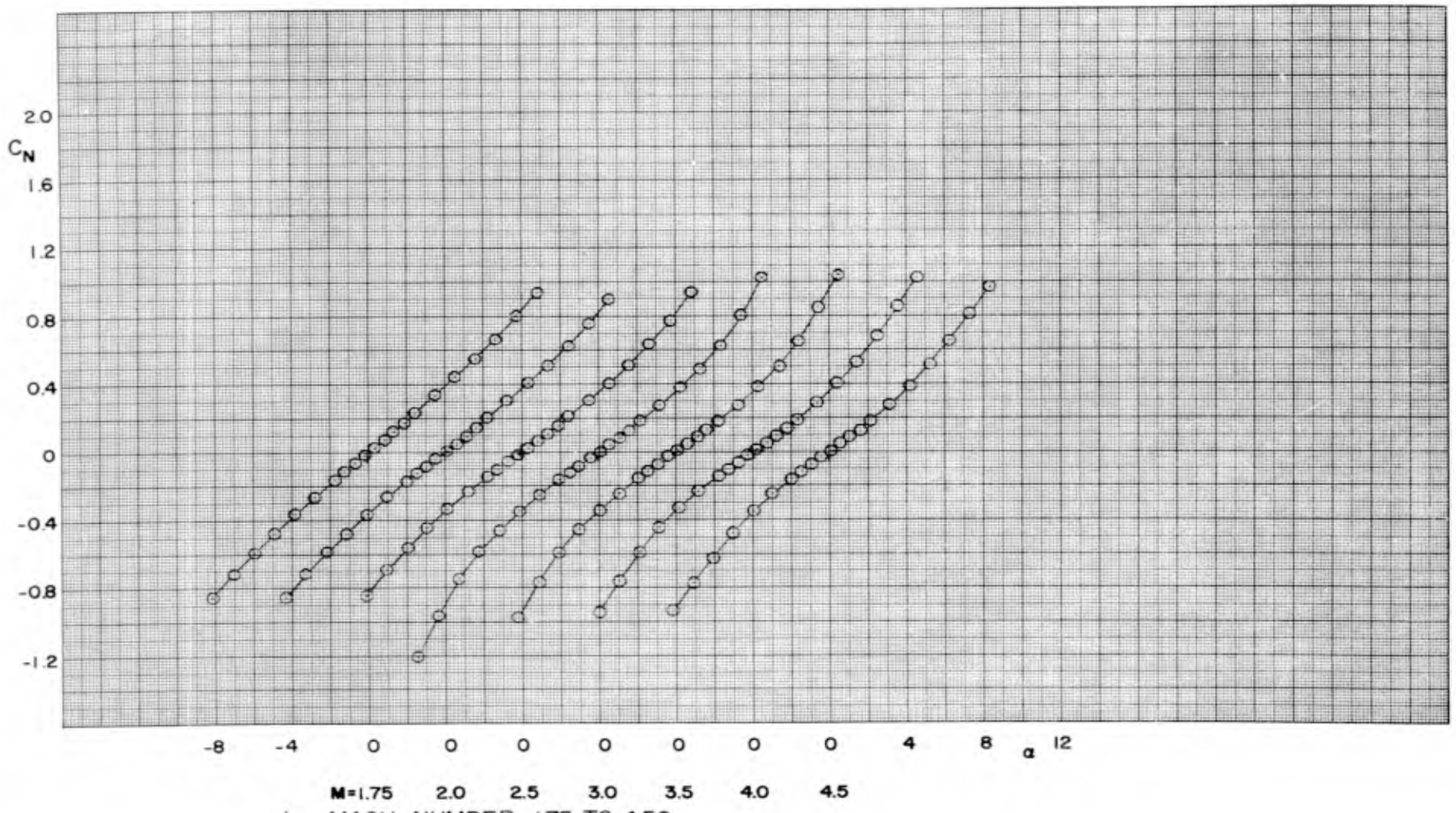

b. MACH NUMBER 1.75 TO 4.50

FIGURE 14 CONCLUDED

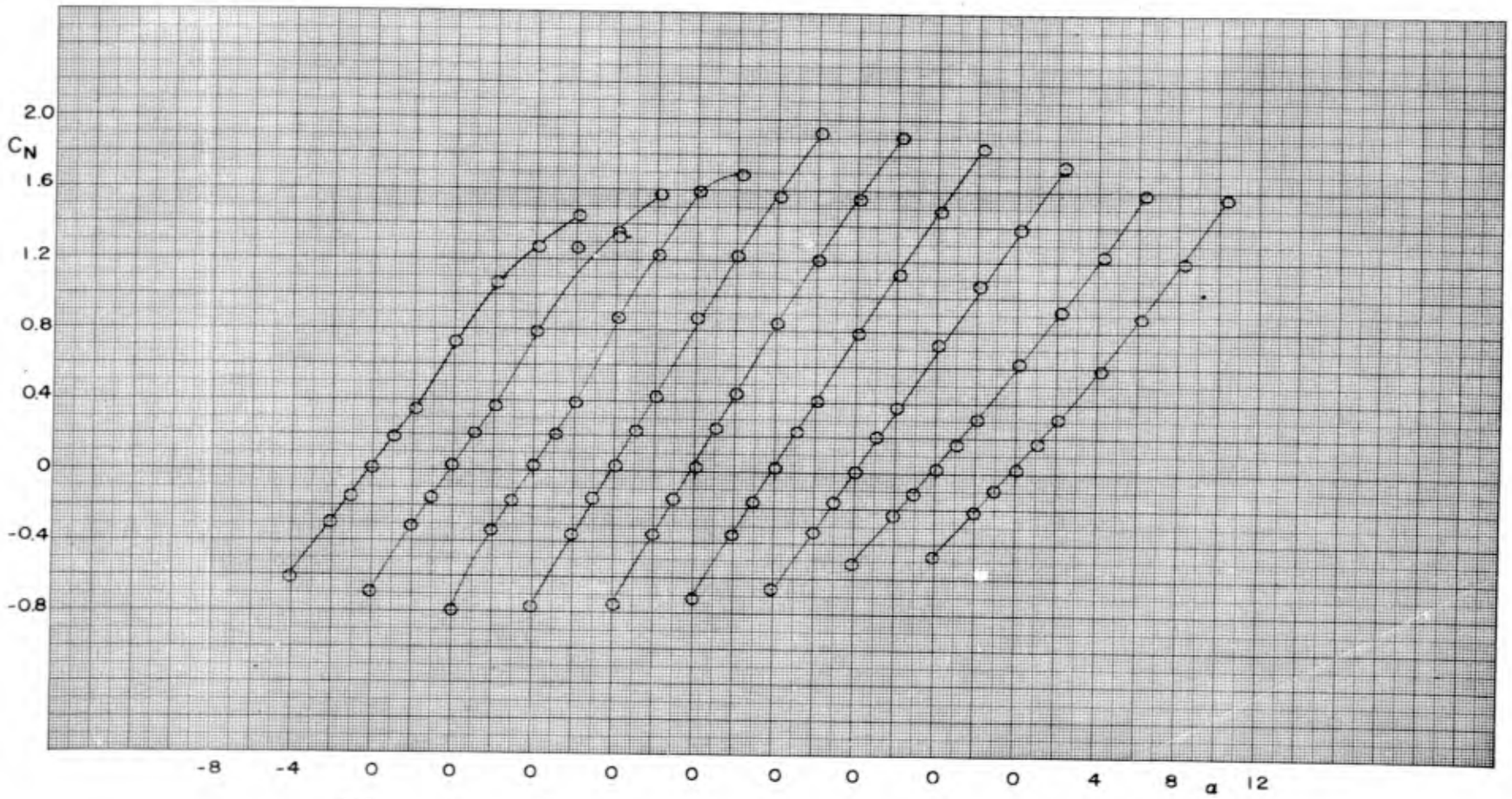

a. MACH NUMBER 0.80 TO 1.50

FIGURE 15 NORMAL-FORCE COEFFICIENT VERSUS ANGLE OF ATTACK FOR CONFIGURATION BF_{6A}

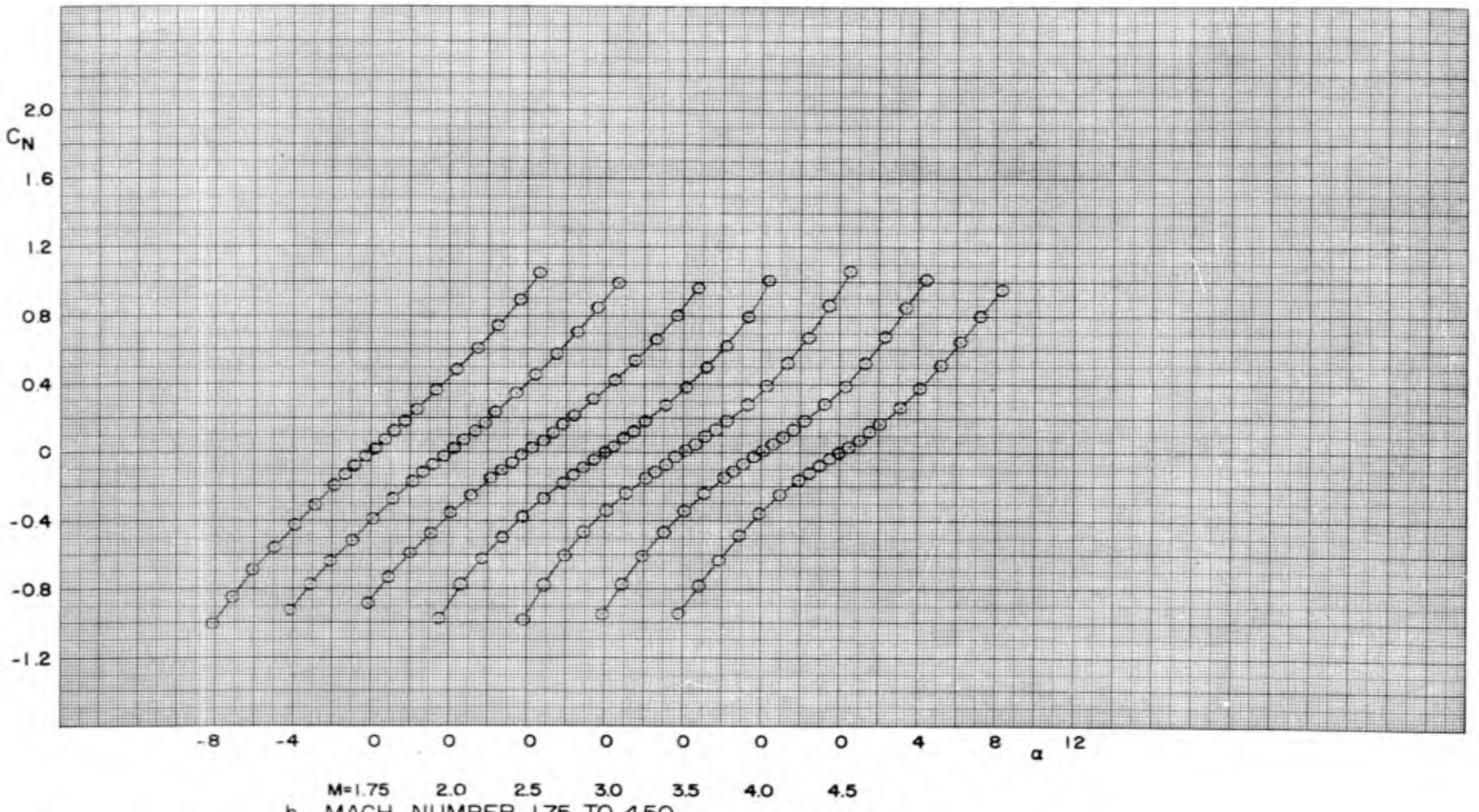

b. MACH NUMBER 1.75 TO 4.50

FIGURE 15 CONCLUDED

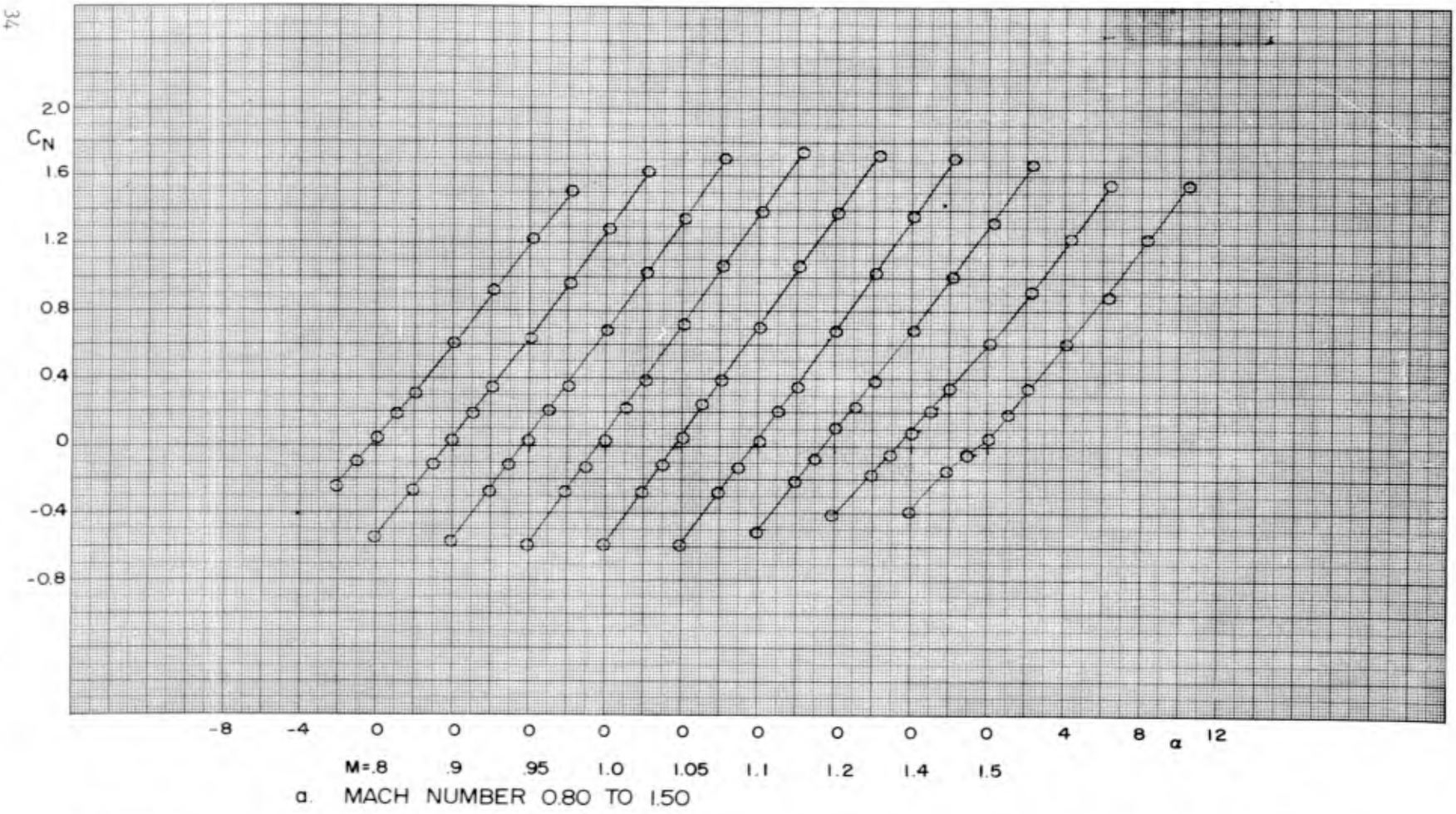

a. MACH NUMBER 0.80 TO 1.50

FIGURE 16 NORMAL-FORCE COEFFICIENT VERSUS ANGLE OF ATTACK FOR CONFIGURATION BF_{6B}

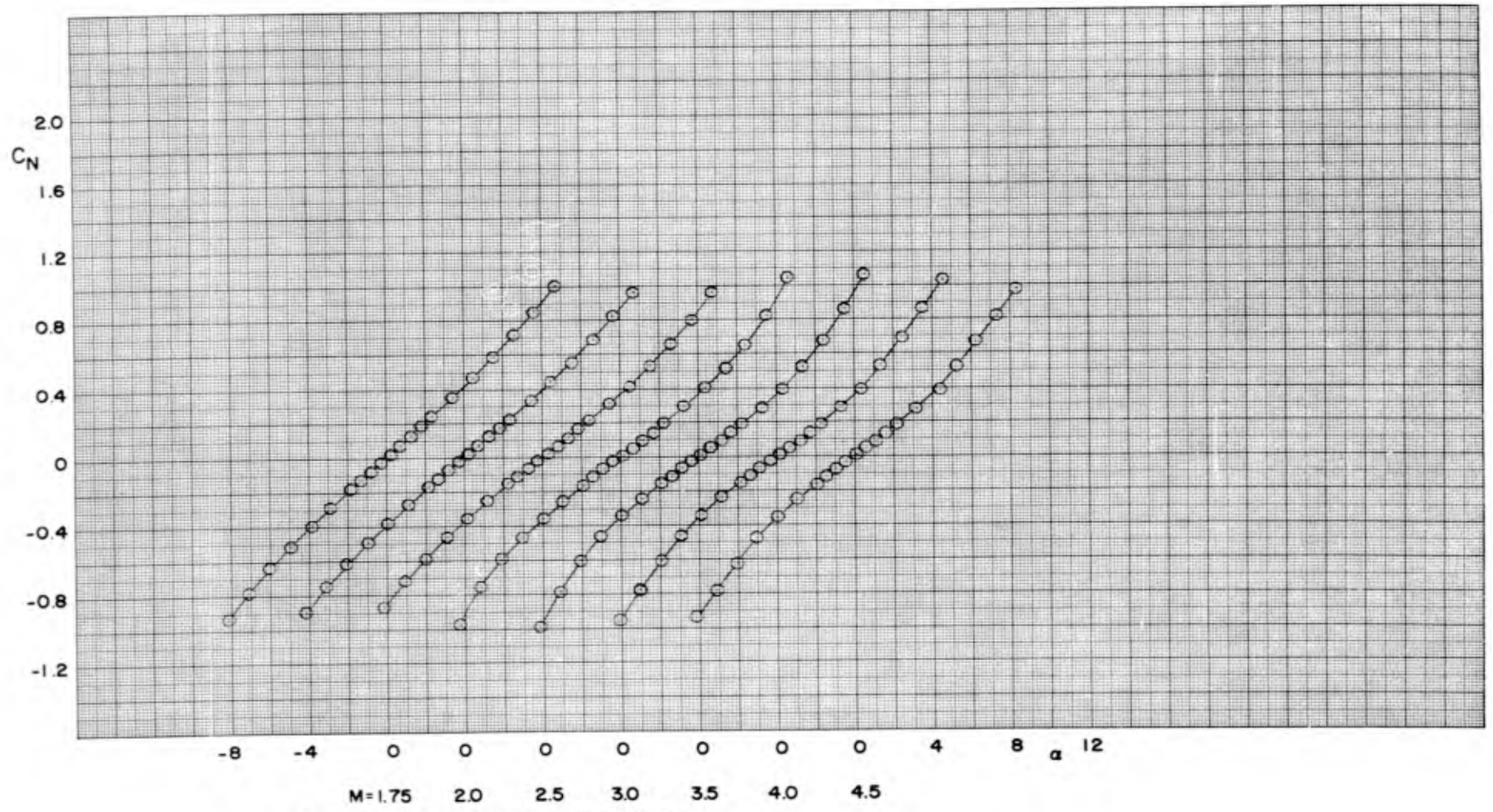

b. MACH NUMBER 1.75 TO 4.50

FIGURE 16 CONCLUDED

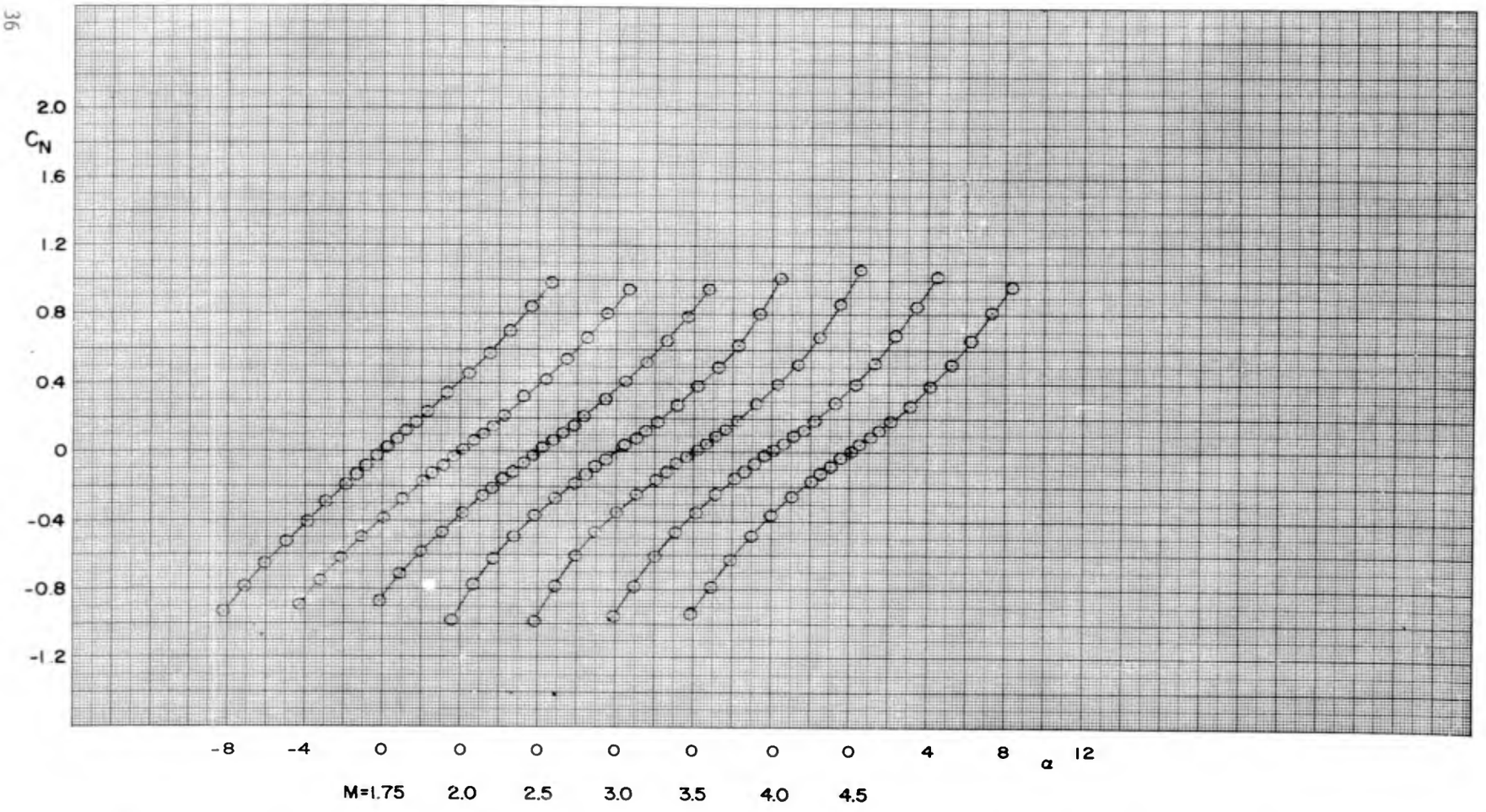

FIGURE 17 NORMAL-FORCE COEFFICIENT VERSUS ANGLE OF ATTACK FOR CONFIGURATION BF_{6C}

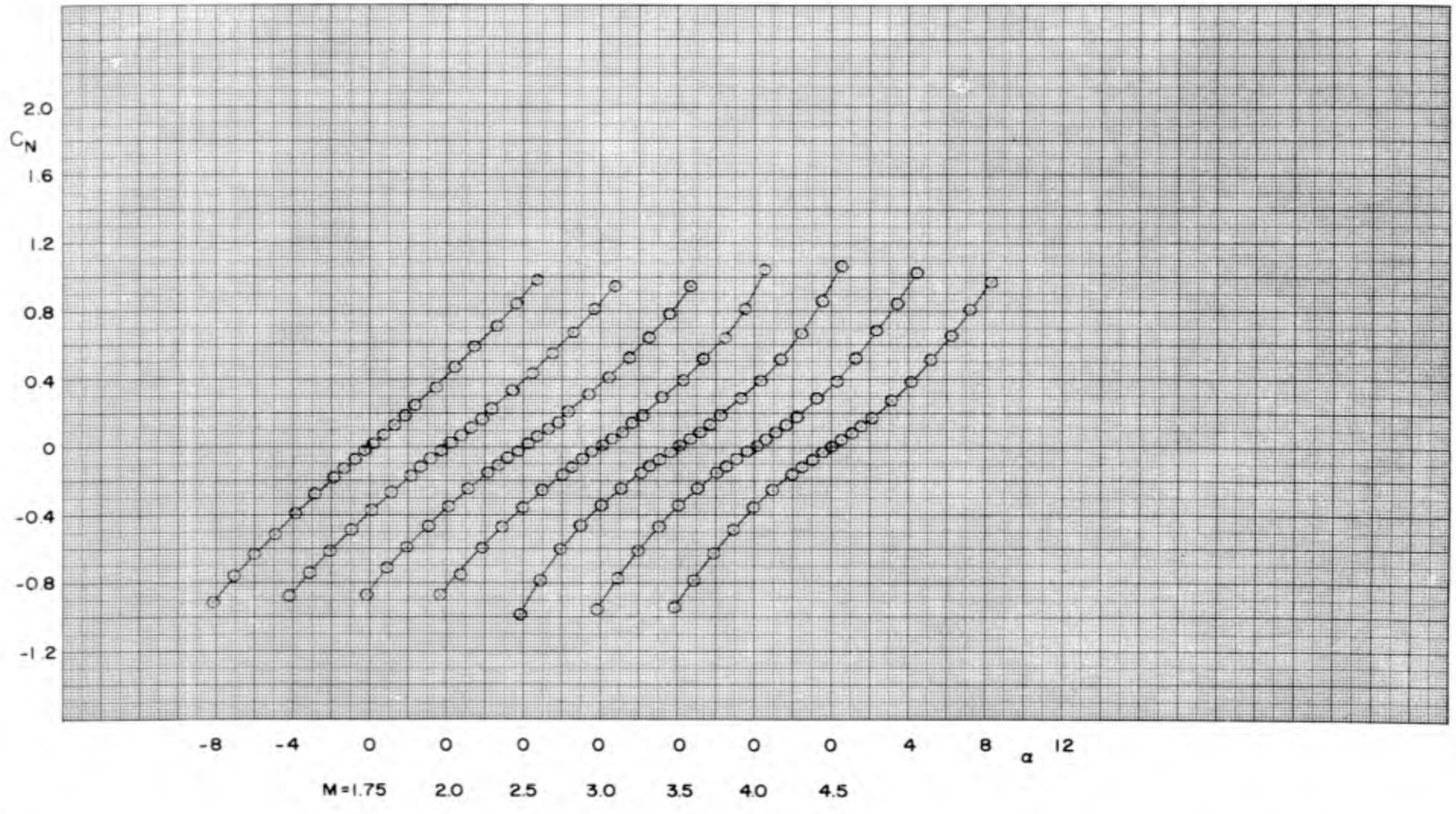

FIGURE 18 NORMAL-FORCE COEFFICIENT VERSUS ANGLE OF ATTACK FOR CONFIGURATION BF_{6D}

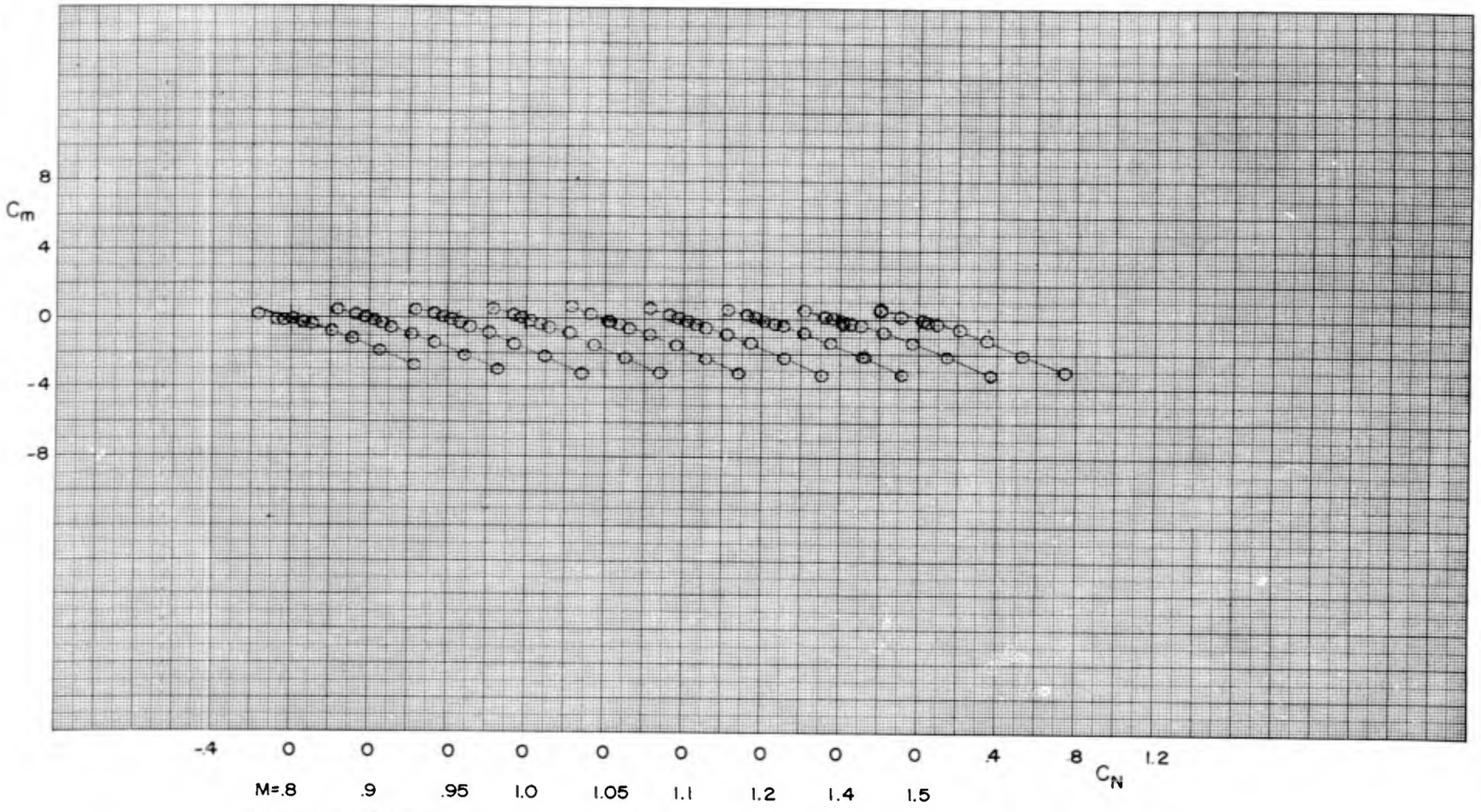

a. MACH NUMBER 0.80 TO 1.50

FIGURE 19 PITCHING-MOMENT COEFFICIENT VERSUS NORMAL-FORCE COEFFICIENT FOR CONFIGURATION B

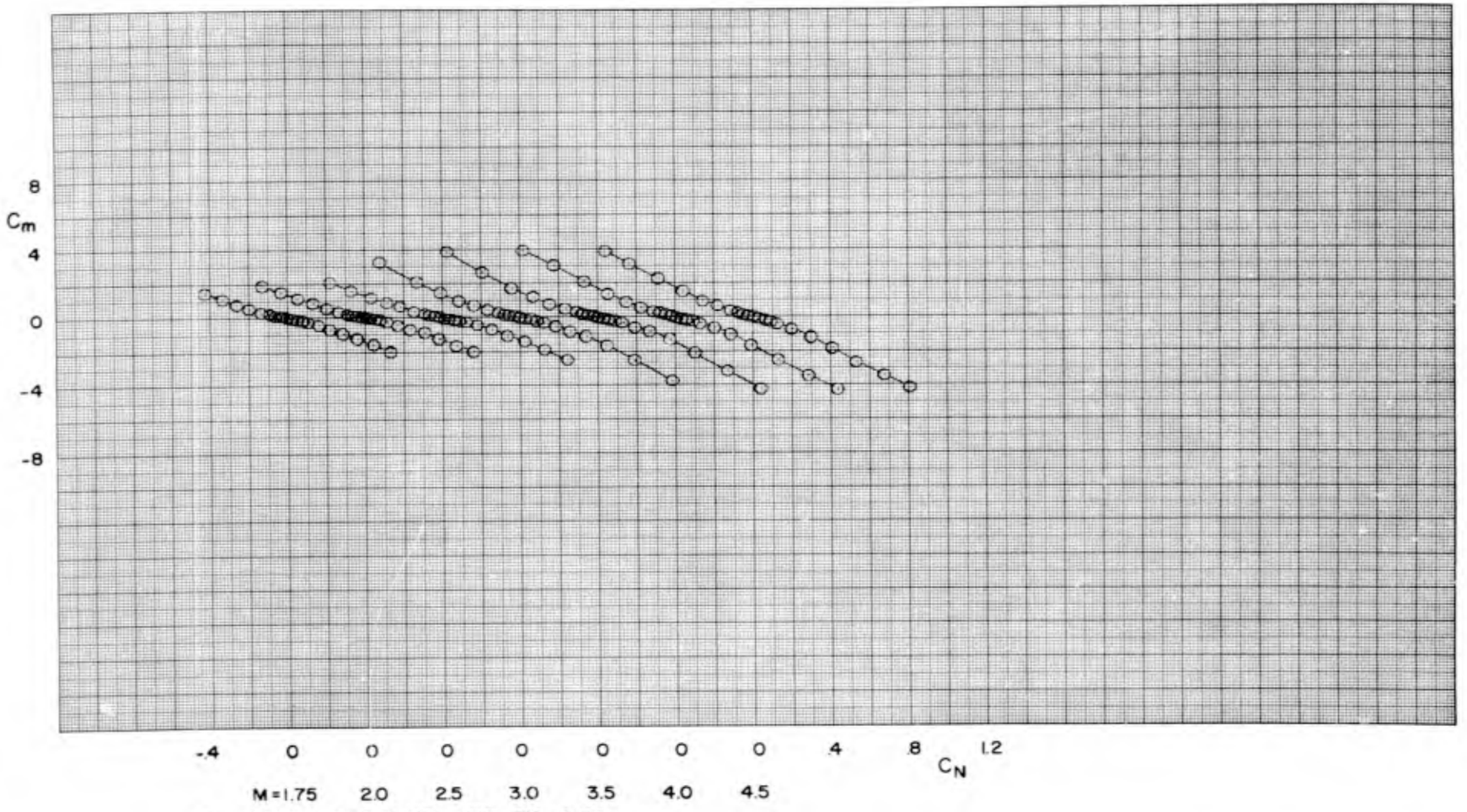

b. MACH NUMBER 1.75 TO 4.50

FIGURE 19 CONCLUDED

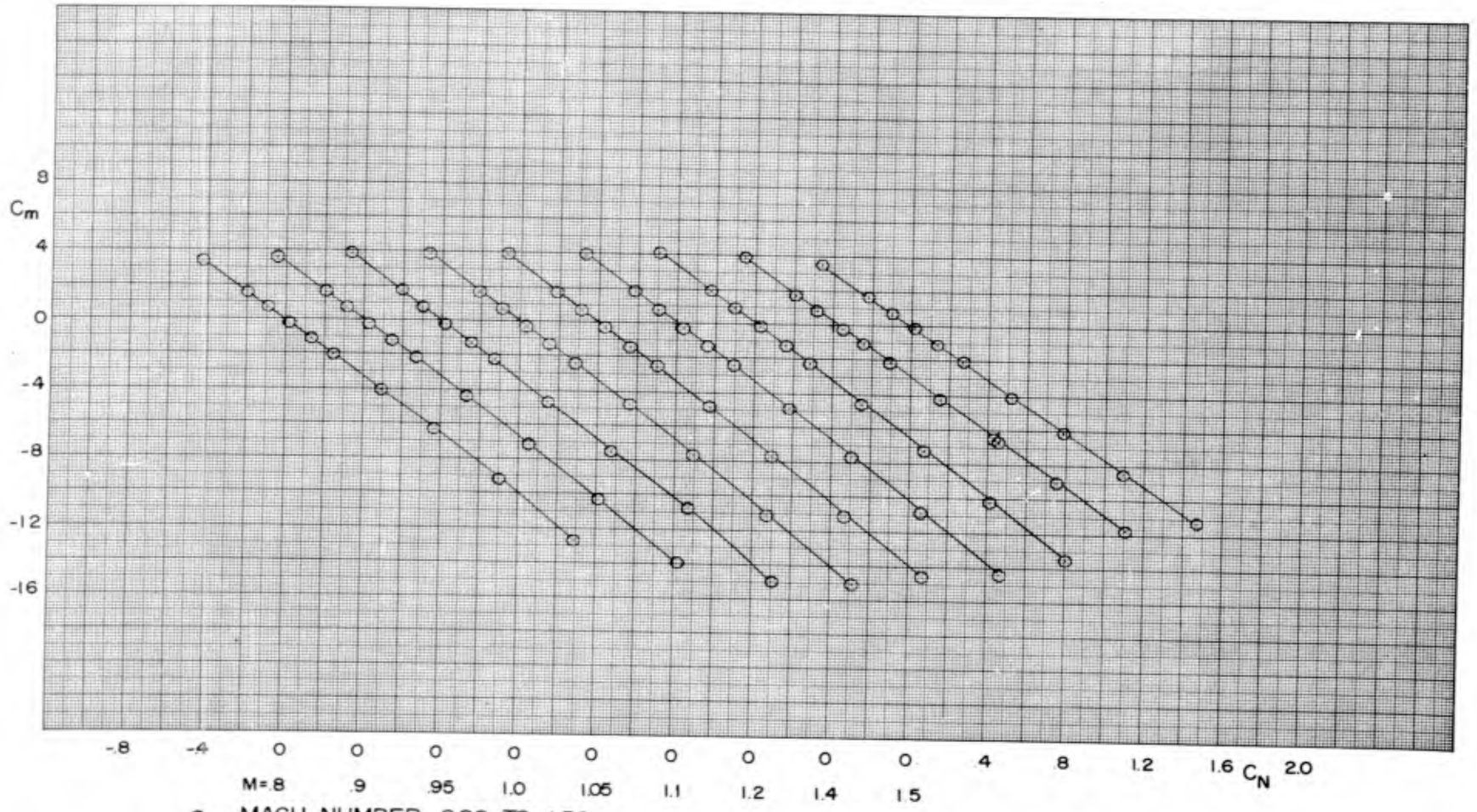

a. MACH NUMBER 0.80 TO 1.50

FIGURE 20 PITCHING-MOMENT COEFFICIENT VERSUS NORMAL-FORCE COEFFICIENT FOR CONFIGURATION BF_{4A}

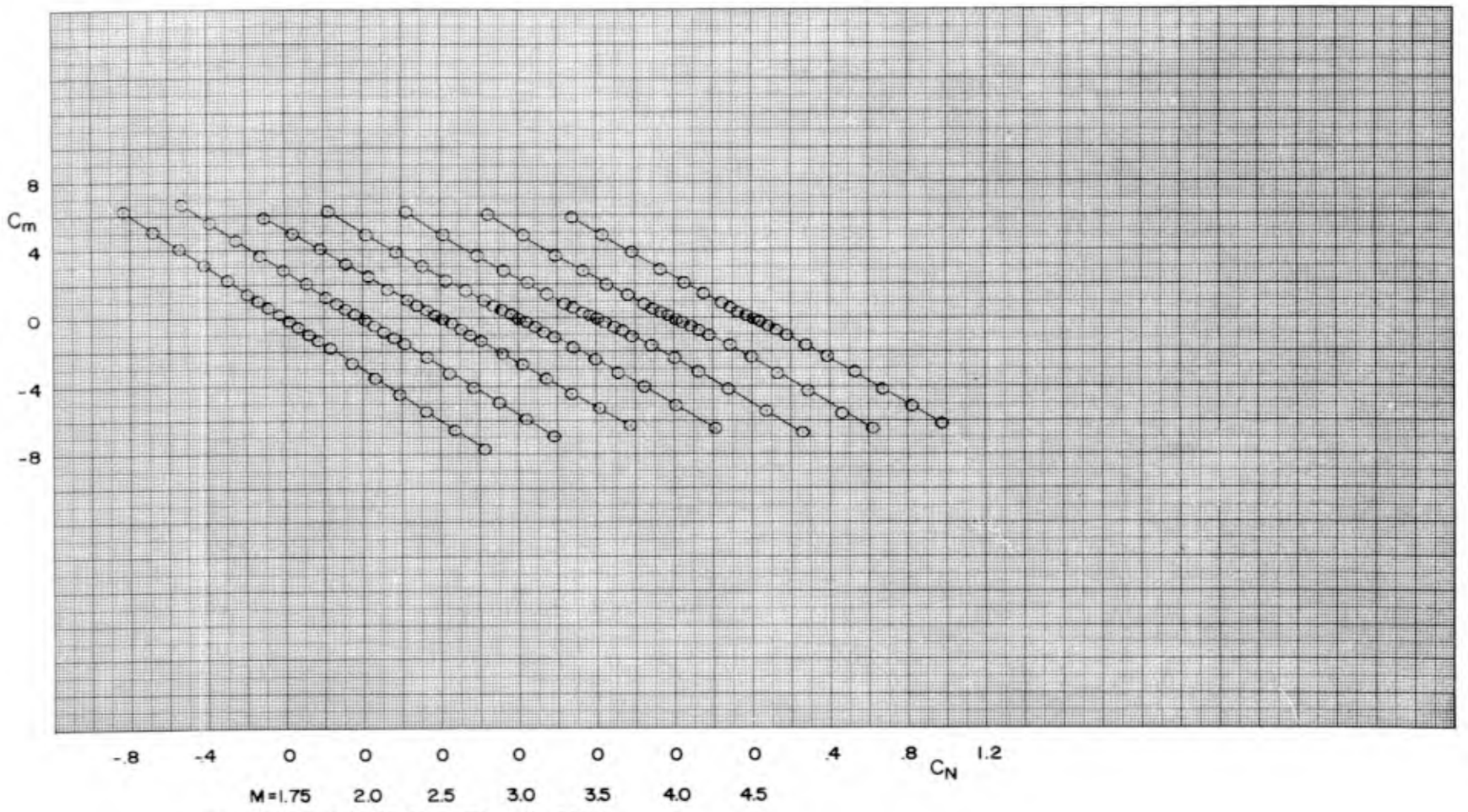

b. MACH NUMBER 1.75 TO 4.50

FIGURE 20 CONCLUDED

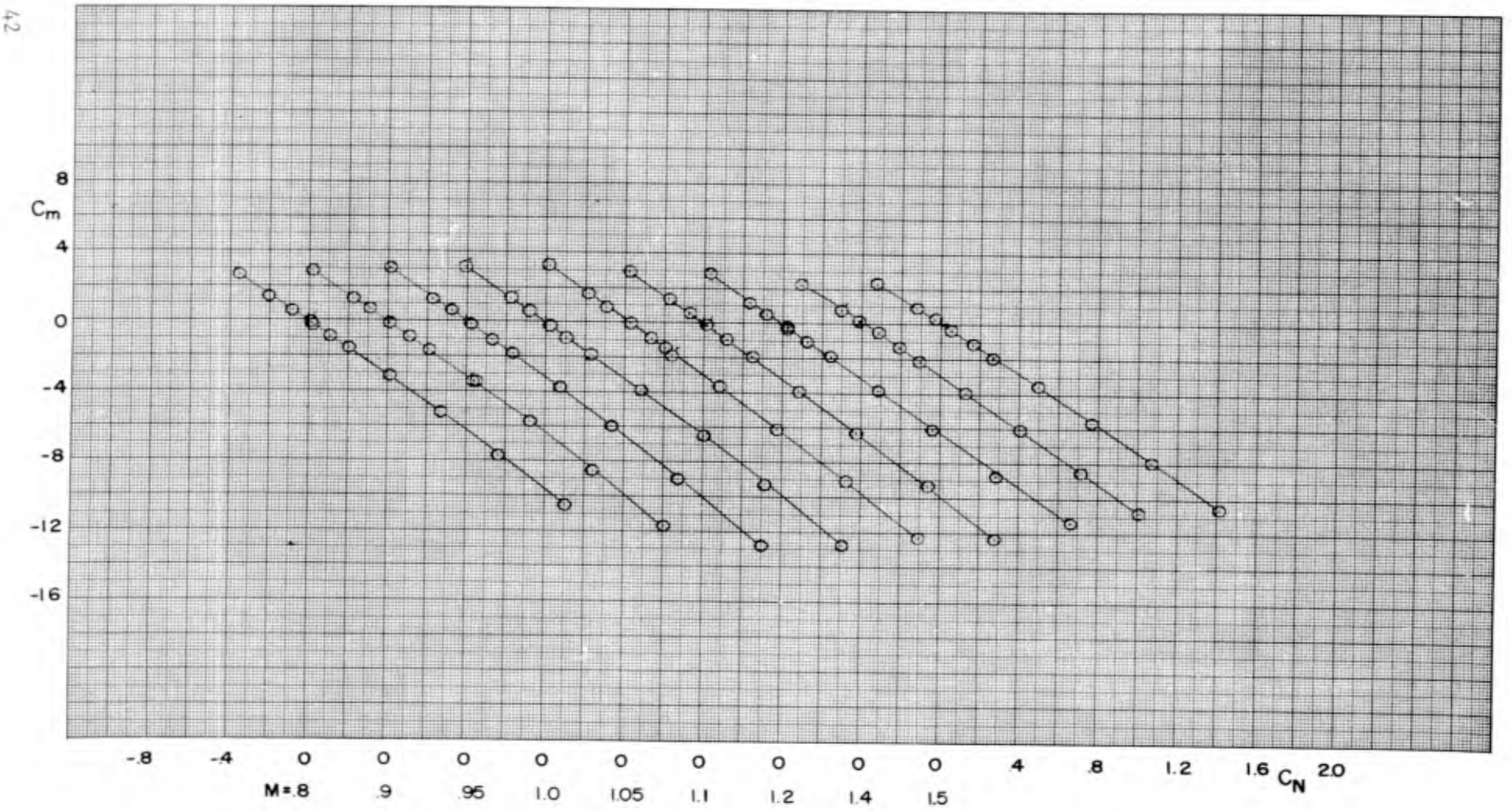

a. MACH NUMBER 0.80 TO 1.50

FIGURE 21 PITCHING-MOMENT COEFFICIENT VERSUS NORMAL-FORCE COEFFICIENT FOR CONFIGURATION BF_{4B}

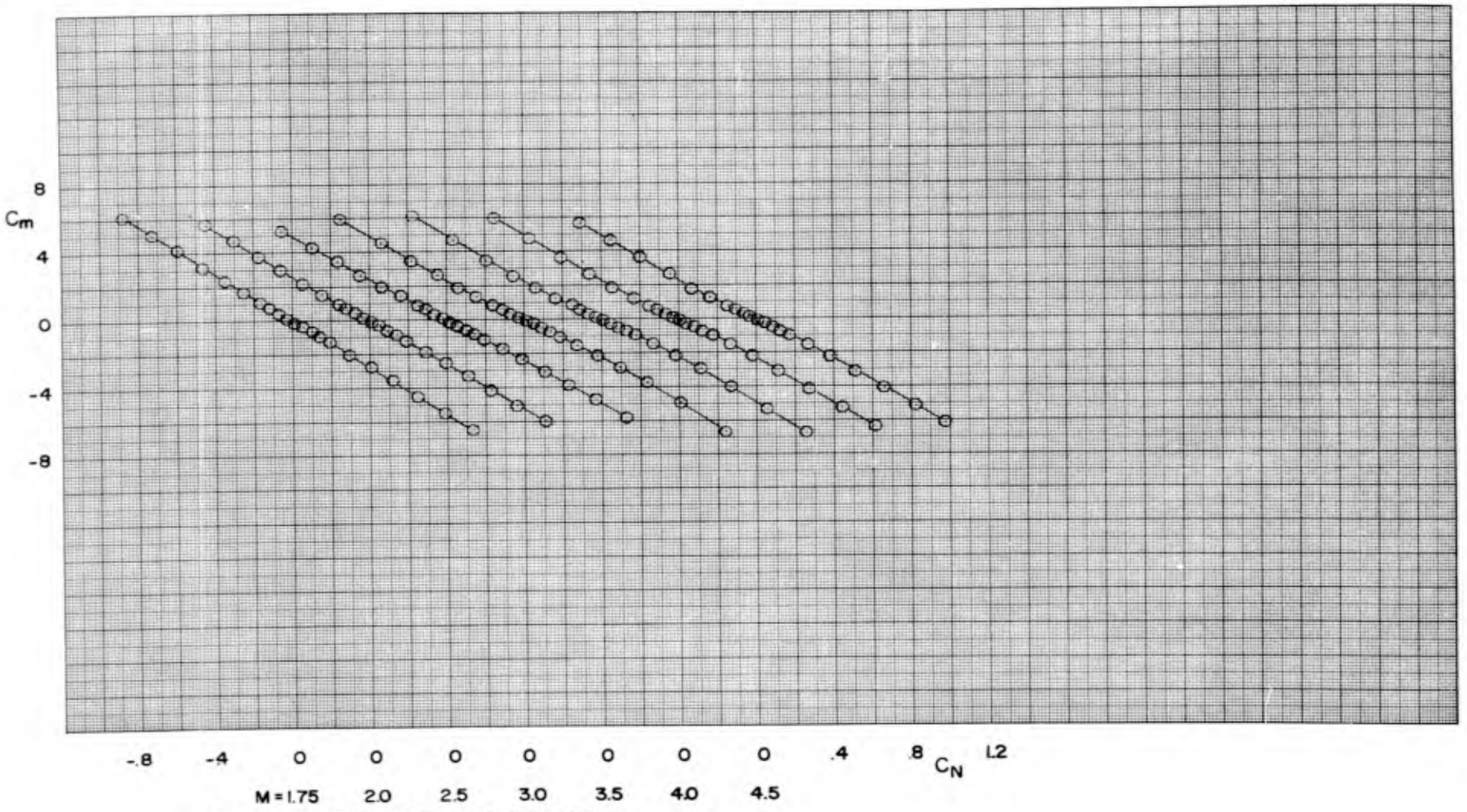

b. MACH NUMBER 1.75 TO 4.50

FIGURE 21 CONCLUDED

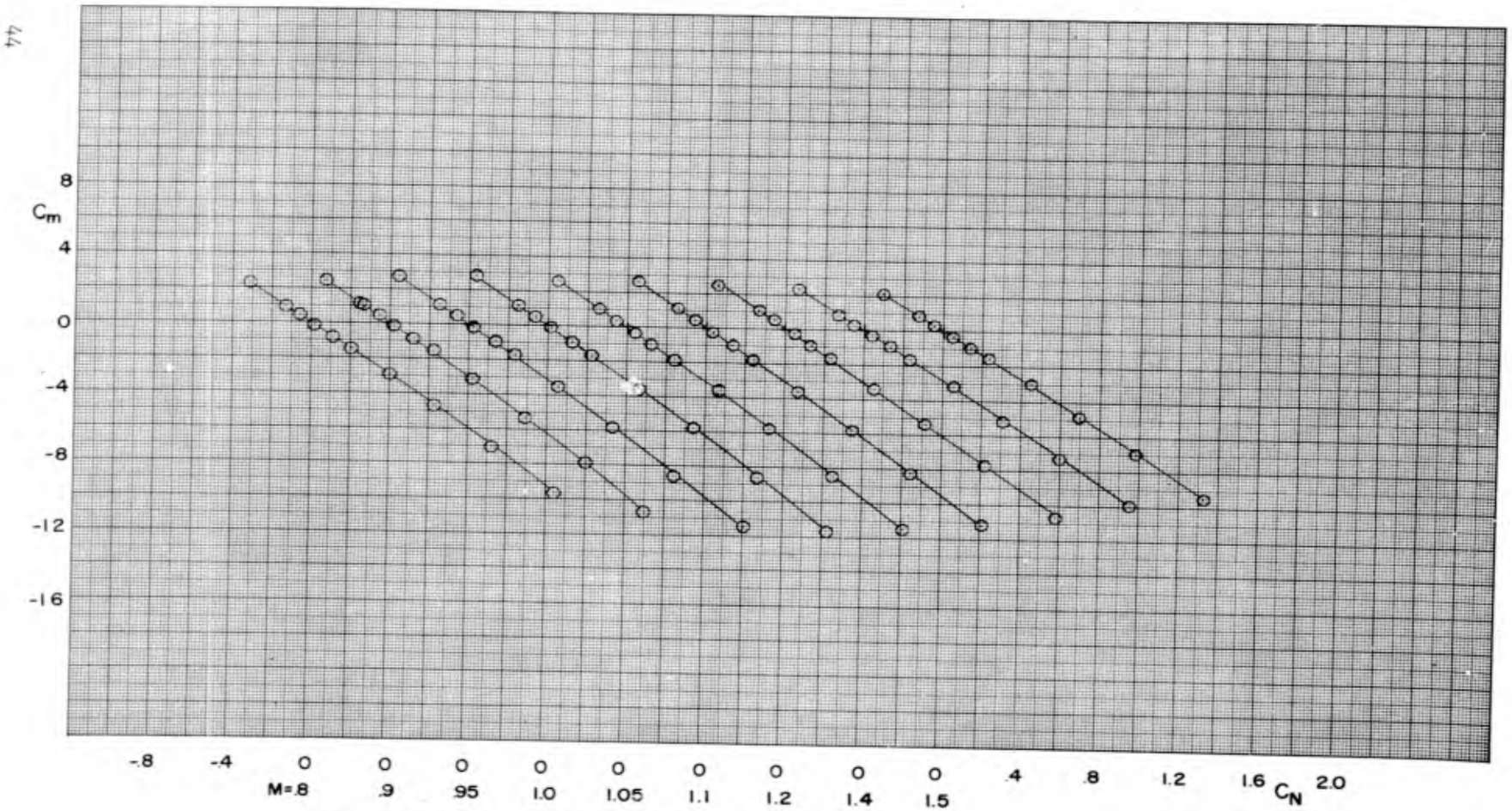

a. MACH NUMBER 0.80 TO 1.50

FIGURE 22 PITCHING-MOMENT COEFFICIENT VERSUS NORMAL-FORCE COEFFICIENT FOR CONFIGURATION BF_{4C}

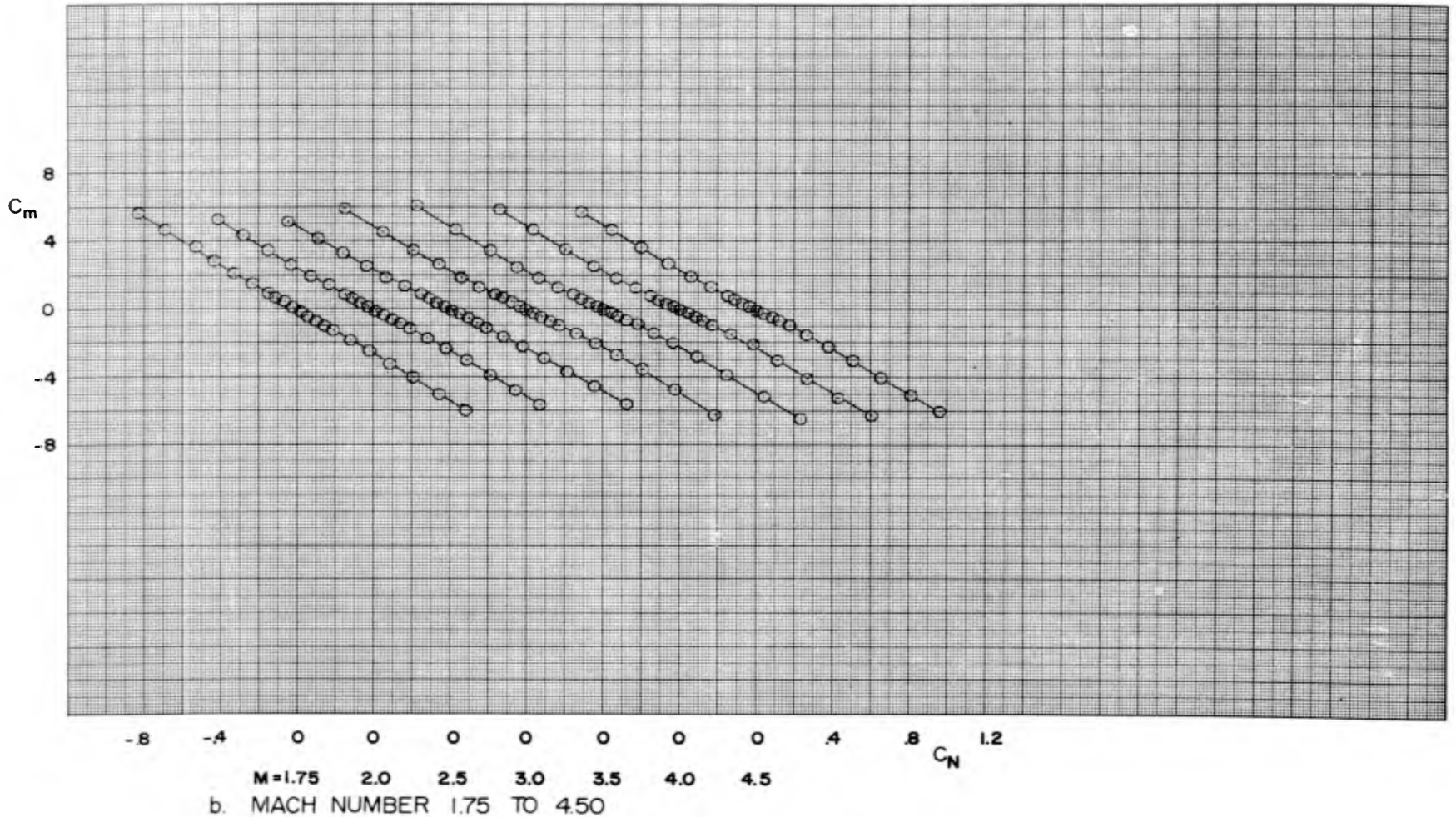

b. MACH NUMBER 1.75 TO 4.50

FIGURE 22 CONCLUDED

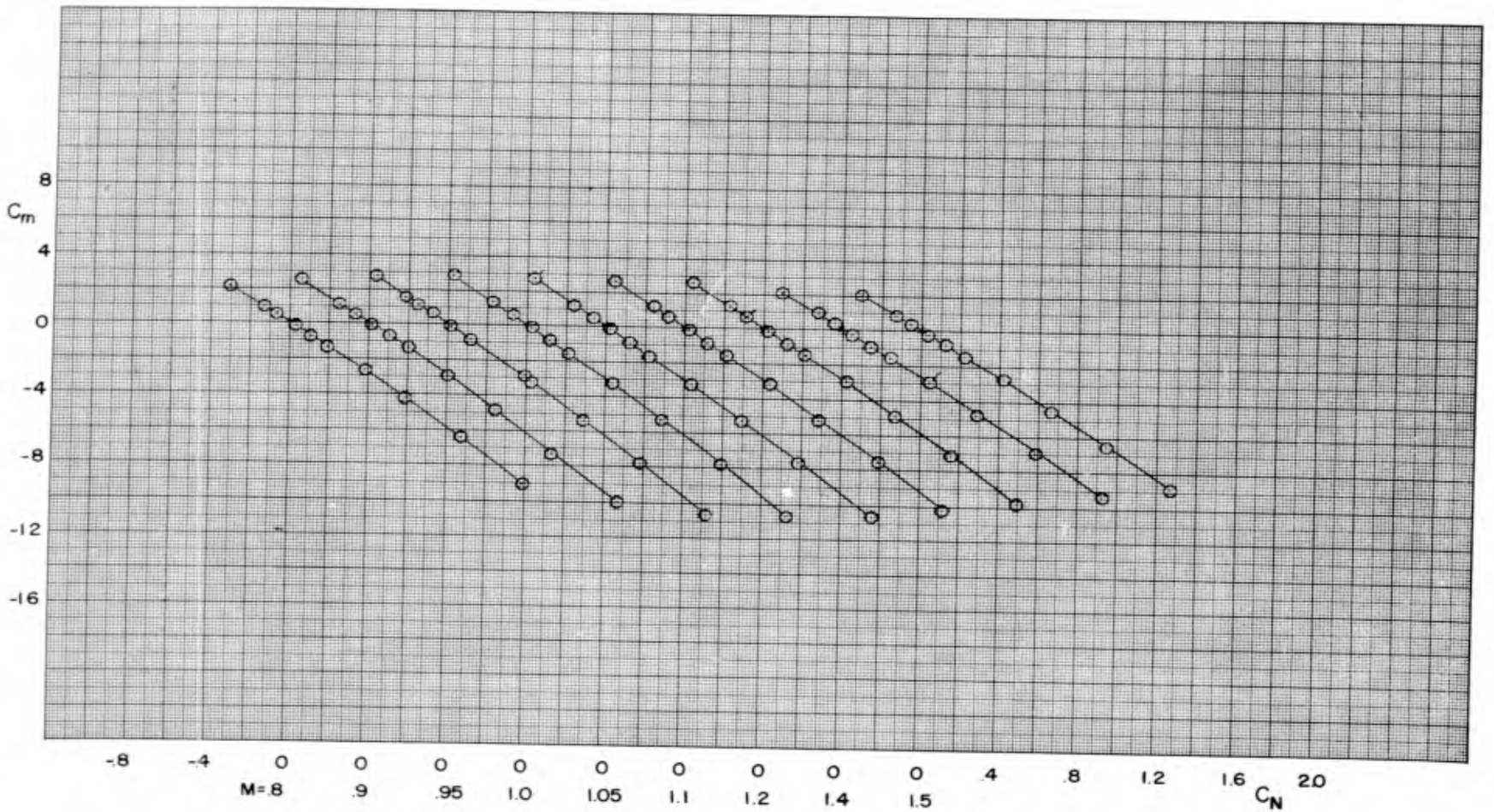

a. MACH NUMBER 0.80 TO 1.50

FIGURE 23 PITCHING-MOMENT COEFFICIENT VERSUS NORMAL-FORCE COEFFICIENT FOR CONFIGURATION BF_4D

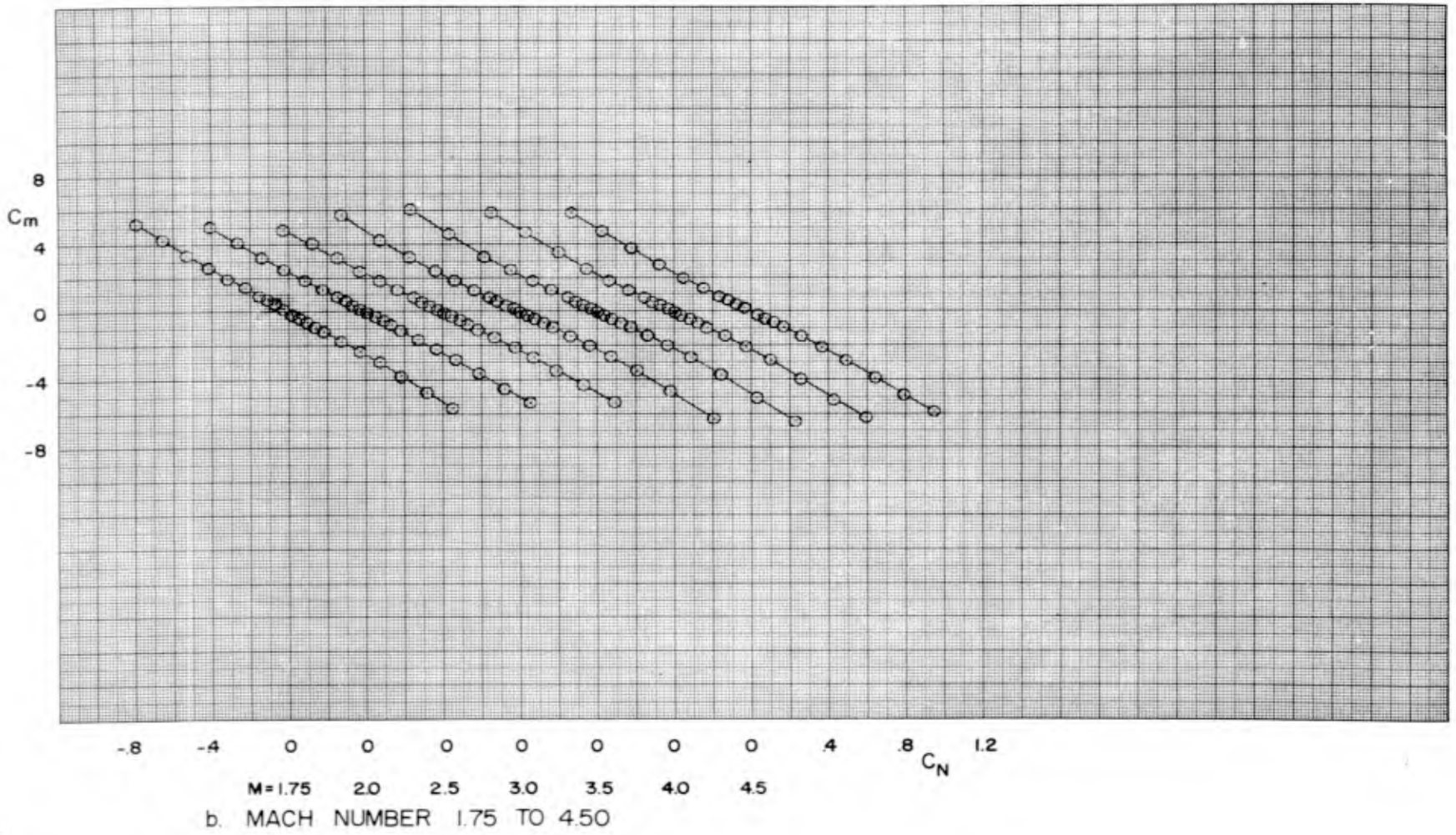

b. MACH NUMBER 1.75 TO 4.50

FIGURE 23 CONCLUDED

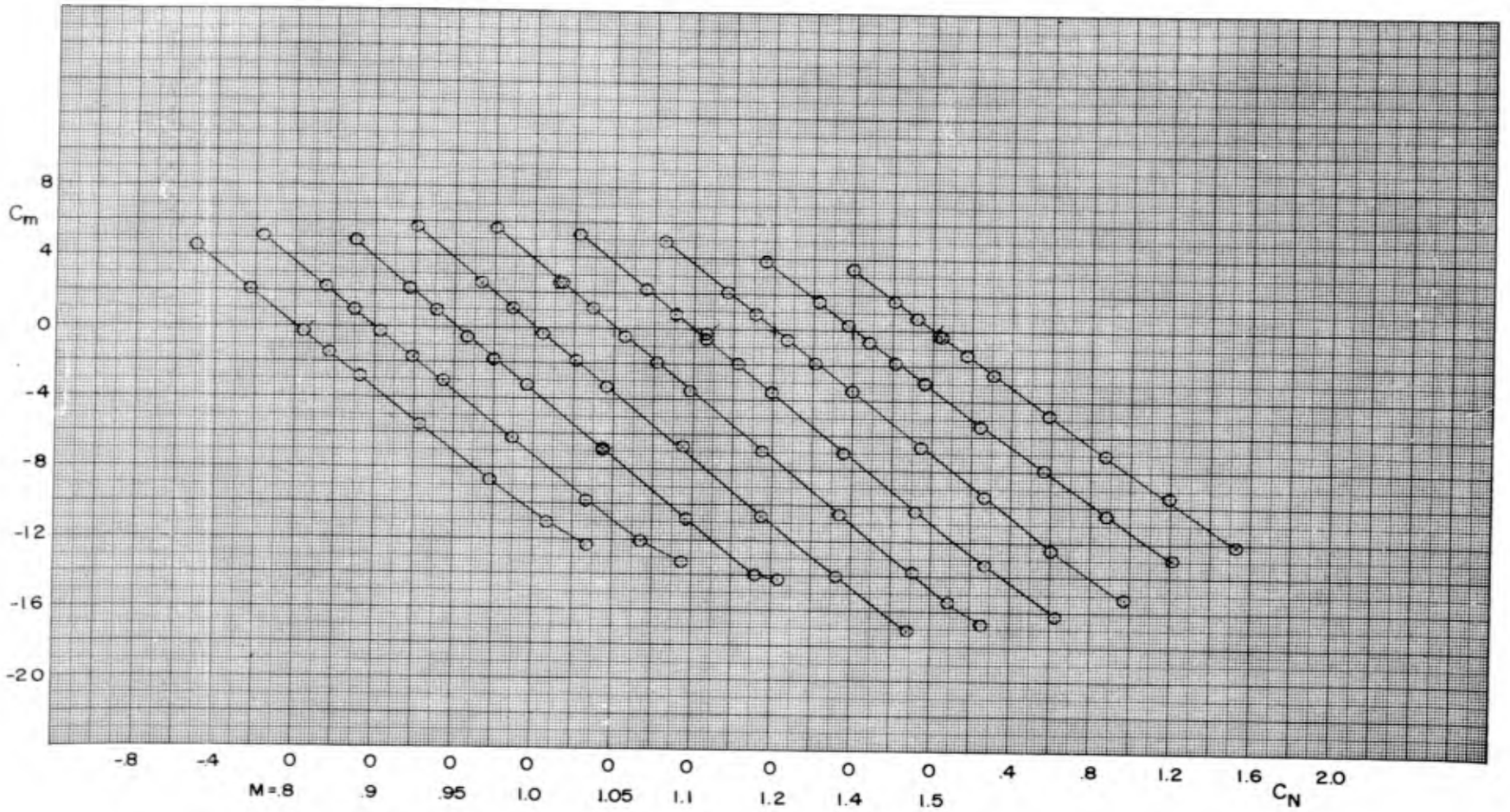

a. MACH NUMBER 0.80 TO 1.50

FIGURE 24 PITCHING-MOMENT COEFFICIENT VERSUS NORMAL-FORCE COEFFICIENT FOR CONFIGURATION BF_{5A}

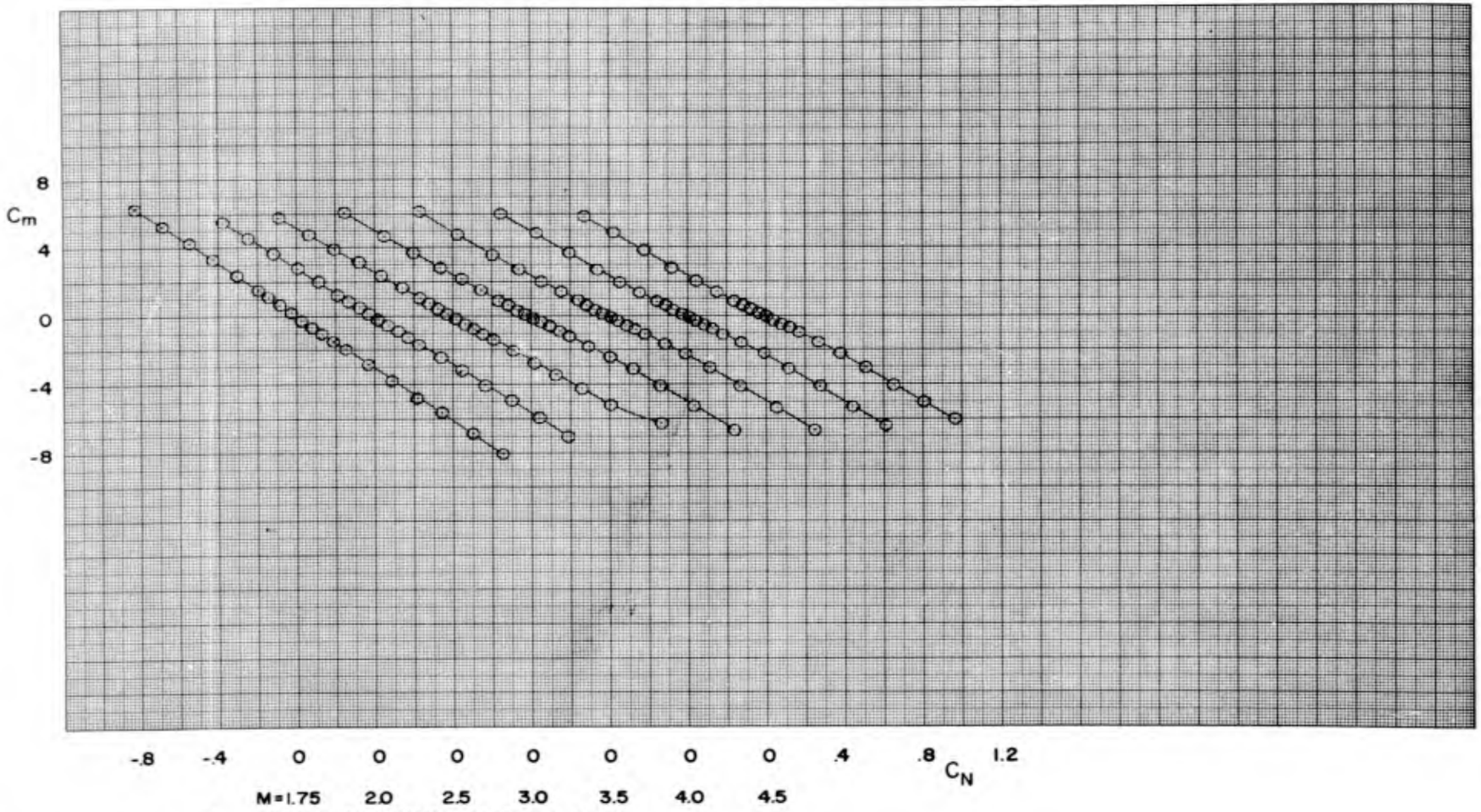

b. MACH NUMBER 1.75 TO 4.50

FIGURE 24 CONCLUDED

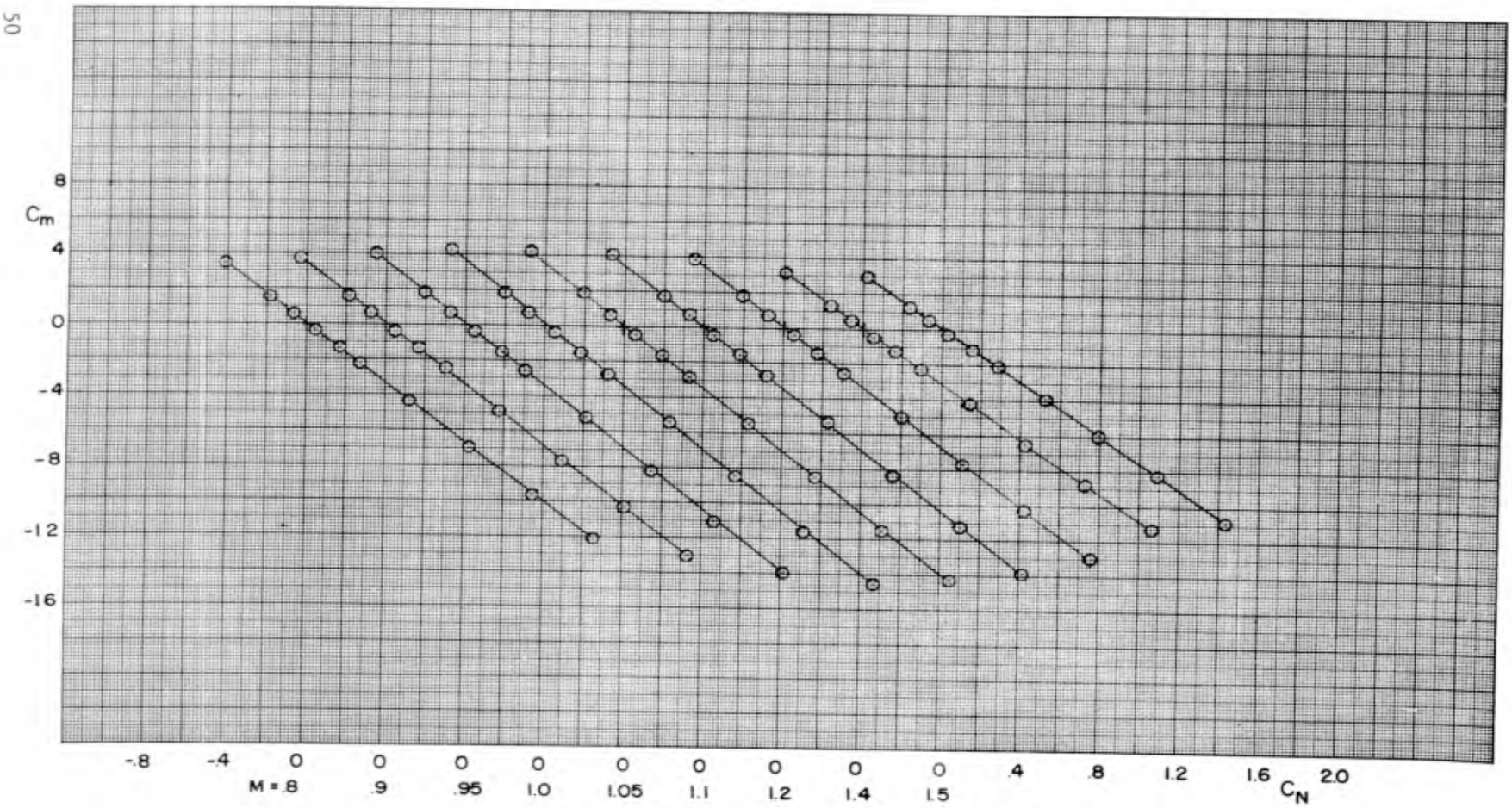

a. MACH NUMBER 0.80 TO 1.50

FIGURE 25 PITCHING-MOMENT COEFFICIENT VERSUS NORMAL-FORCE COEFFICIENT FOR CONFIGURATION BF_{5B}

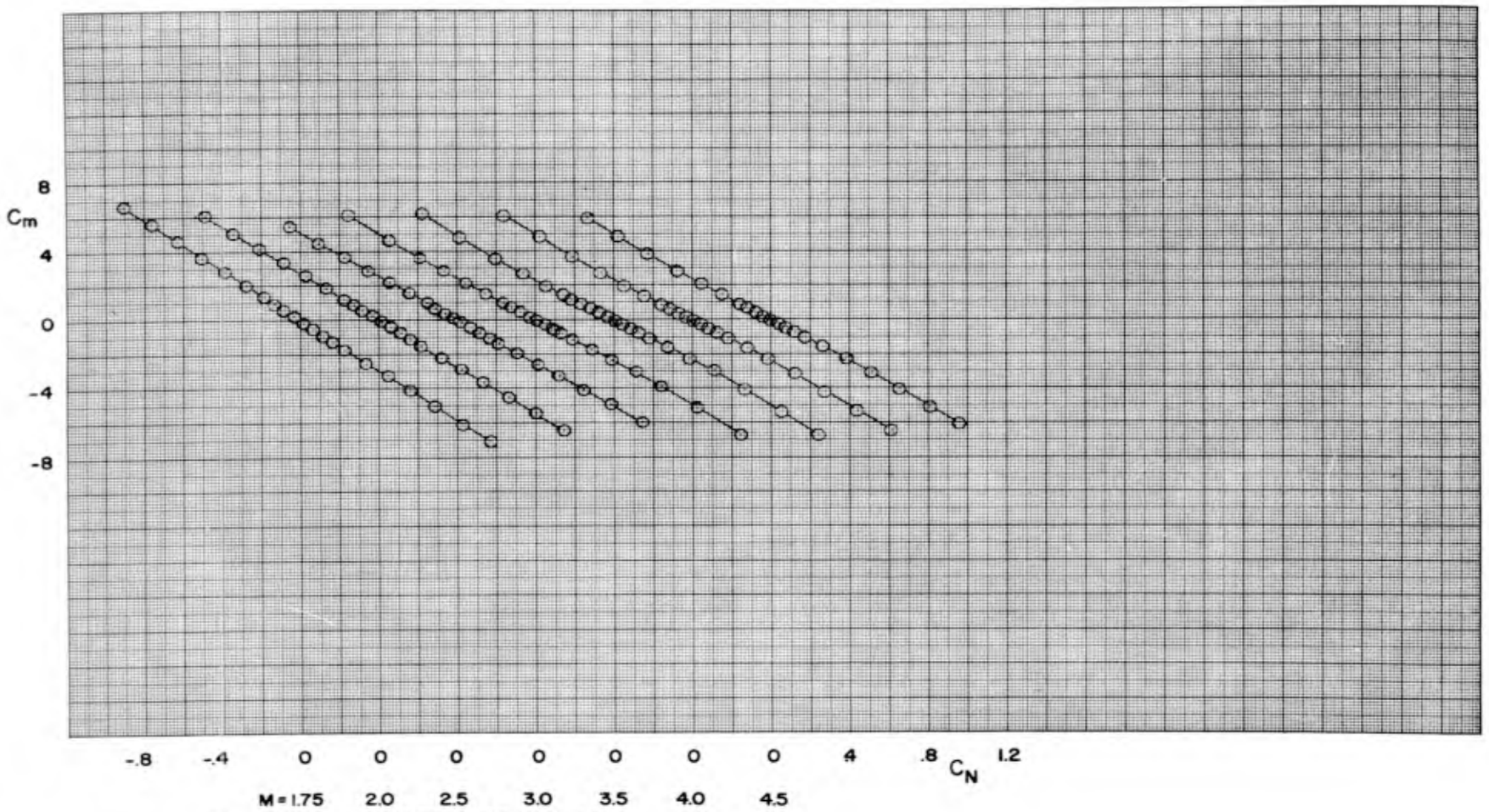

b. MACH NUMBER 1.75 TO 4.50

FIGURE 25 CONCLUDED

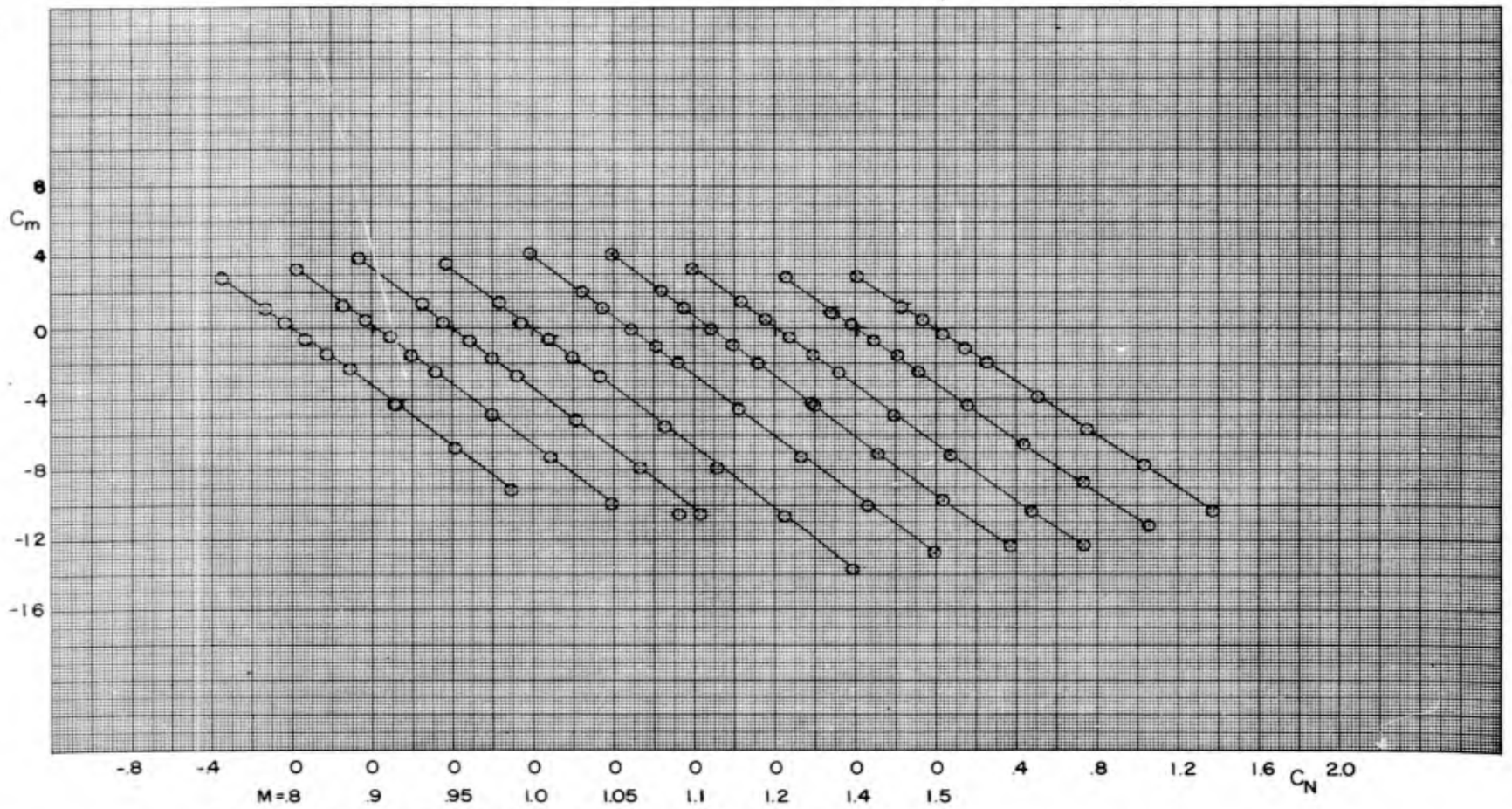

a. MACH NUMBER 0.80 TO 1.50

FIGURE 26 PITCHING-MOMENT COEFFICIENT VERSUS NORMAL-FORCE COEFFICIENT FOR CONFIGURATION BF_{5C}

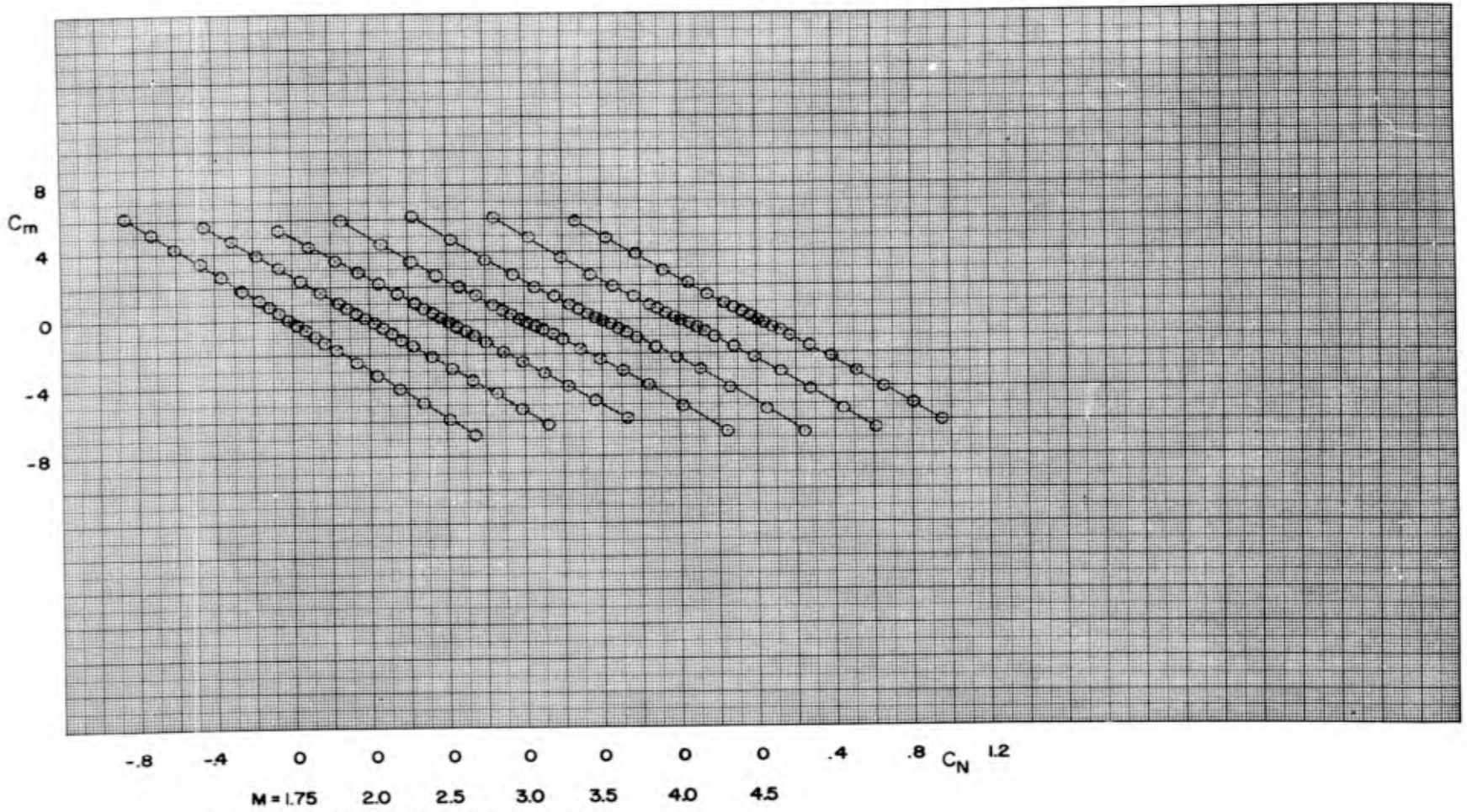

b. MACH NUMBER 1.75 TO 4.50

FIGURE 26 CONCLUDED

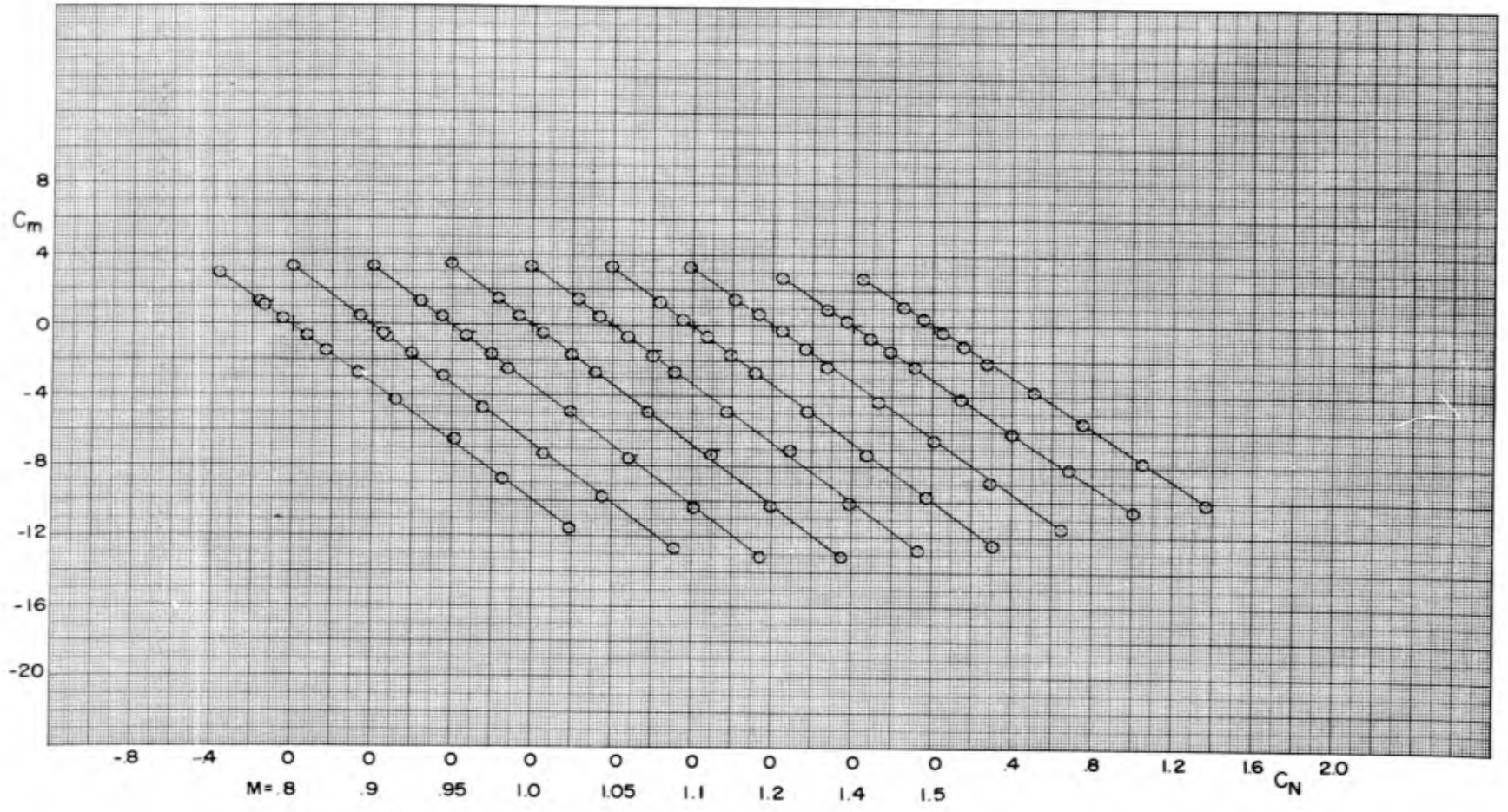

a. MACH NUMBER 0.80 TO 1.50

FIGURE 27 PITCHING-MOMENT COEFFICIENT VERSUS NORMAL-FORCE COEFFICIENT FOR CONFIGURATION BF_{5D}

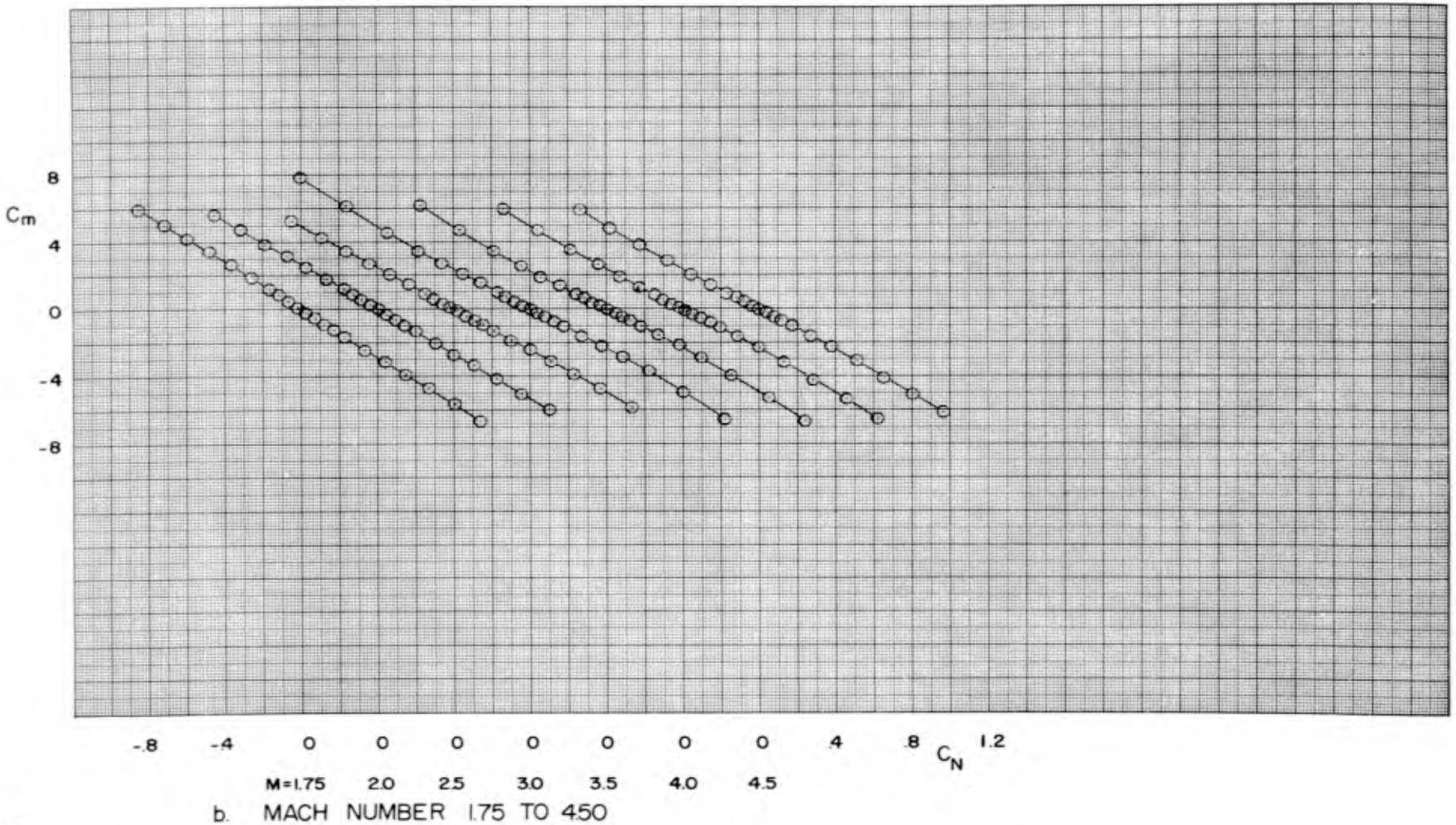

b. MACH NUMBER 1.75 TO 4.50

FIGURE 27 CONCLUDED

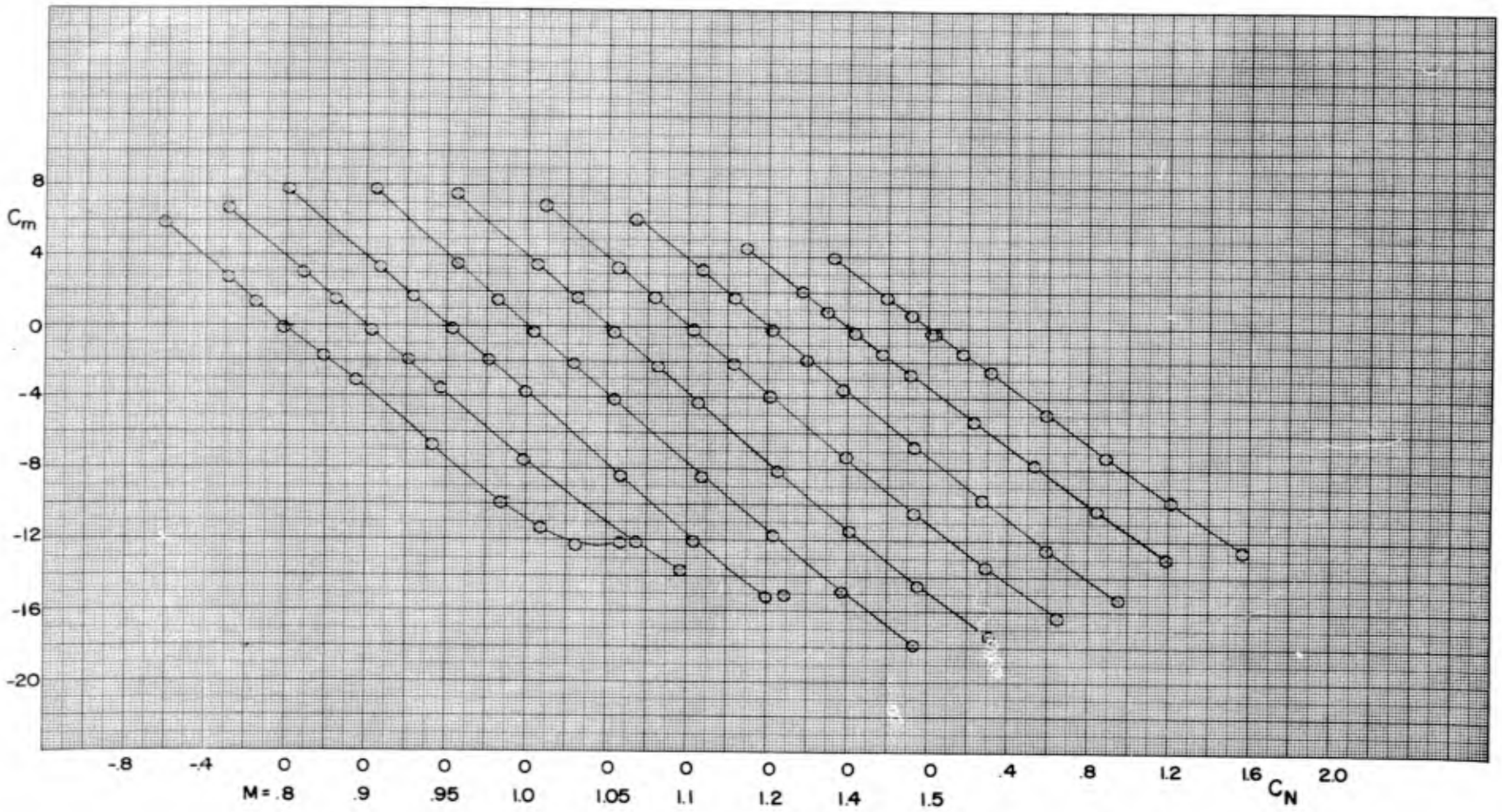

a. MACH NUMBER 0.80 TO 1.50

FIGURE 28 PITCHING-MOMENT COEFFICIENT VERSUS NORMAL-FORCE COEFFICIENT FOR CONFIGURATION BF_{6A}

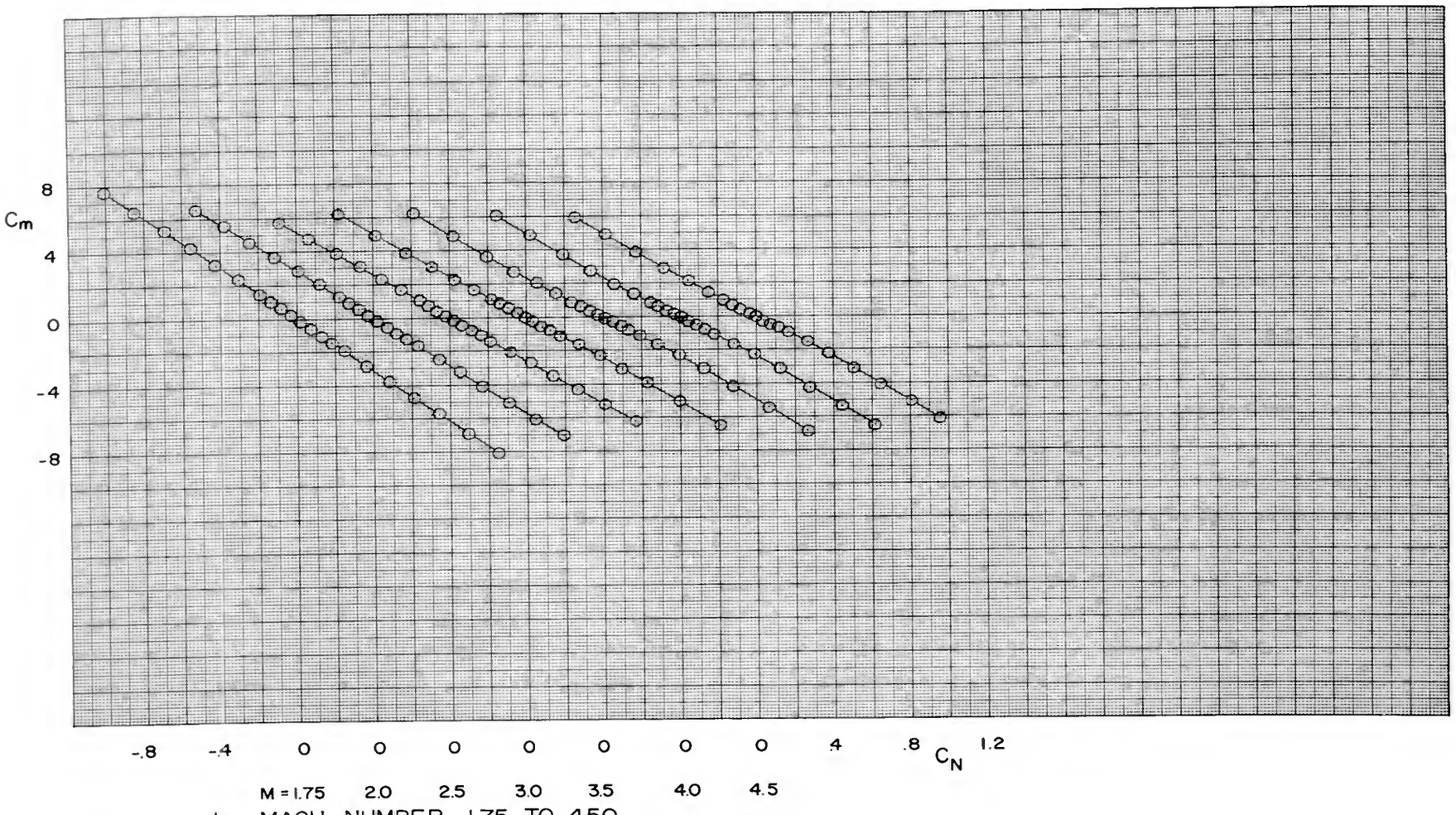

b. MACH NUMBER 1.75 TO 4.50

FIGURE 28 CONCLUDED

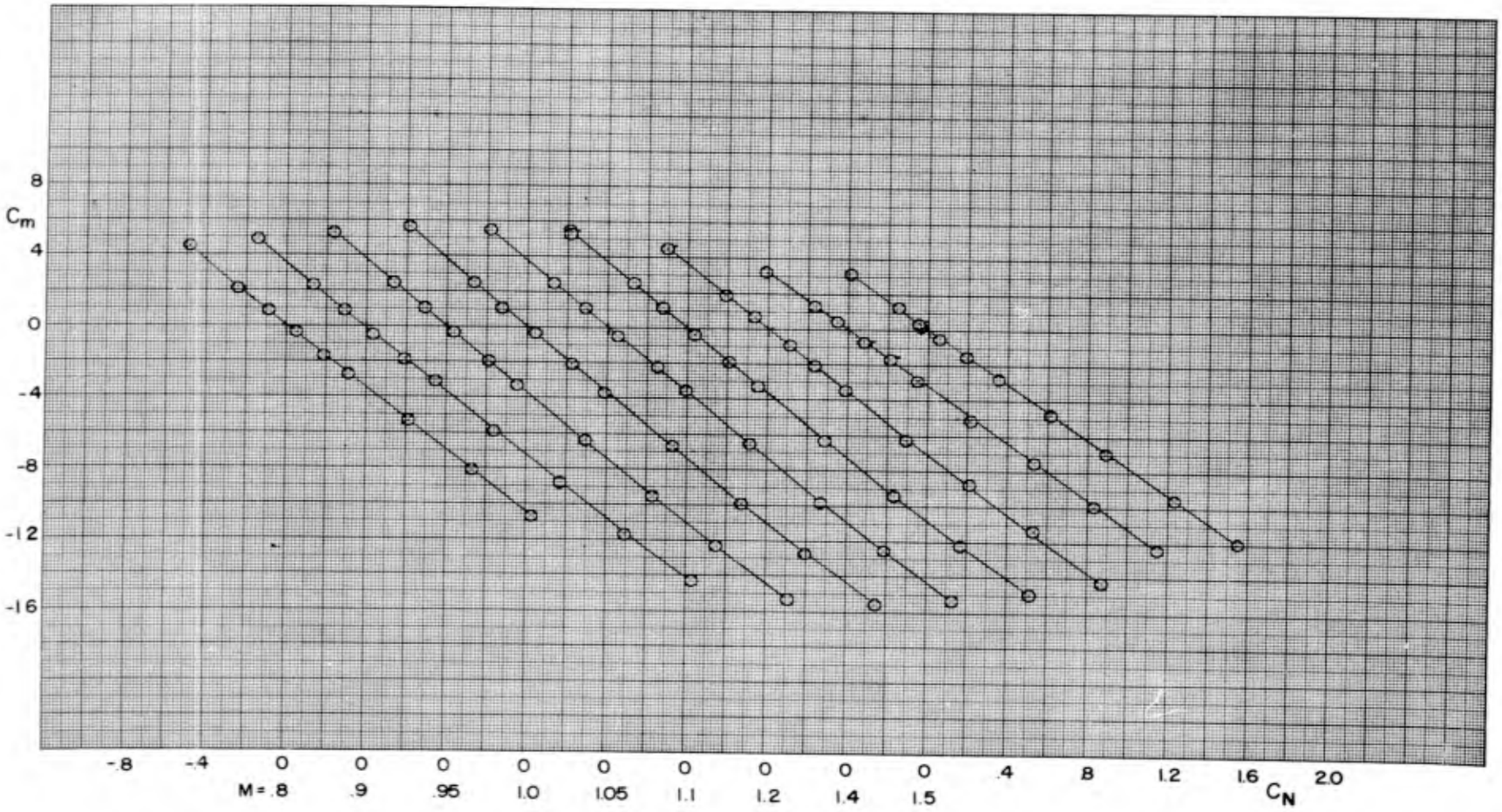

a. MACH NUMBER 0.80 TO 1.50

FIGURE 29 PITCHING-MOMENT COEFFICIENT VERSUS NORMAL-FORCE COEFFICIENT FOR CONFIGURATION BF_{6B}

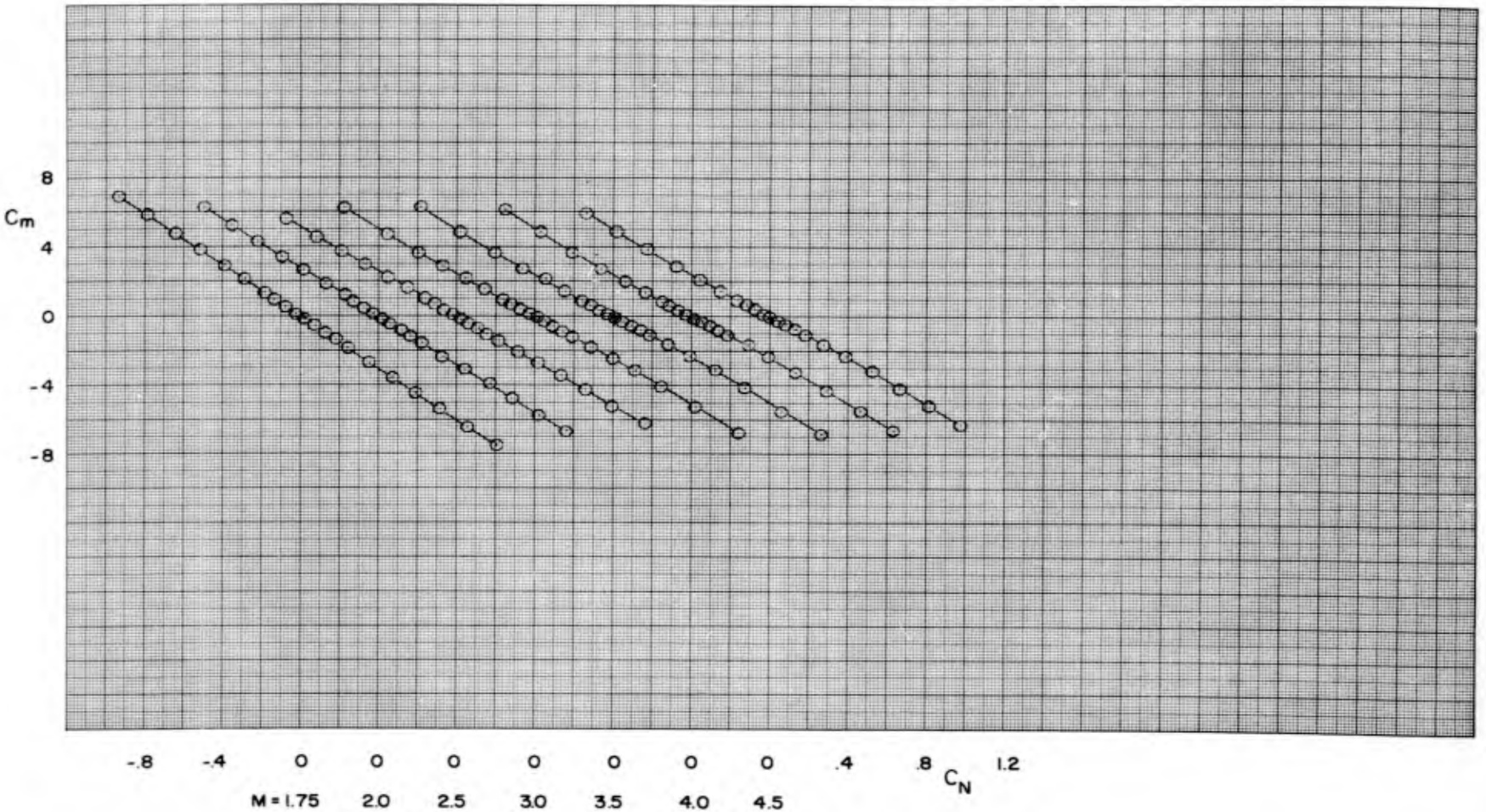

b. MACH NUMBER 1.75 TO 4.50

FIGURE 29 CONCLUDED

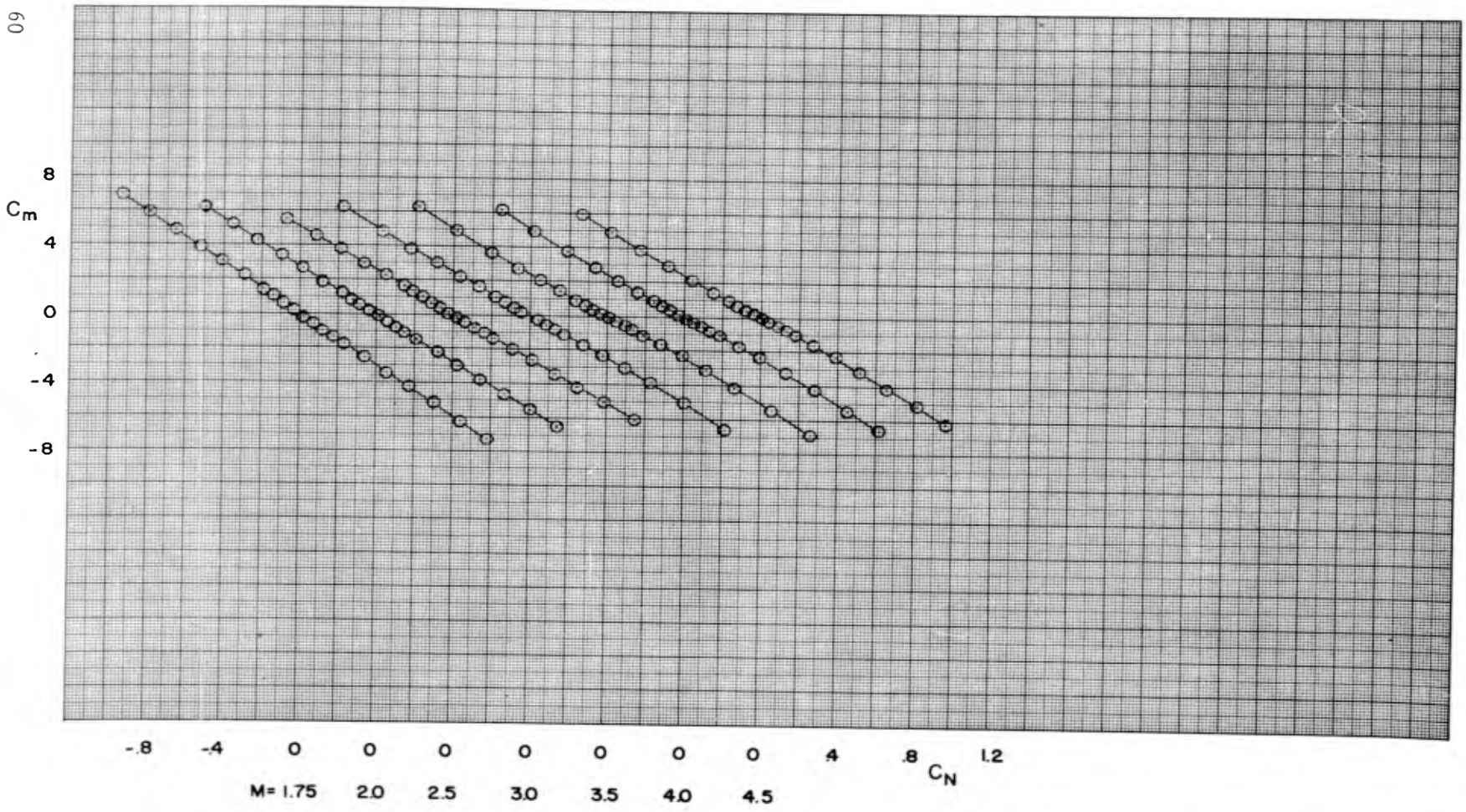

FIGURE 30 PITCHING-MOMENT COEFFICIENT VERSUS NORMAL-FORCE COEFFICIENT FOR CONFIGURATION BF_{6C}

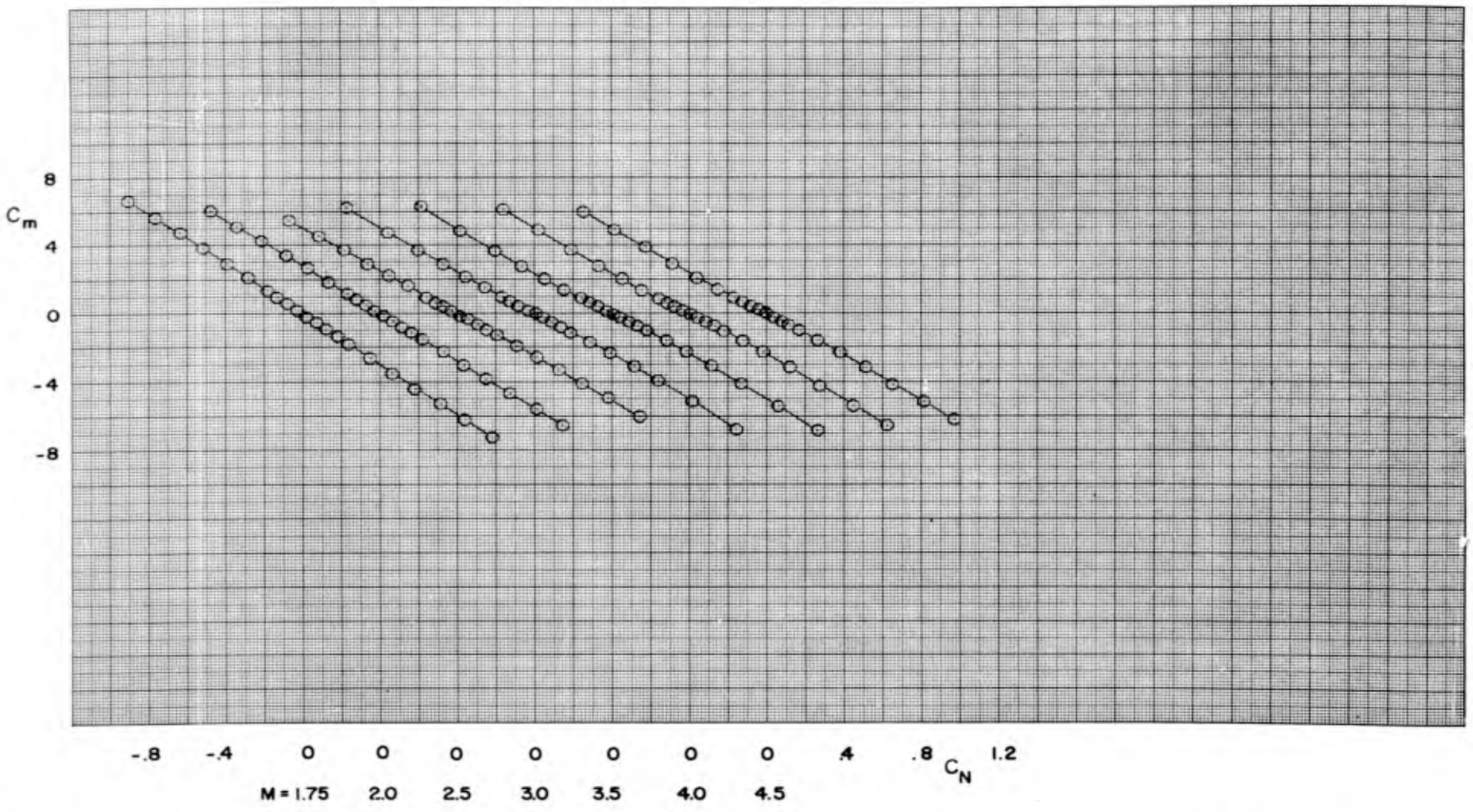

FIGURE 31 PITCHING-MOMENT COEFFICIENT VERSUS NORMAL-FORCE COEFFICIENT FOR CONFIGURATION BF_{6D}

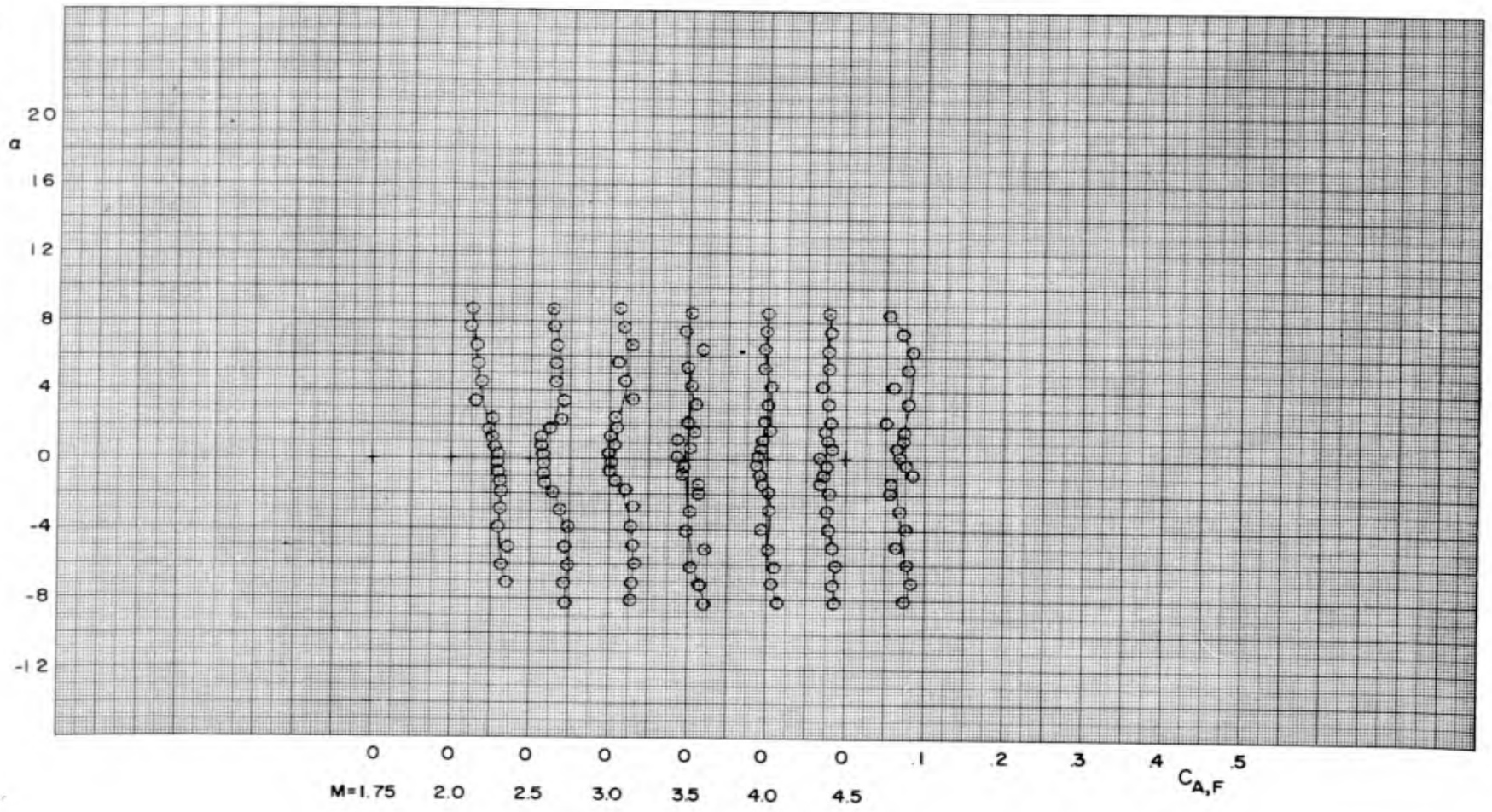

FIGURE 32 ANGLE OF ATTACK VERSUS AXIAL FORCE COEFFICIENT FOR CONFIGURATION B

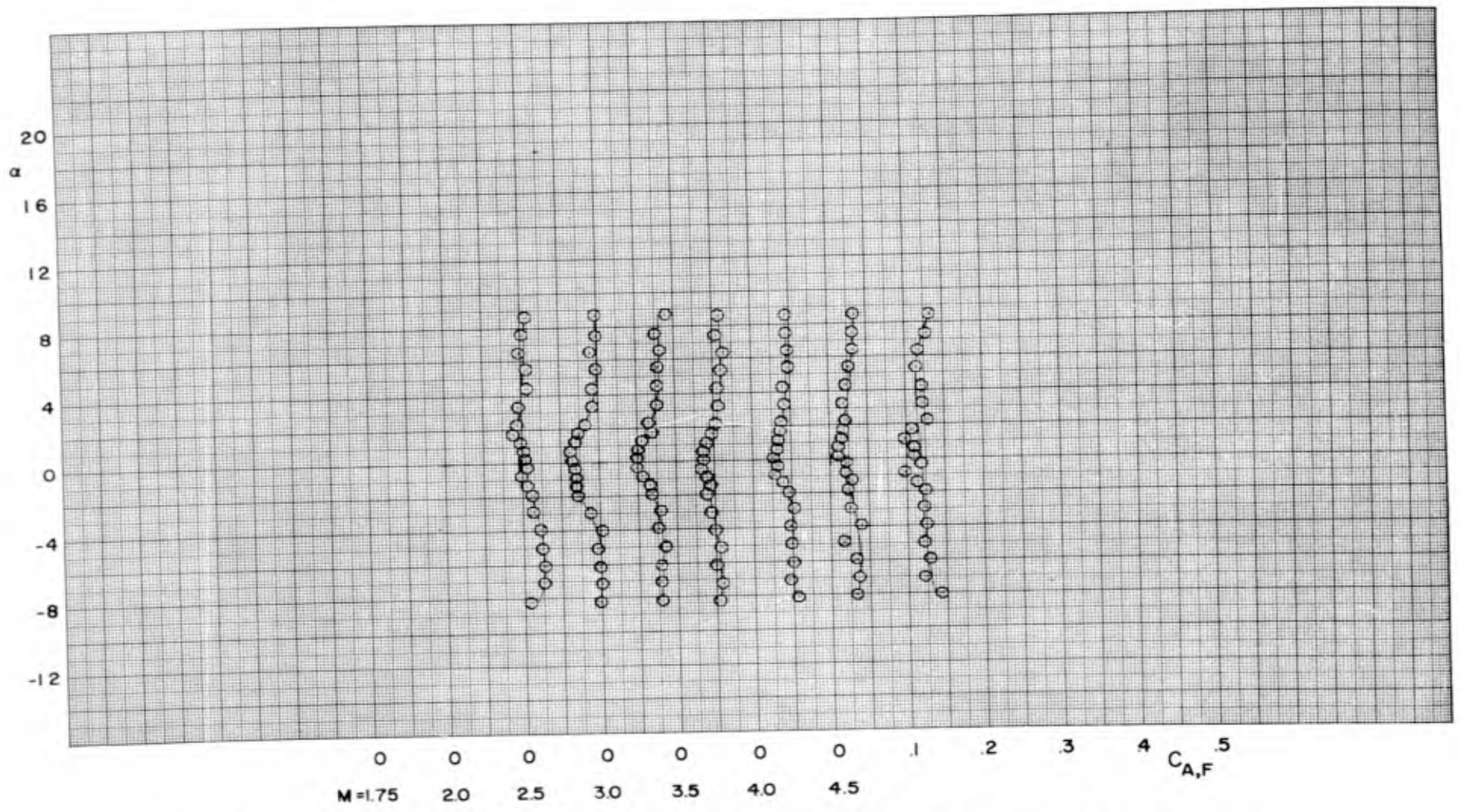

FIGURE 33 ANGLE OF ATTACK VERSUS AXIAL FORCE COEFFICIENT FOR CONFIGURATION BF_{4A}

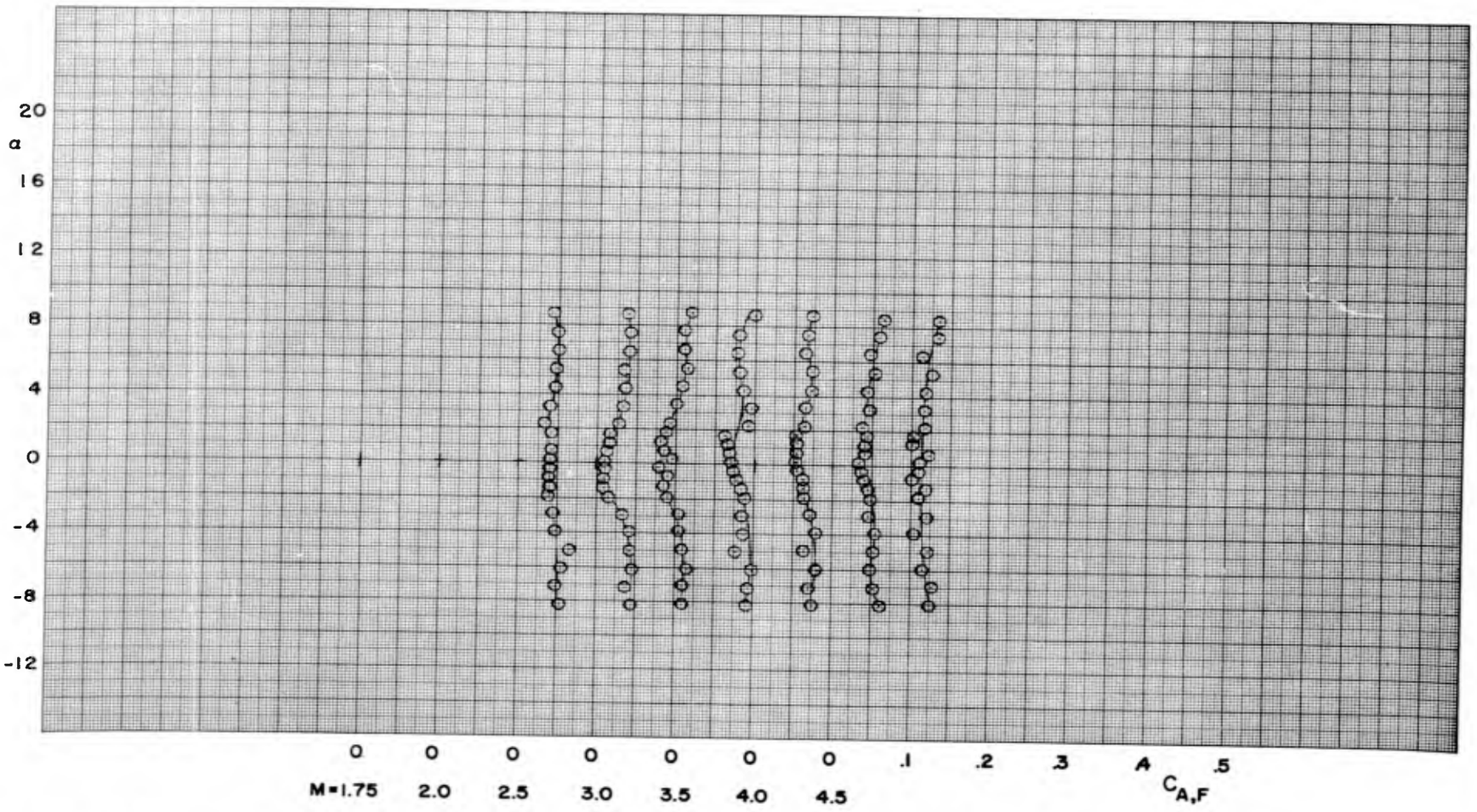

FIGURE 34 ANGLE OF ATTACK VERSUS AXIAL FORCE COEFFICIENT FOR CONFIGURATION BF_{4B}

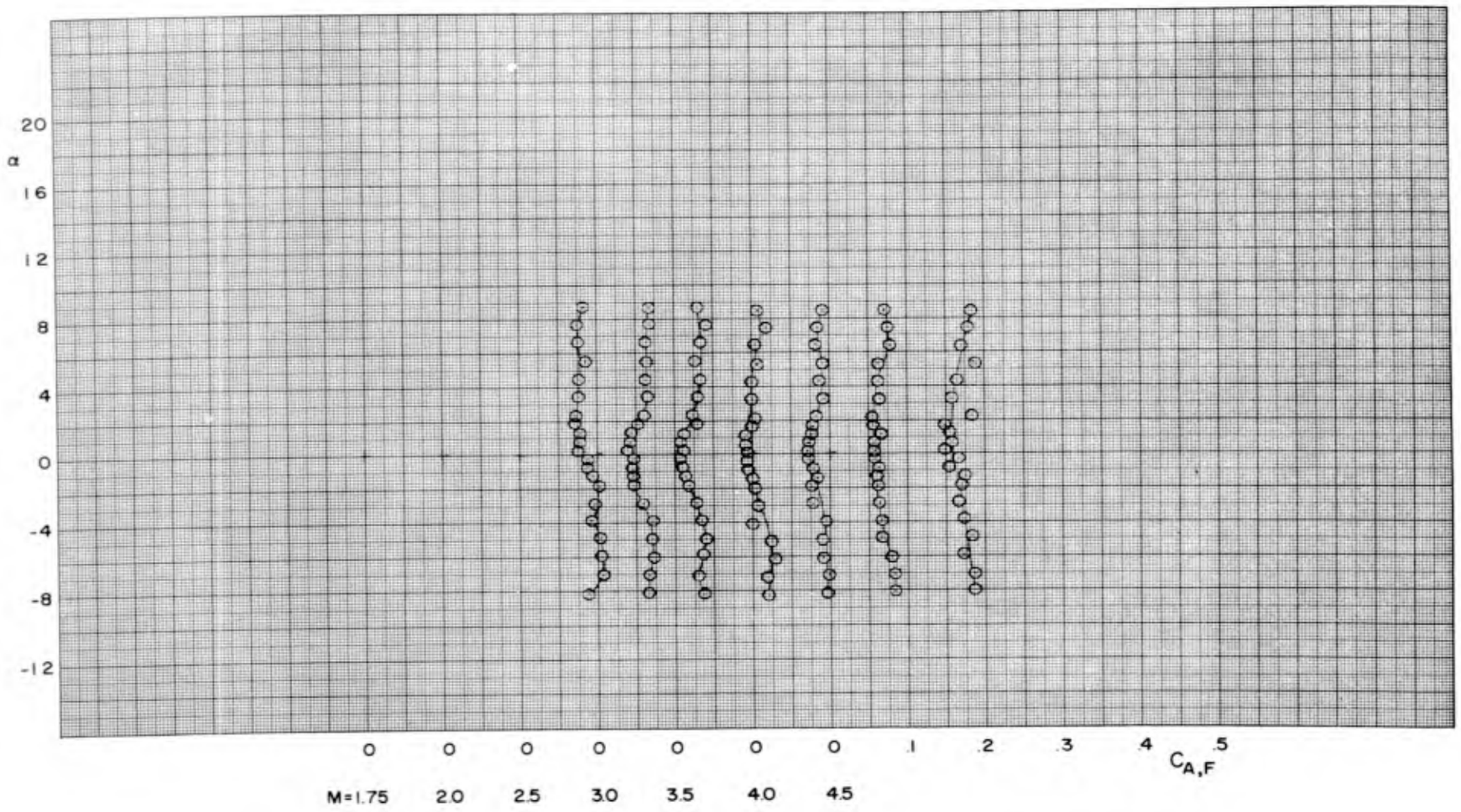

FIGURE 35 ANGLE OF ATTACK VERSUS AXIAL FORCE COEFFICIENT FOR CONFIGURATION BF_{4C}

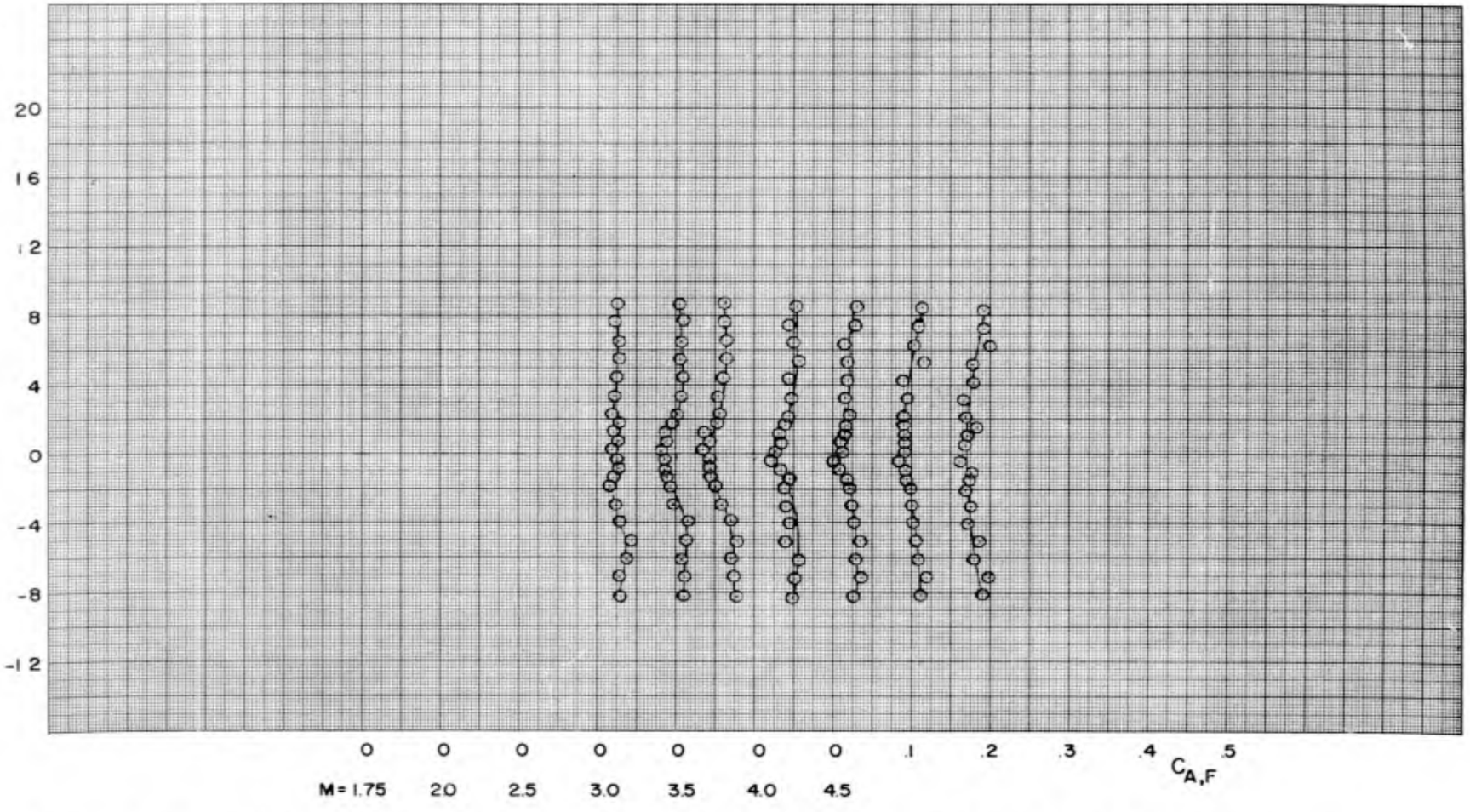

FIGURE 36 ANGLE OF ATTACK VERSUS AXIAL FORCE COEFFICIENT FOR CONFIGURATION BF_{4D}

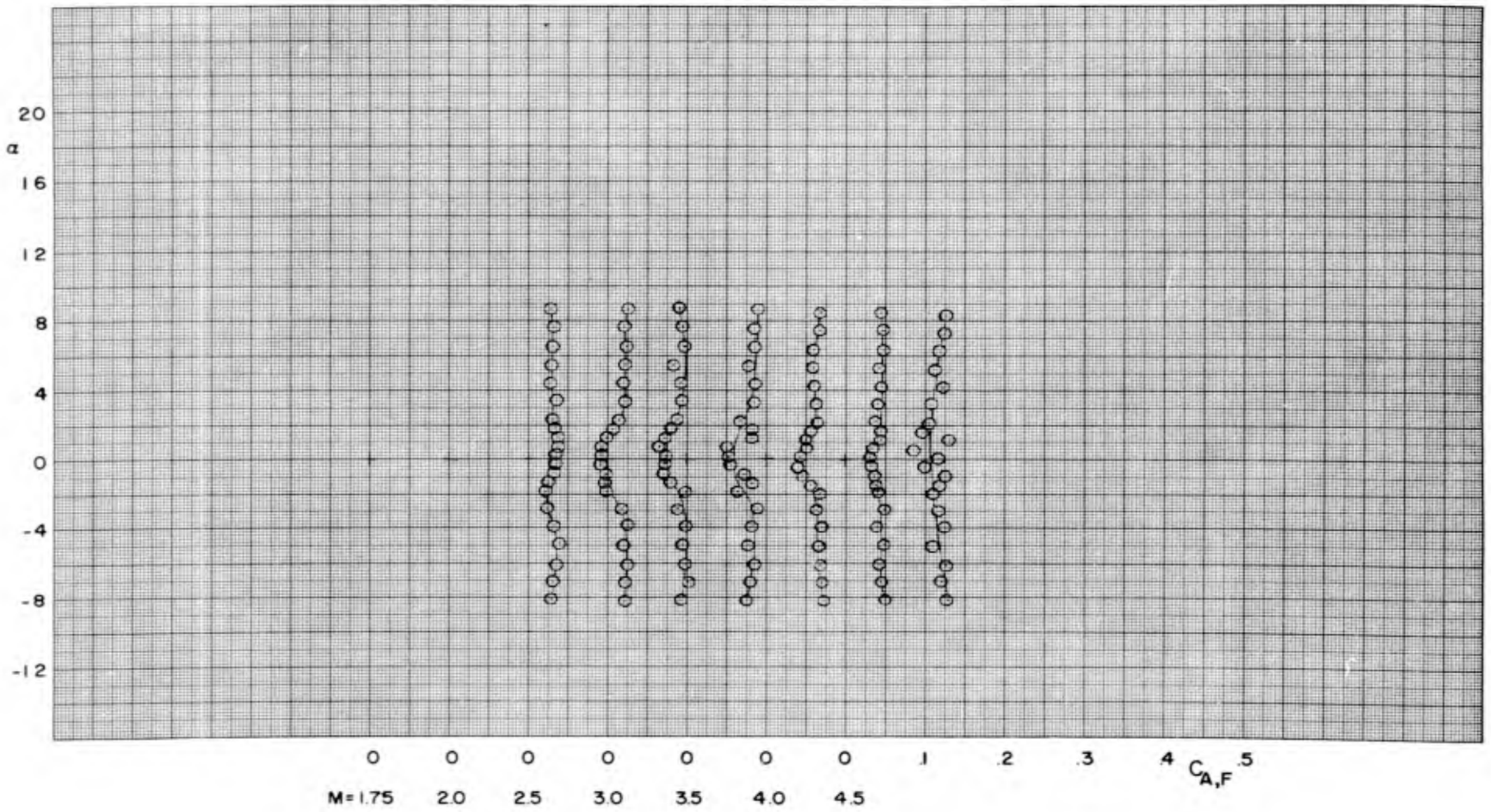

FIGURE 37 ANGLE OF ATTACK VERSUS AXIAL FORCE COEFFICIENT FOR CONFIGURATION BF_{5A}

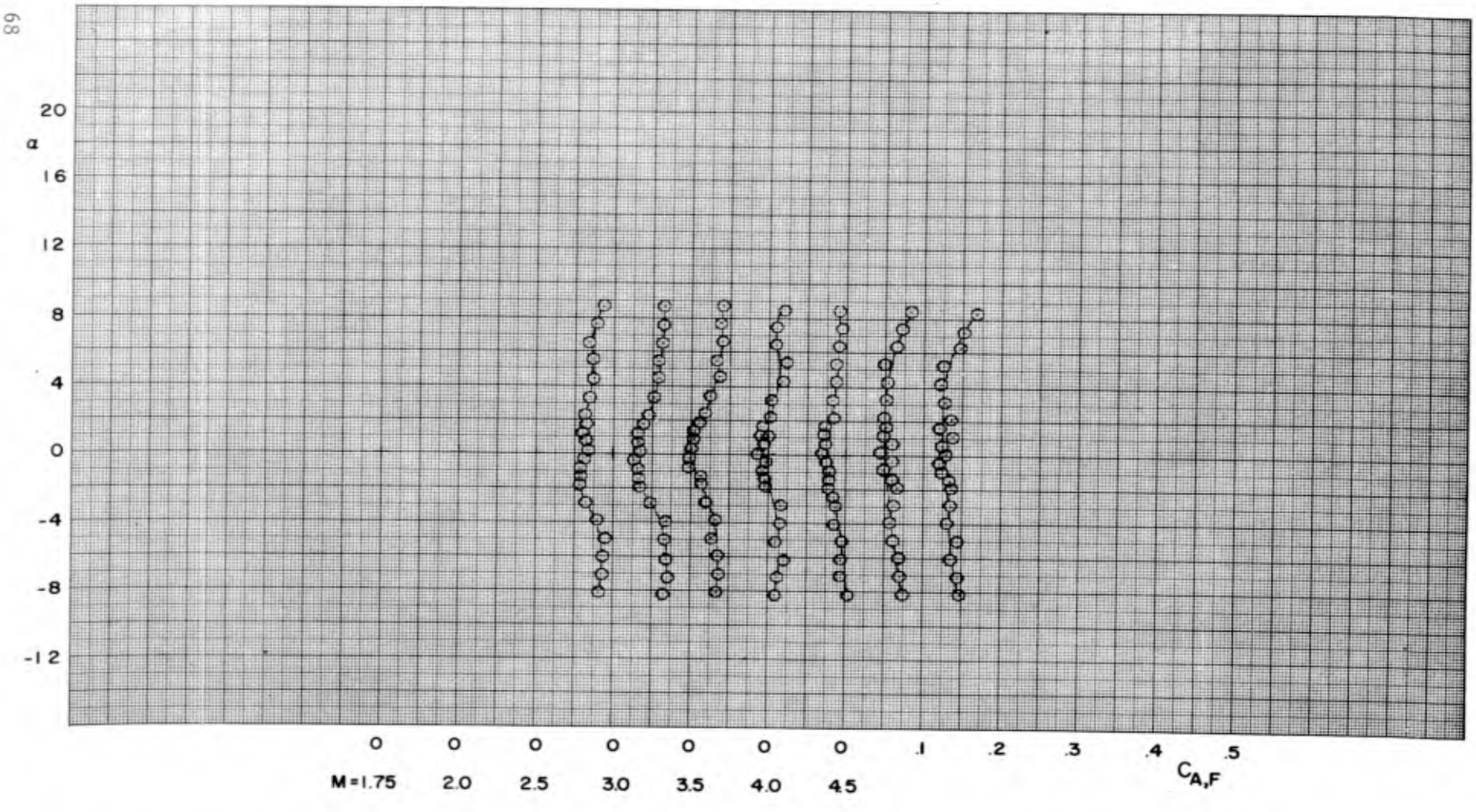

FIGURE 38 ANGLE OF ATTACK VERSUS AXIAL FORCE COEFFICIENT FOR CONFIGURATION BF_{5B}

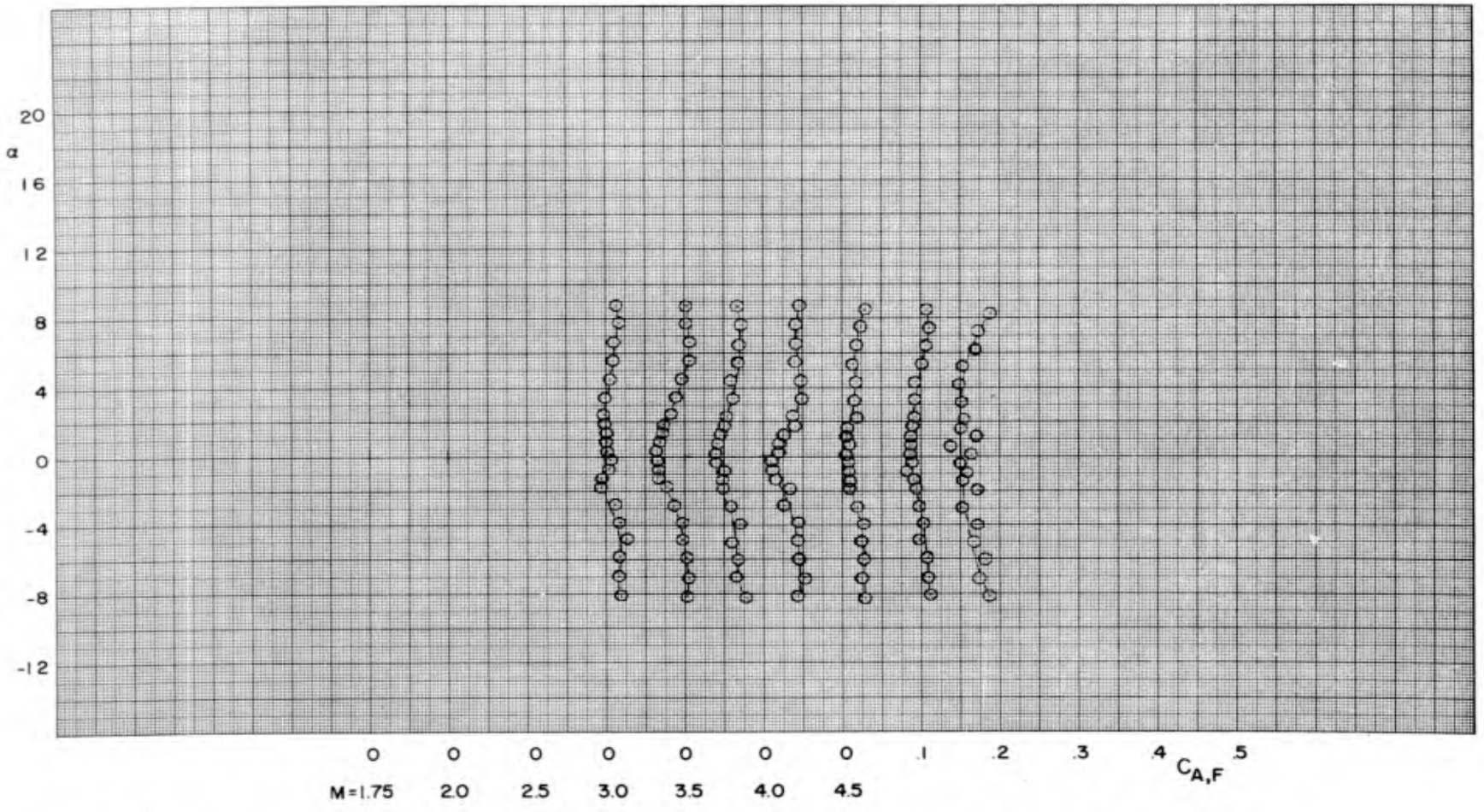

FIGURE 39 ANGLE OF ATTACK VERSUS AXIAL FORCE COEFFICIENT FOR CONFIGURATION BF_{5C}

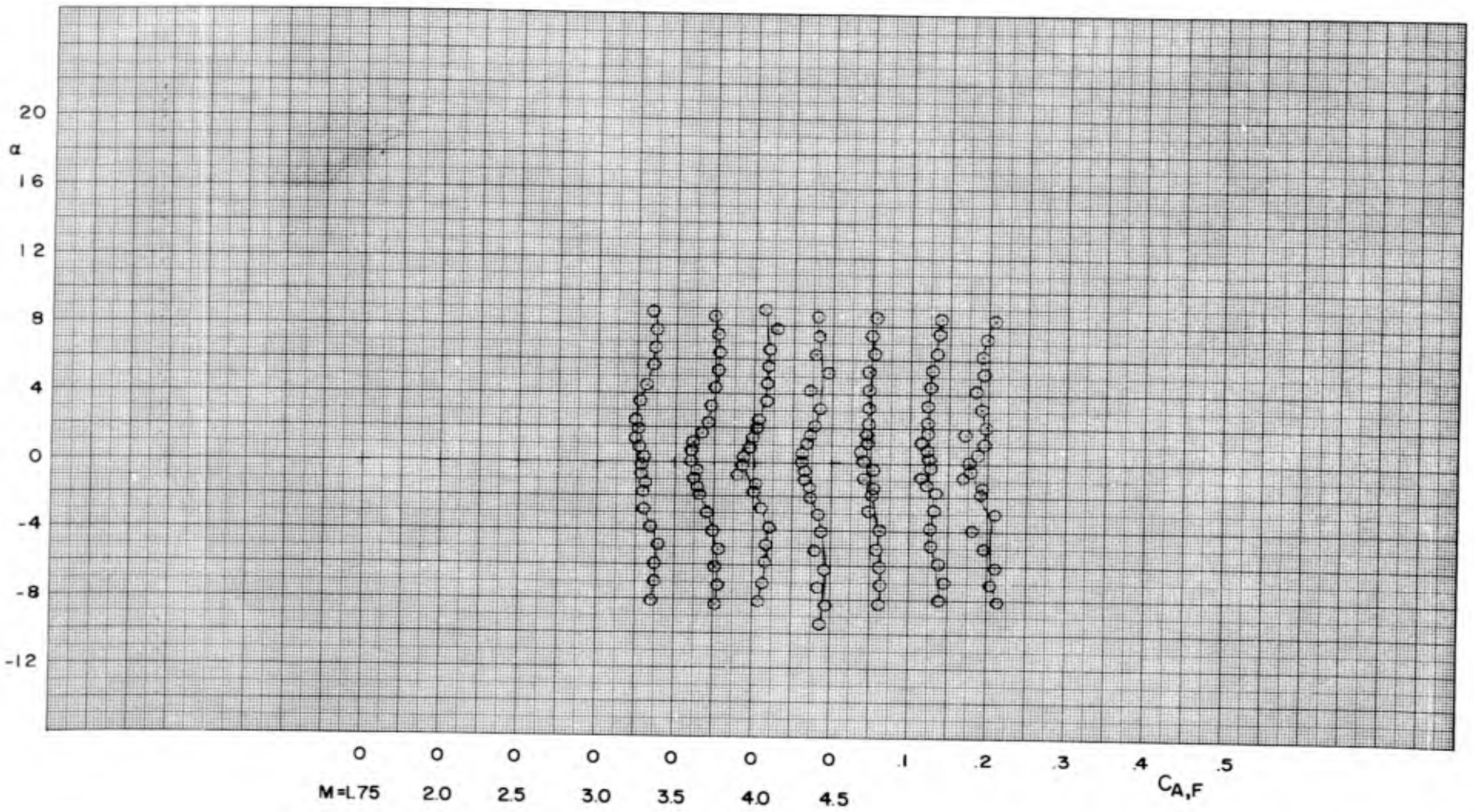

FIGURE 40 ANGLE OF ATTACK VERSUS AXIAL FORCE COEFFICIENT FOR CONFIGURATION BF_{5D}

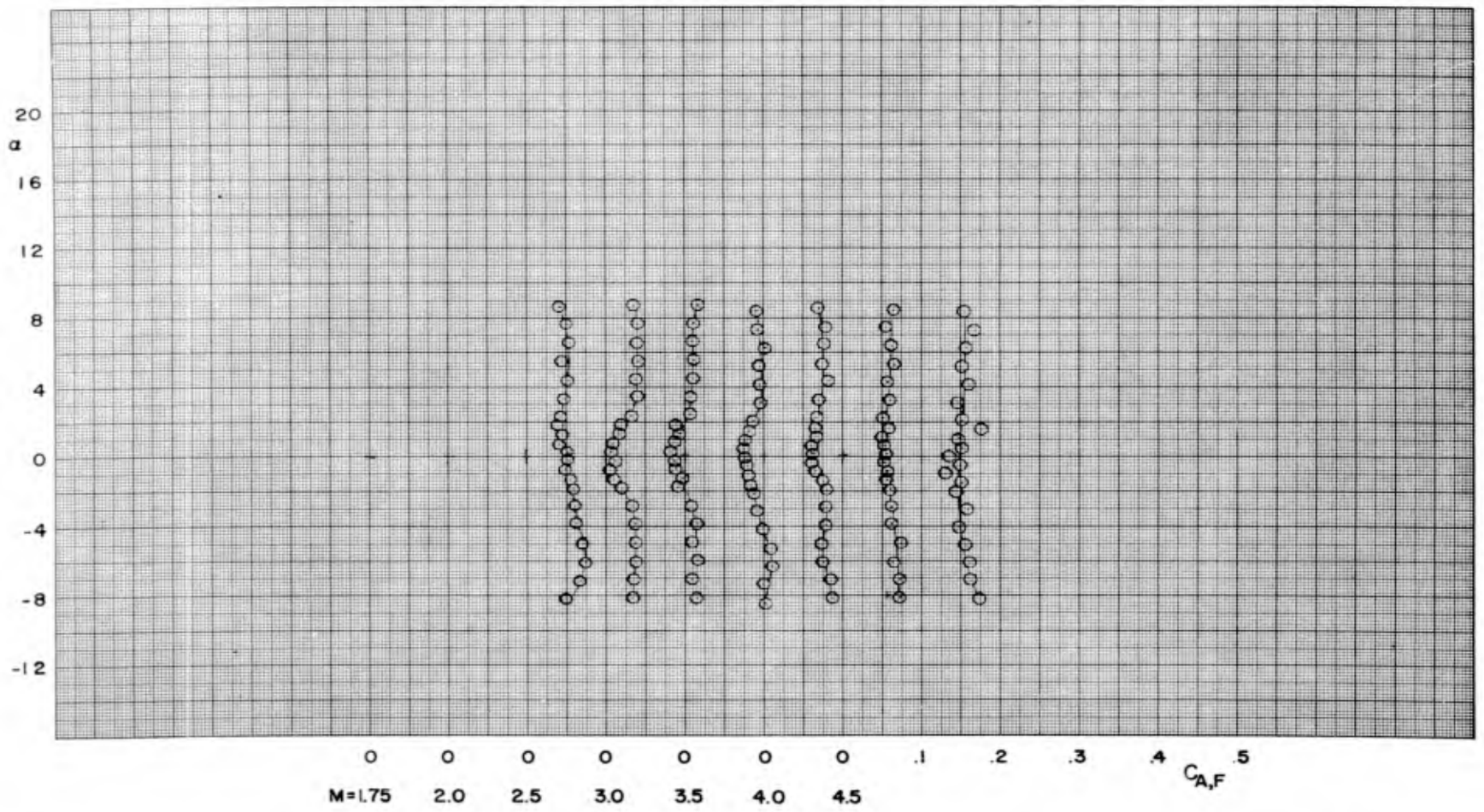

FIGURE 41 ANGLE OF ATTACK VERSUS AXIAL FORCE COEFFICIENT FOR CONFIGURATION BF_{6A}

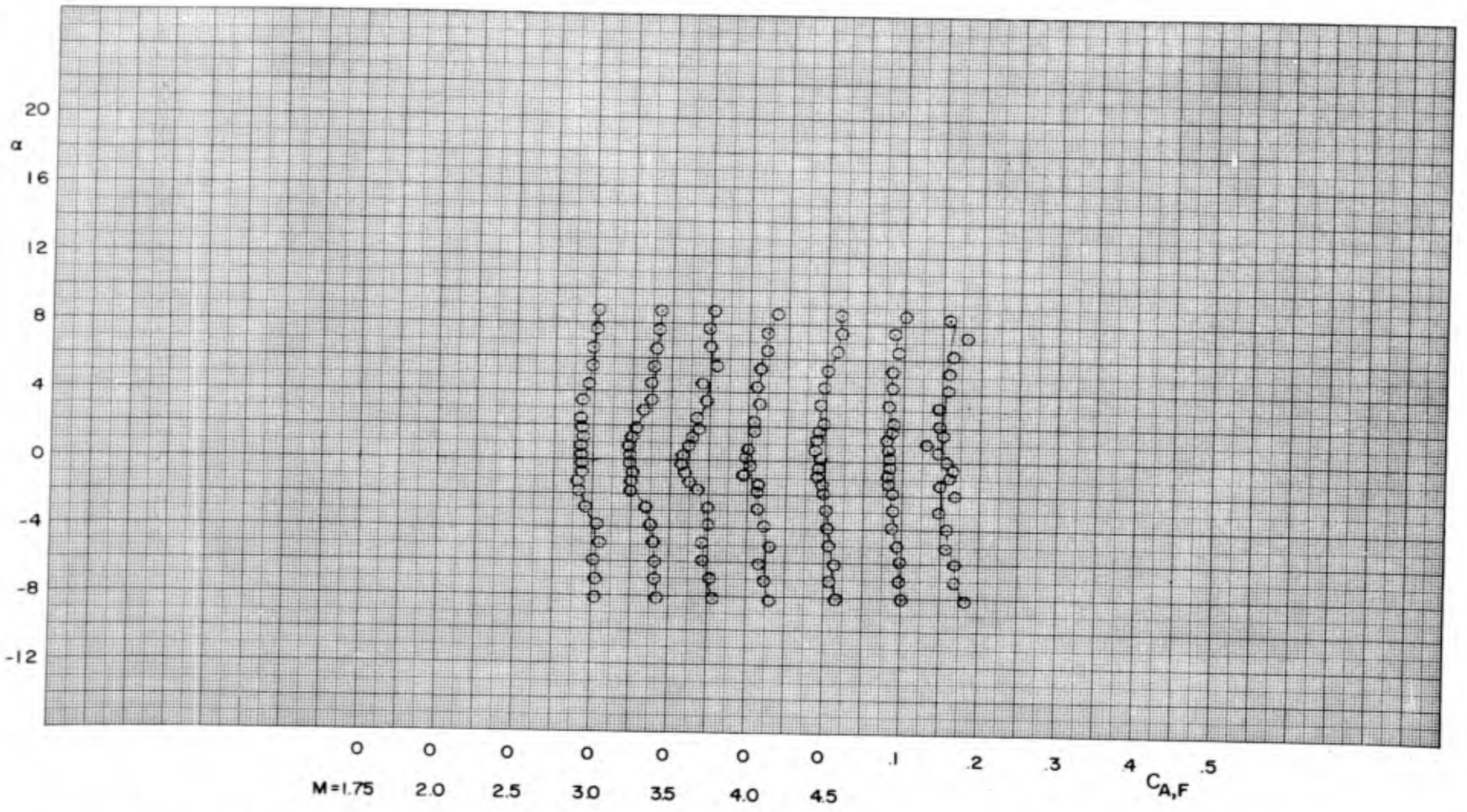

FIGURE 42 ANGLE OF ATTACK VERSUS AXIAL FORCE COEFFICIENT FOR CONFIGURATION BF_{6B}

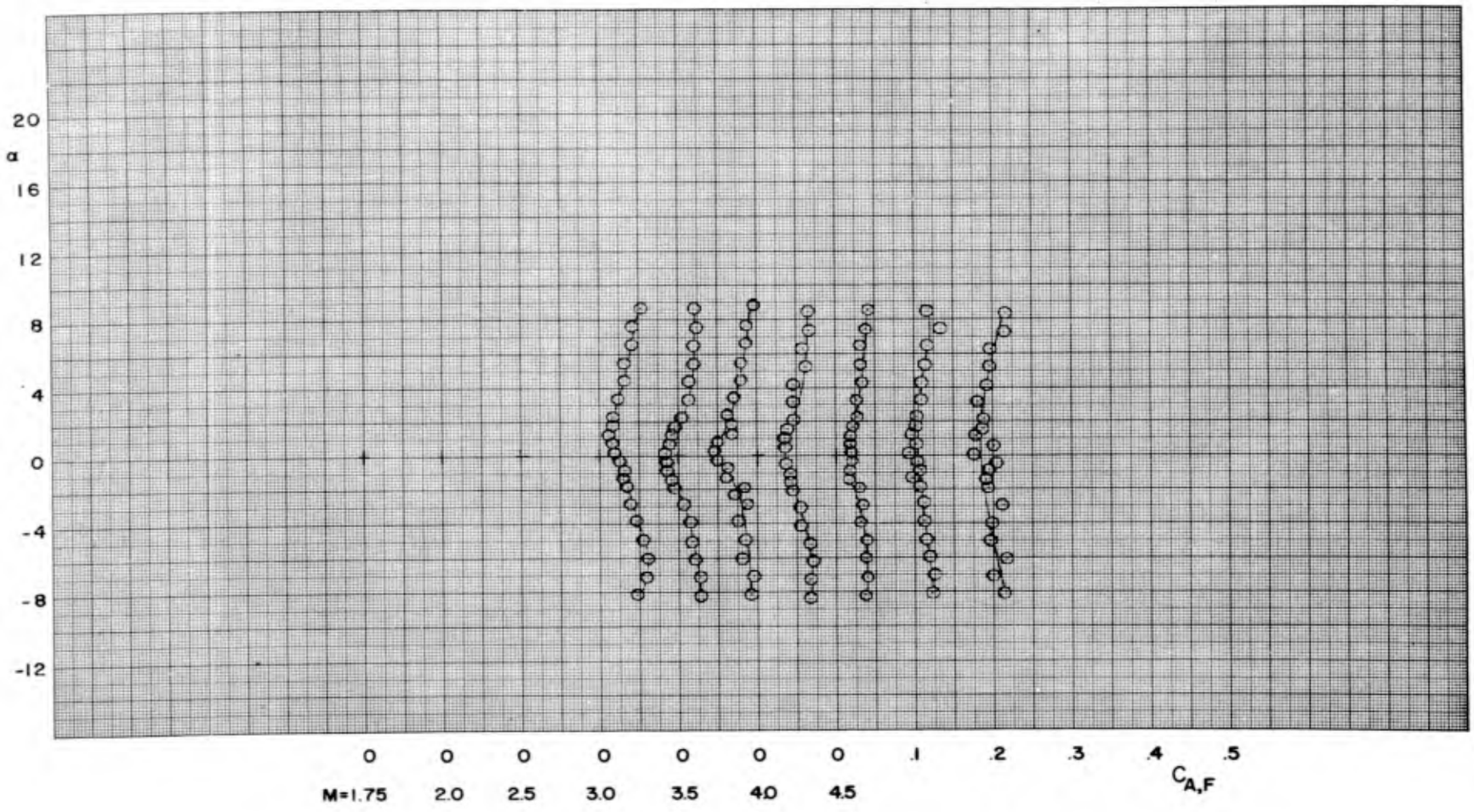

FIGURE 43 ANGLE OF ATTACK VERSUS AXIAL FORCE COEFFICIENT FOR CONFIGURATION BF_{6C}

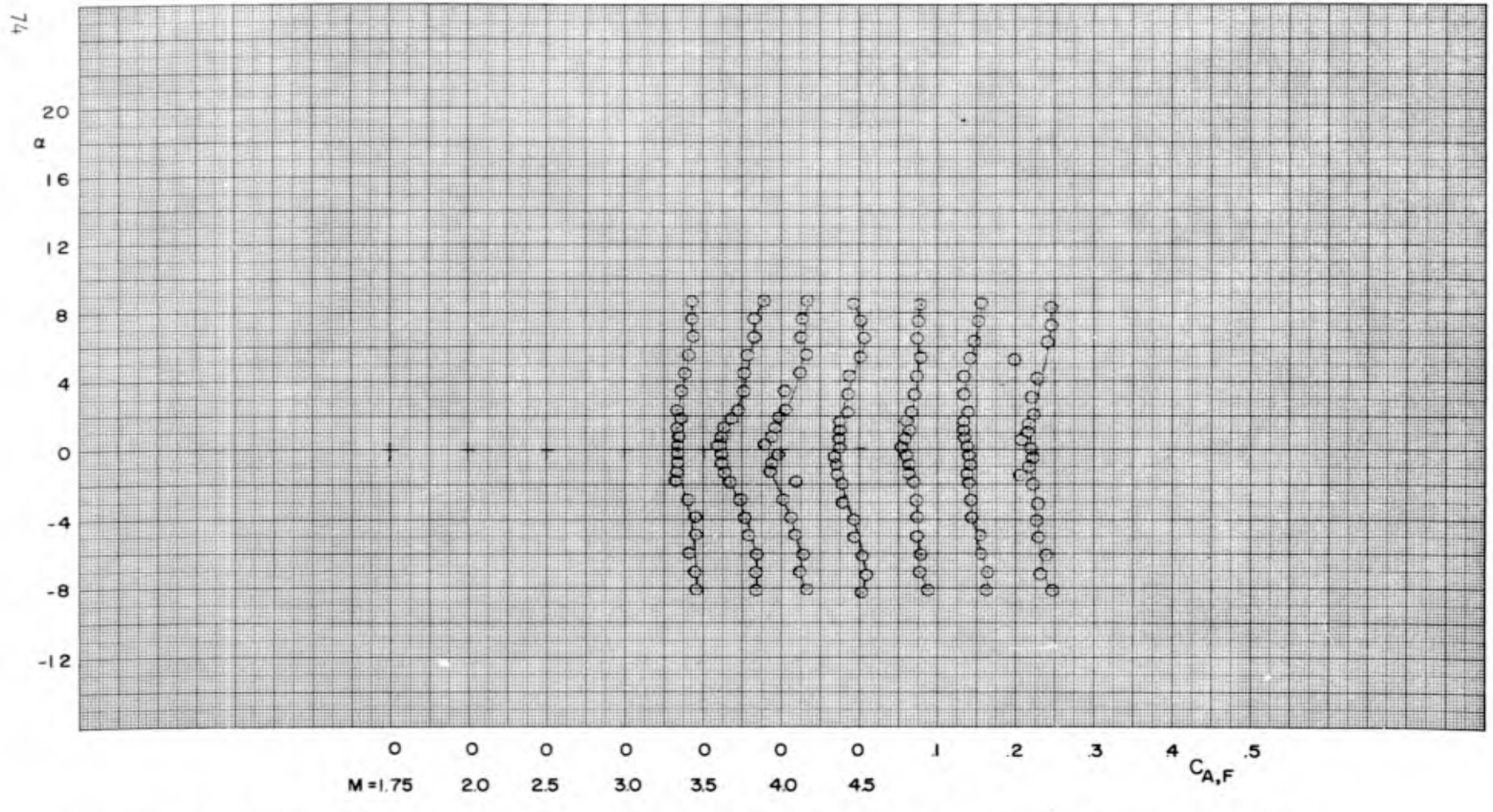

FIGURE 44 ANGLE OF ATTACK VERSUS AXIAL FORCE COEFFICIENT FOR CONFIGURATION $\cdot BF_{6D}$

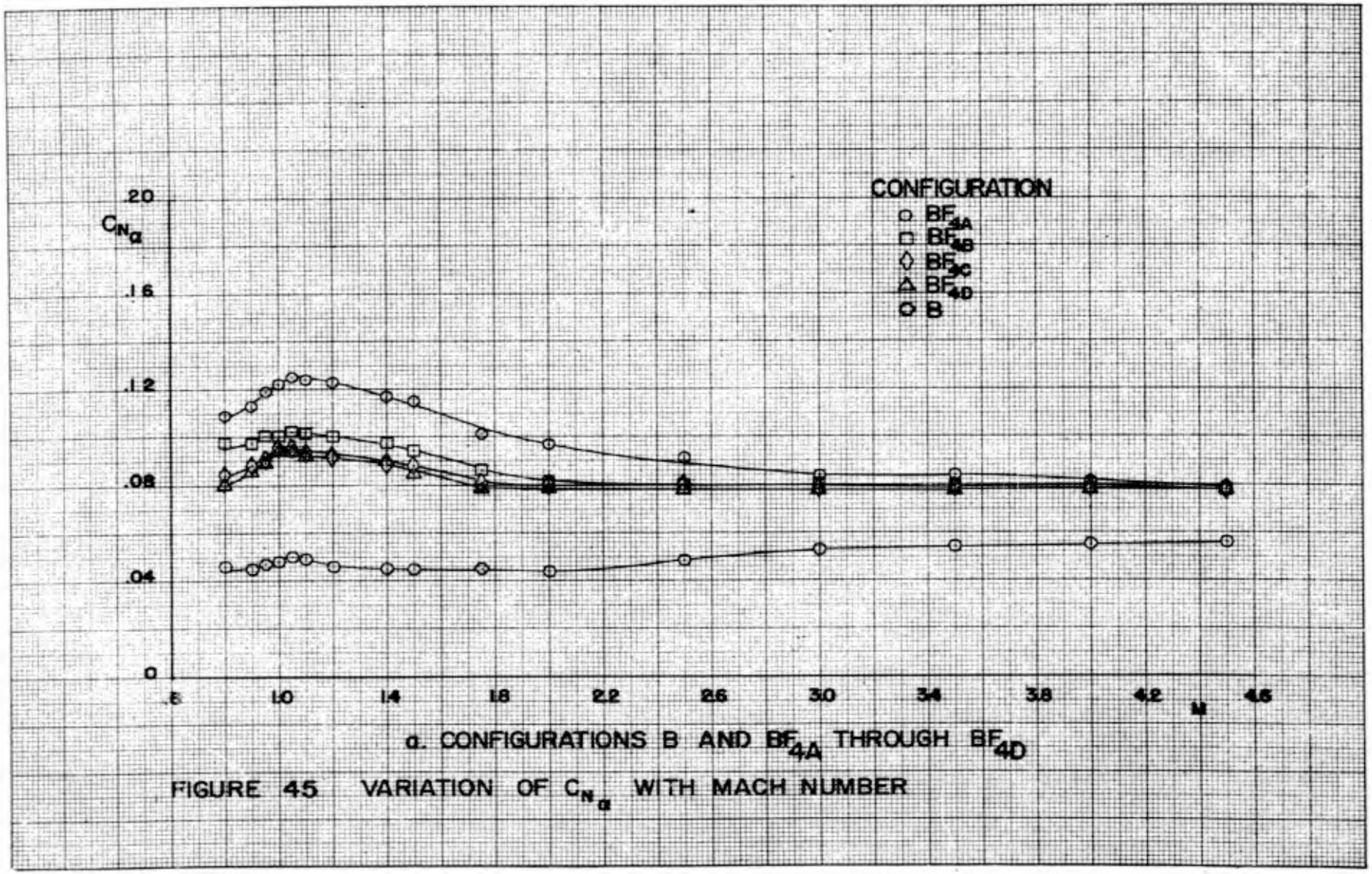

a. CONFIGURATIONS B AND BF_{4A} THROUGH BF_{4D}

FIGURE 45 VARIATION OF C_{N_α} WITH MACH NUMBER

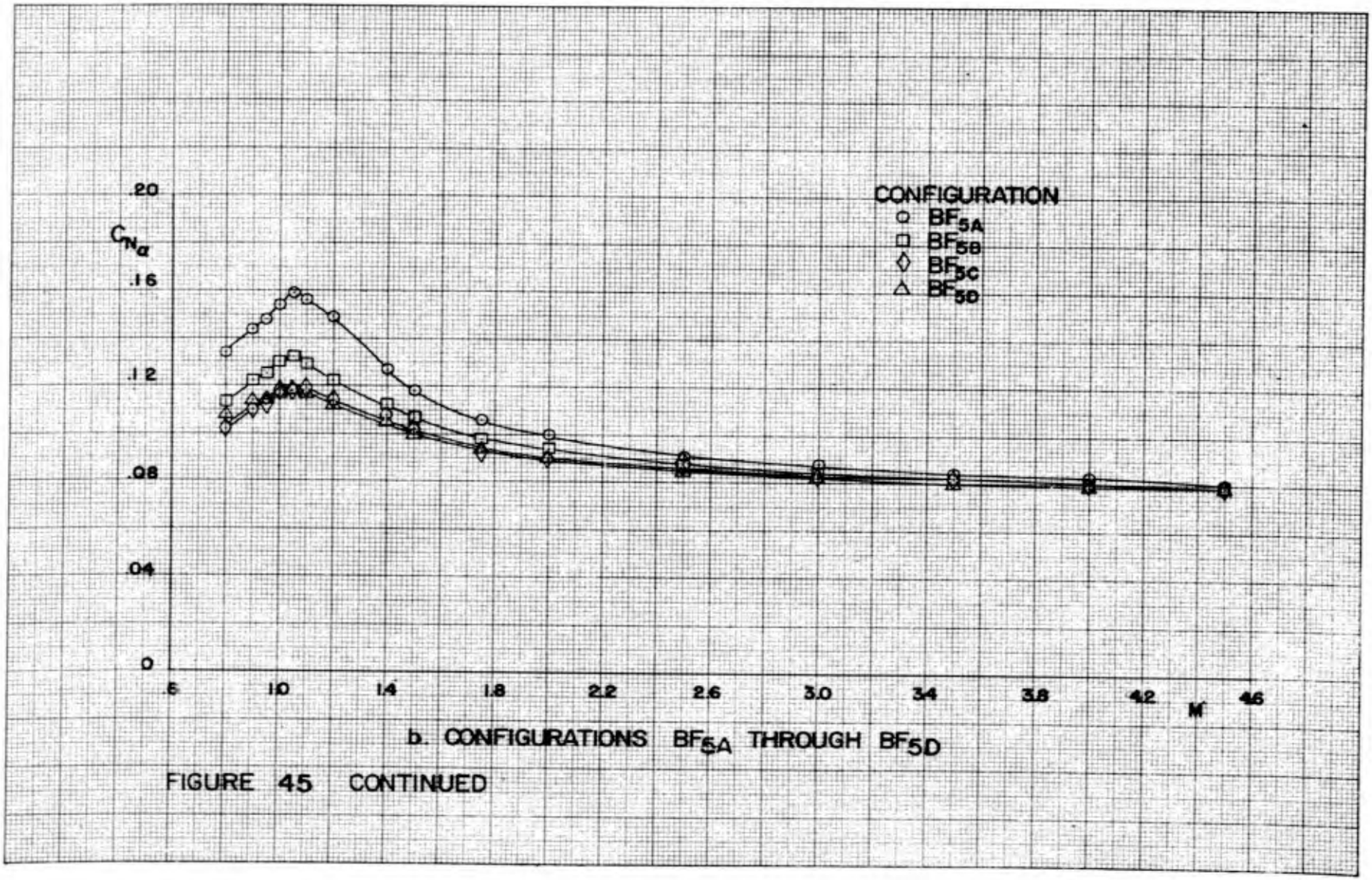

b. CONFIGURATIONS BF_{5A} THROUGH BF_{5D}

FIGURE 45 CONTINUED

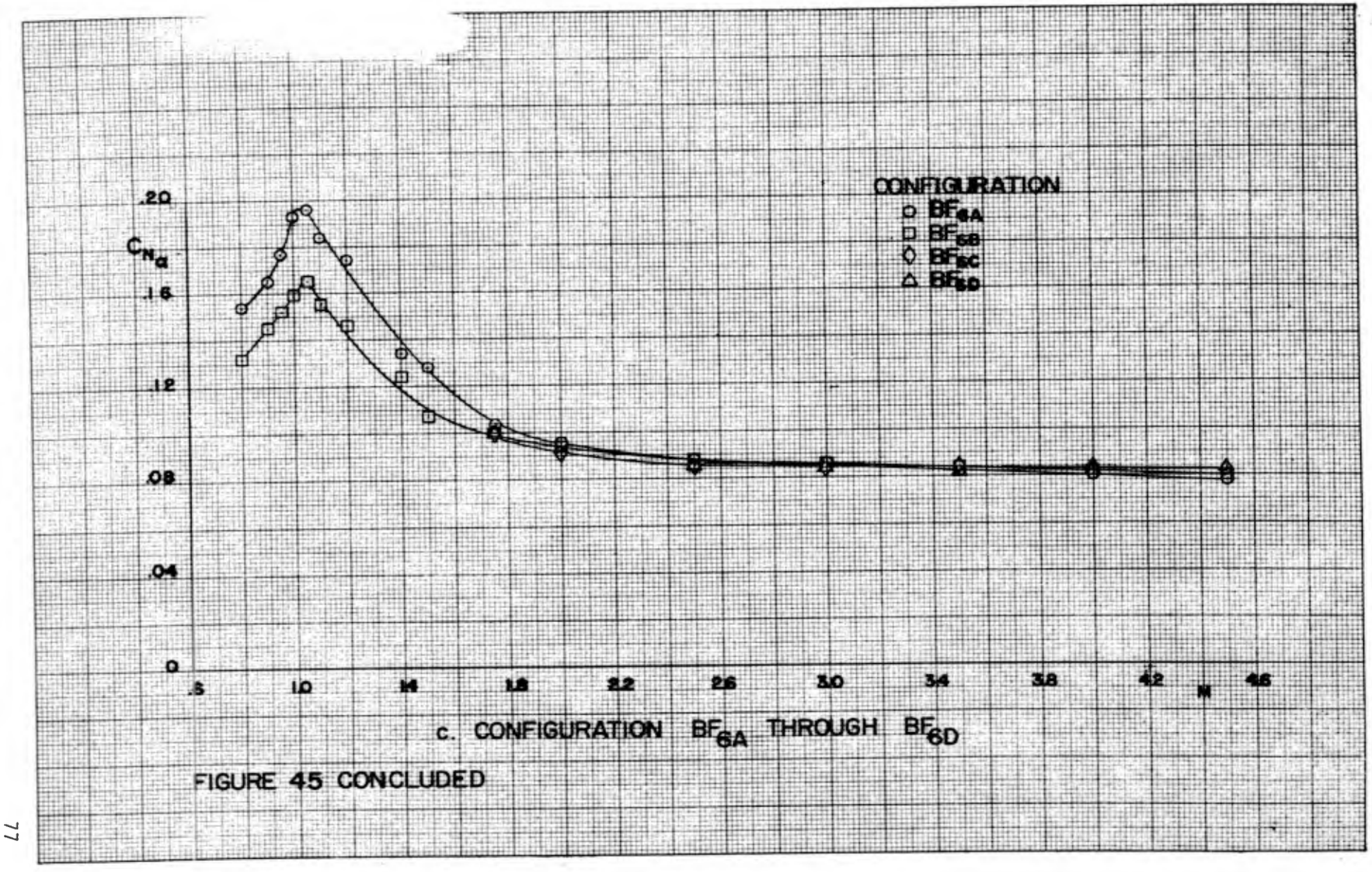

c. CONFIGURATION BF_{6A} THROUGH BF_{6D}

FIGURE 45 CONCLUDED

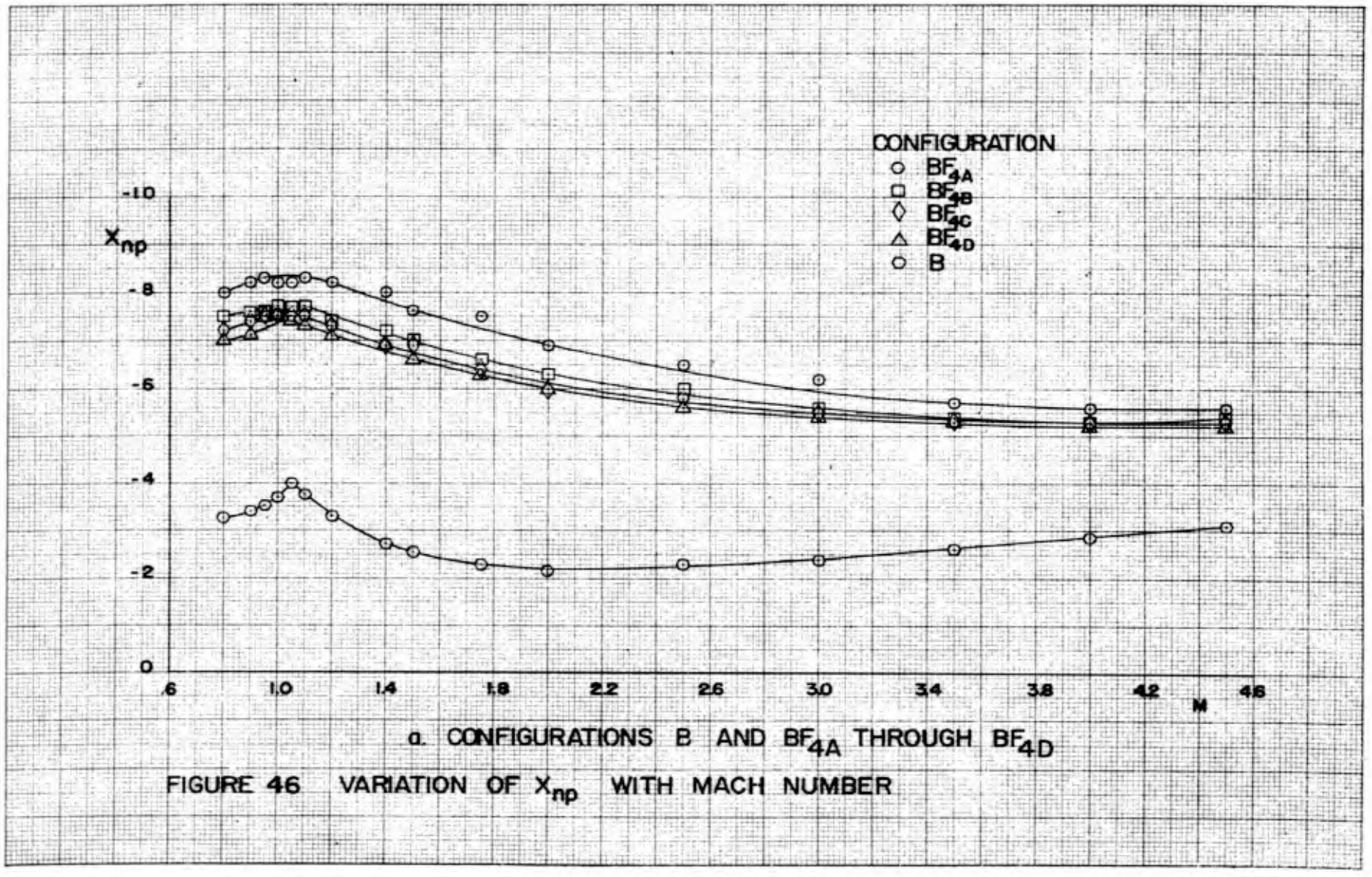

a. CONFIGURATIONS B AND BF_{4A} THROUGH BF_{4D}

FIGURE 46 VARIATION OF X_{np} WITH MACH NUMBER

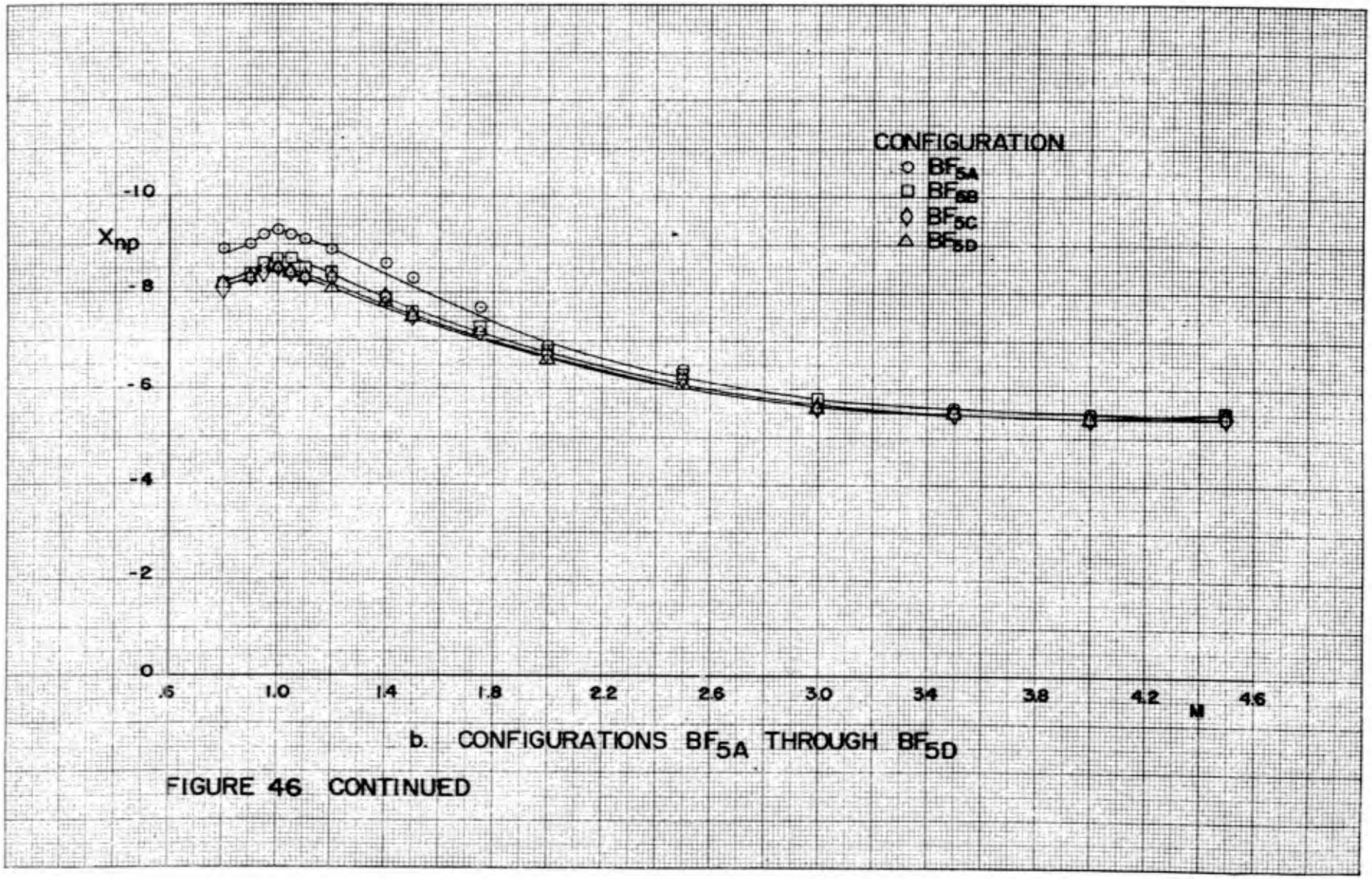

b. CONFIGURATIONS BF_{5A} THROUGH BF_{5D}

FIGURE 46 CONTINUED

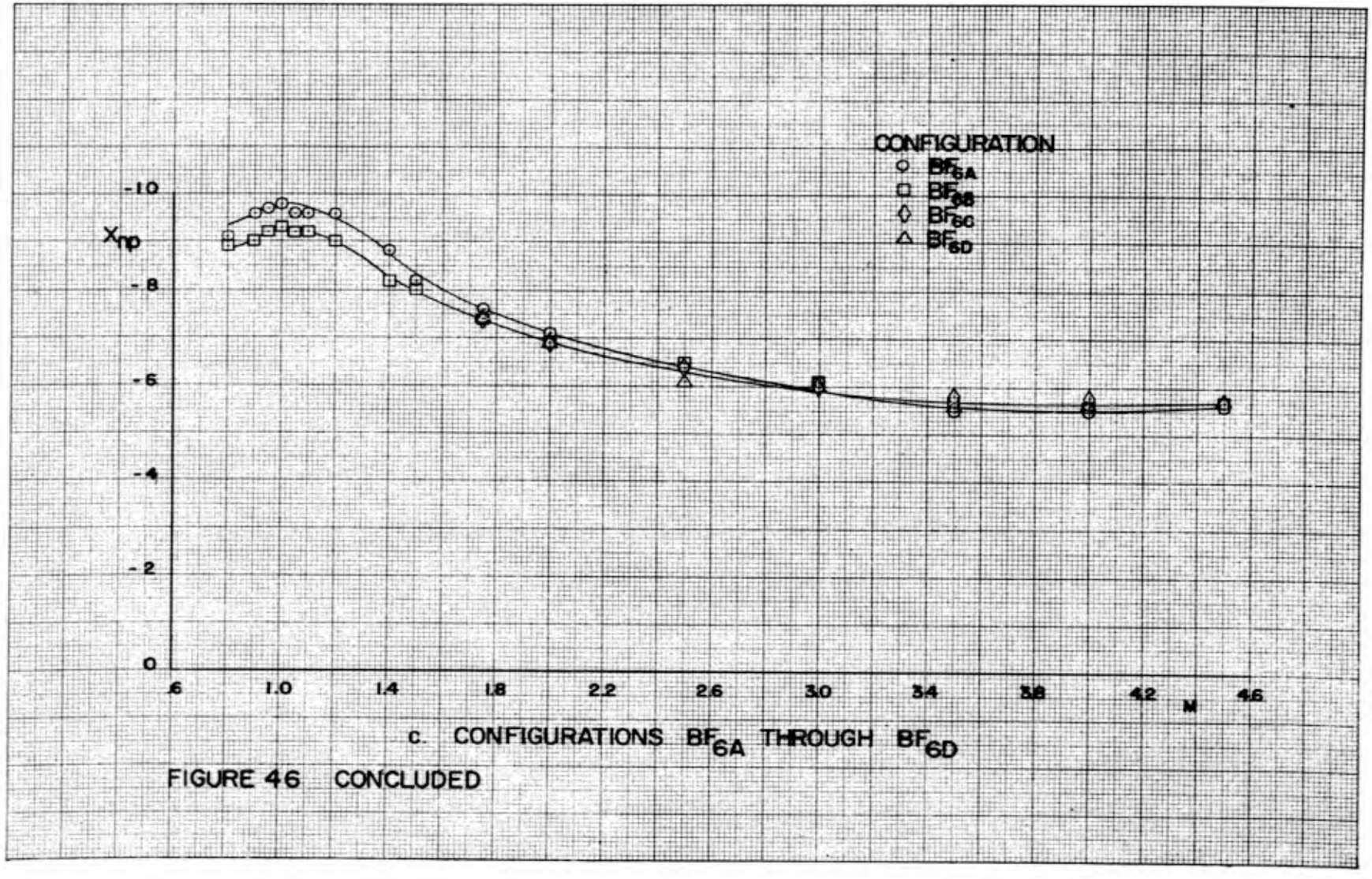

c. CONFIGURATIONS BF_{6A} THROUGH BF_{6D}

FIGURE 46 CONCLUDED

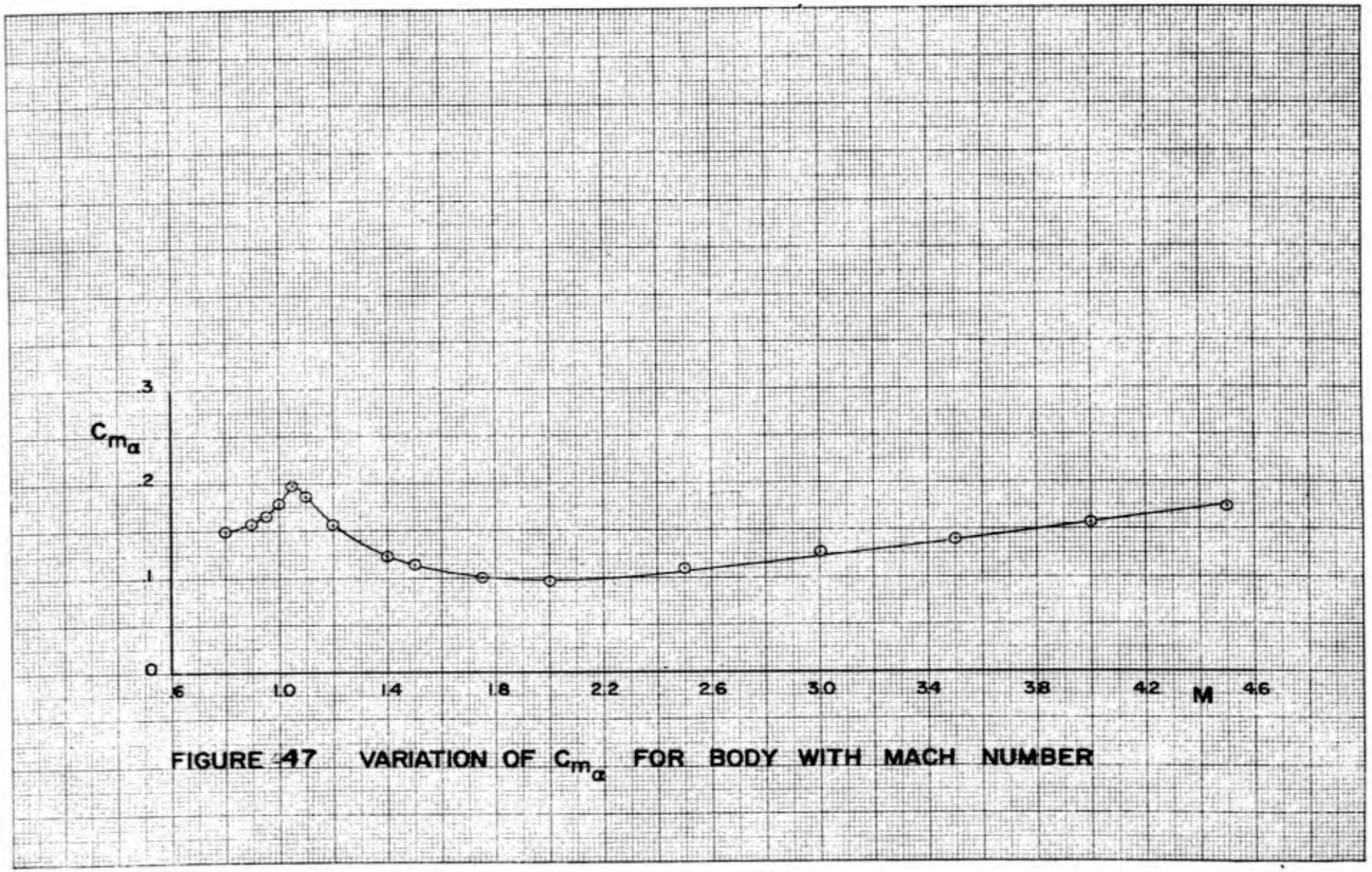

FIGURE 47 VARIATION OF C_{m_α} FOR BODY WITH MACH NUMBER

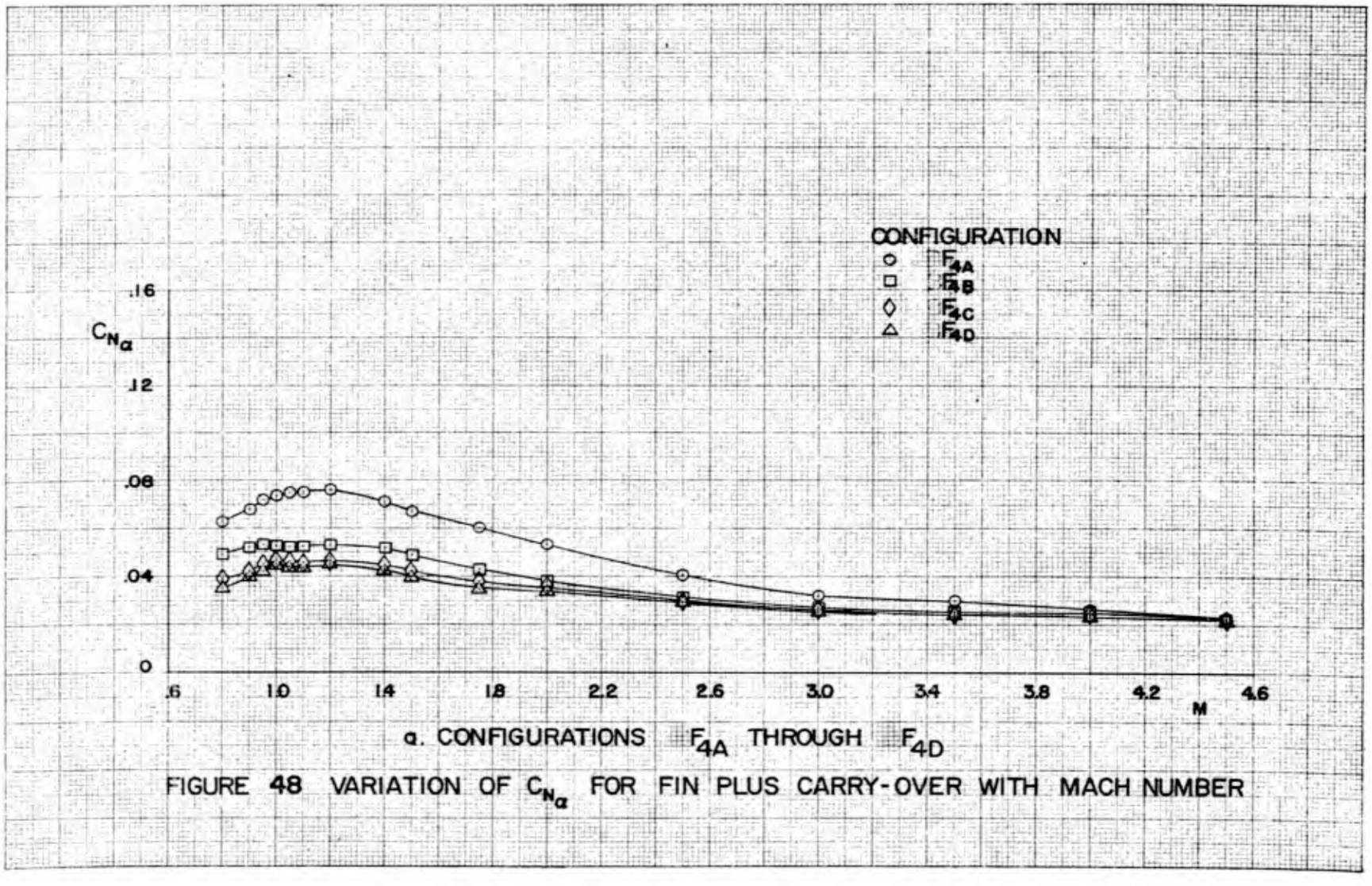

a. CONFIGURATIONS F_{4A} THROUGH F_{4D}

FIGURE 48 VARIATION OF C_{N_α} FOR FIN PLUS CARRY-OVER WITH MACH NUMBER

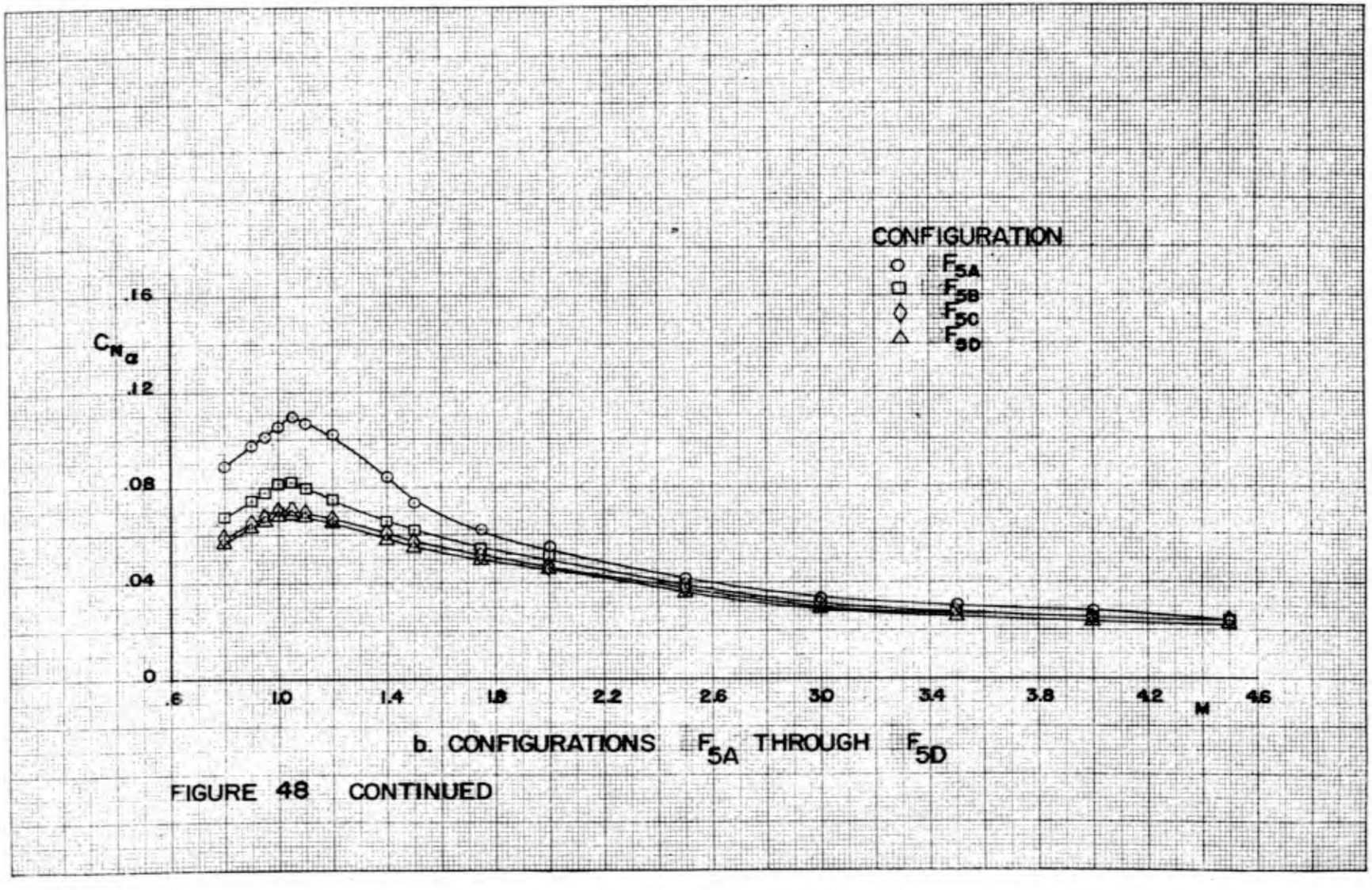

b. CONFIGURATIONS F_{5A} THROUGH F_{5D}

FIGURE 48 CONTINUED

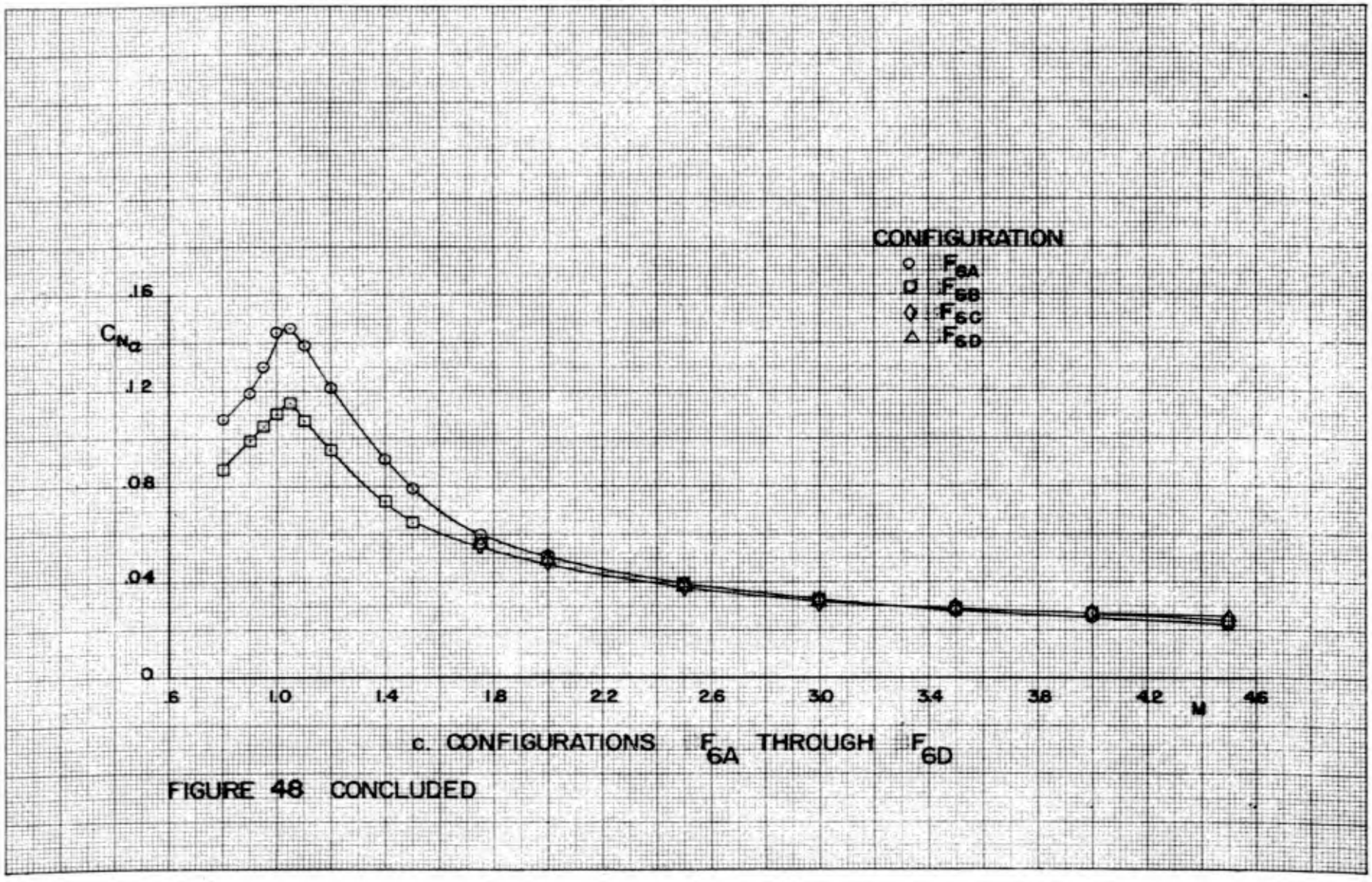

c. CONFIGURATIONS F_{6A} THROUGH F_{6D}

FIGURE 48 CONCLUDED

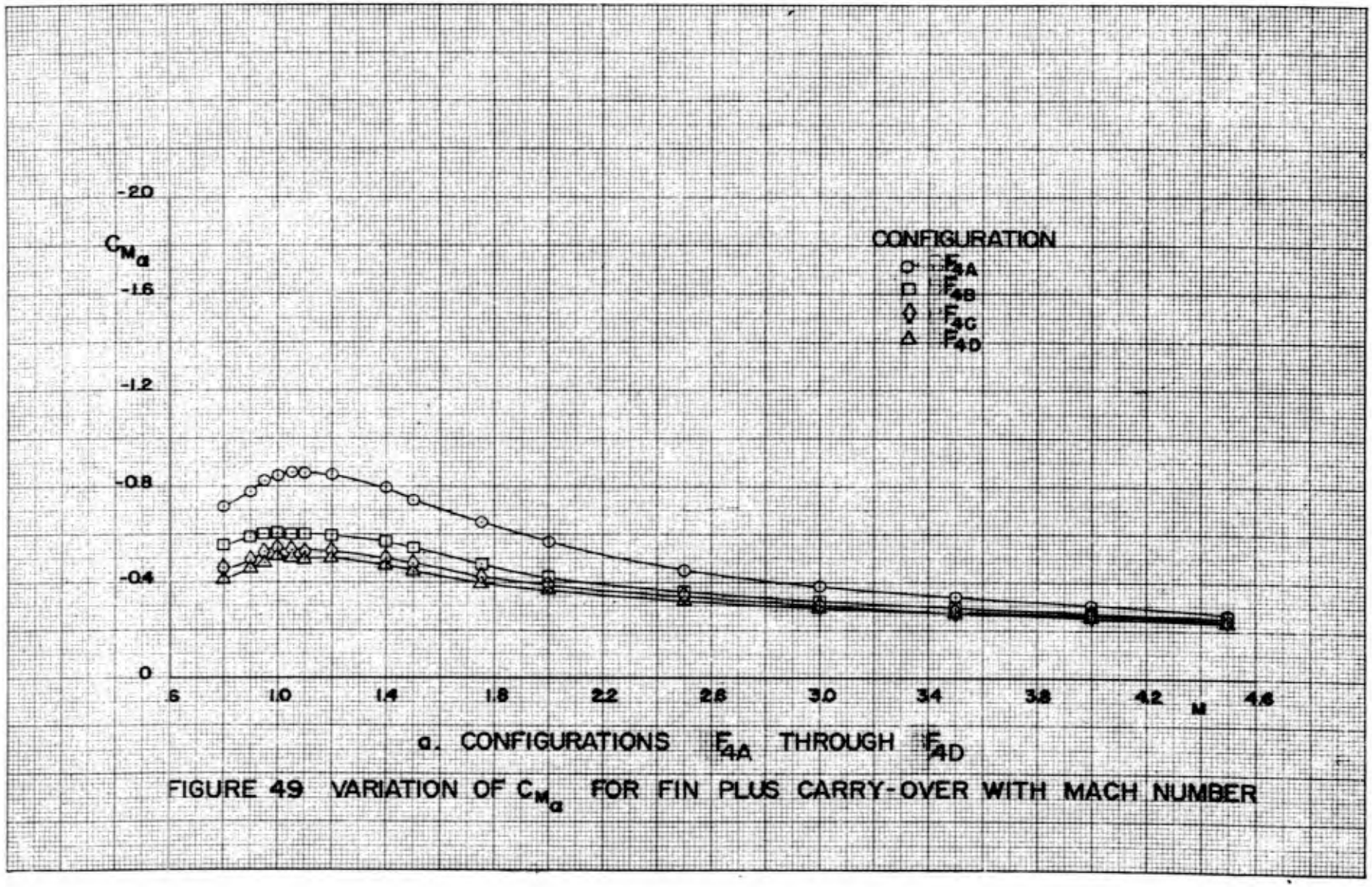

a. CONFIGURATIONS F_{4A} THROUGH F_{4D}

FIGURE 49 VARIATION OF C_{M_α} FOR FIN PLUS CARRY-OVER WITH MACH NUMBER

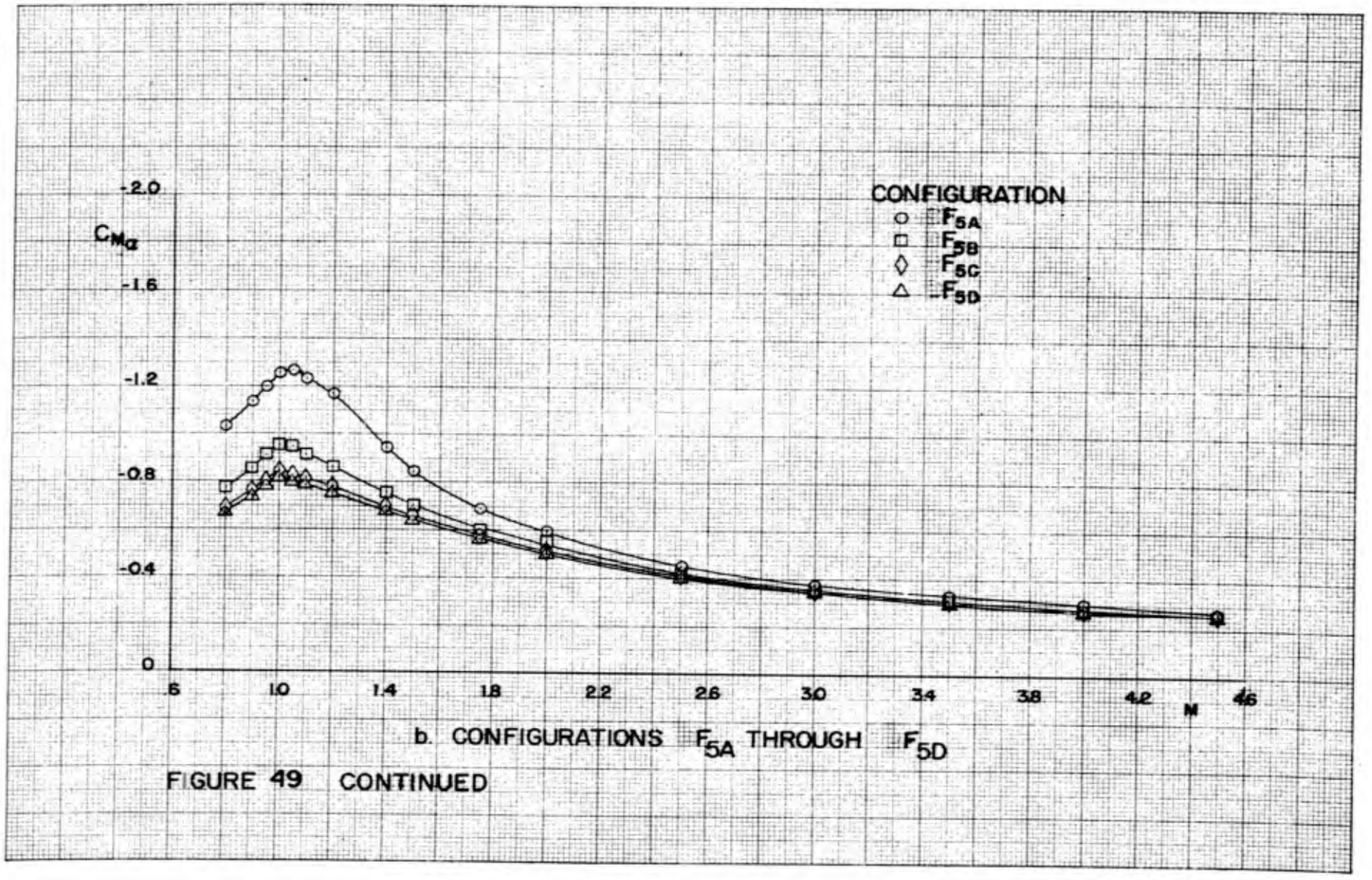

b. CONFIGURATIONS F_{5A} THROUGH F_{5D}

FIGURE 49 CONTINUED

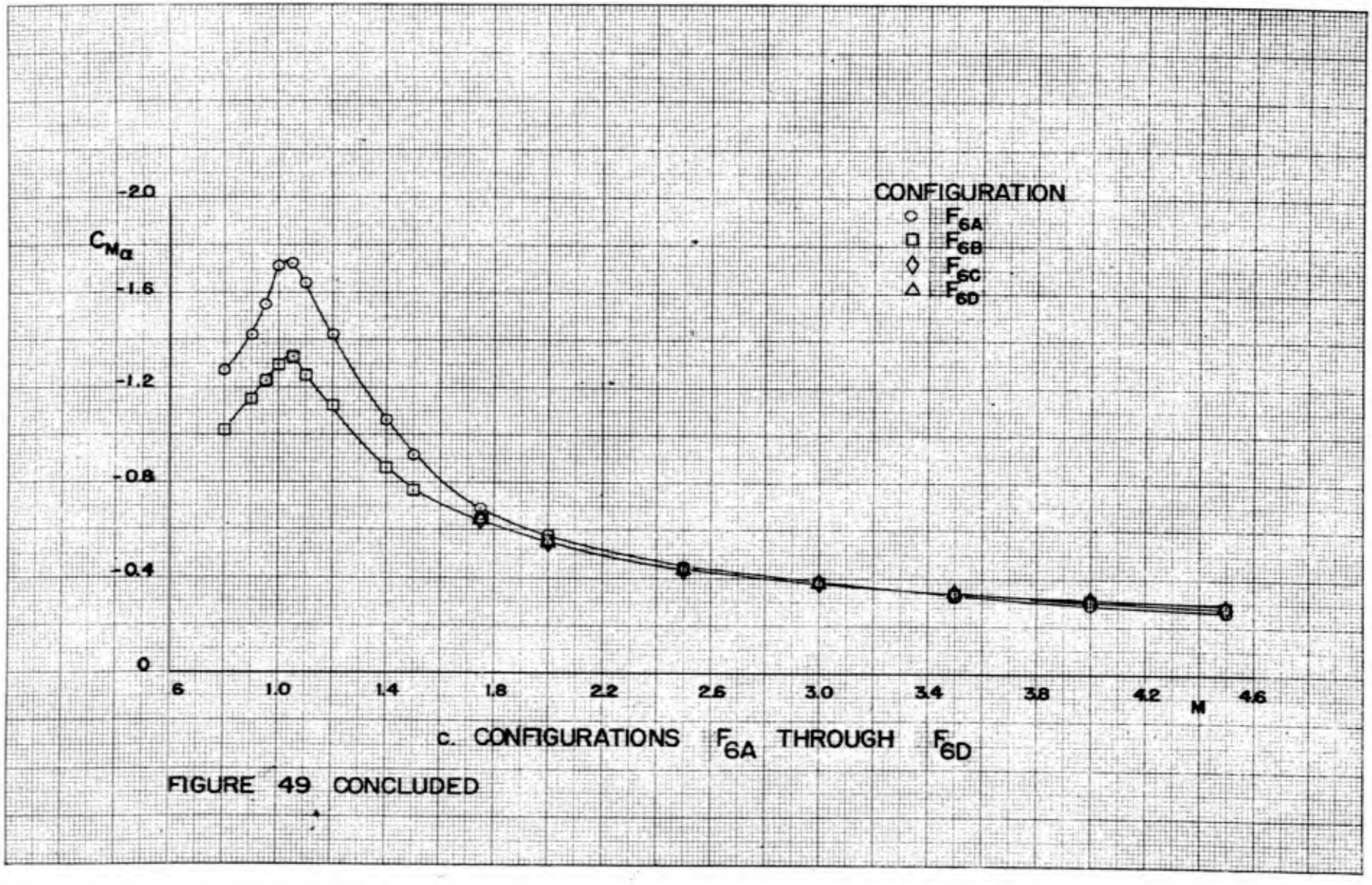

c. CONFIGURATIONS F_{6A} THROUGH F_{6D}

FIGURE 49 CONCLUDED

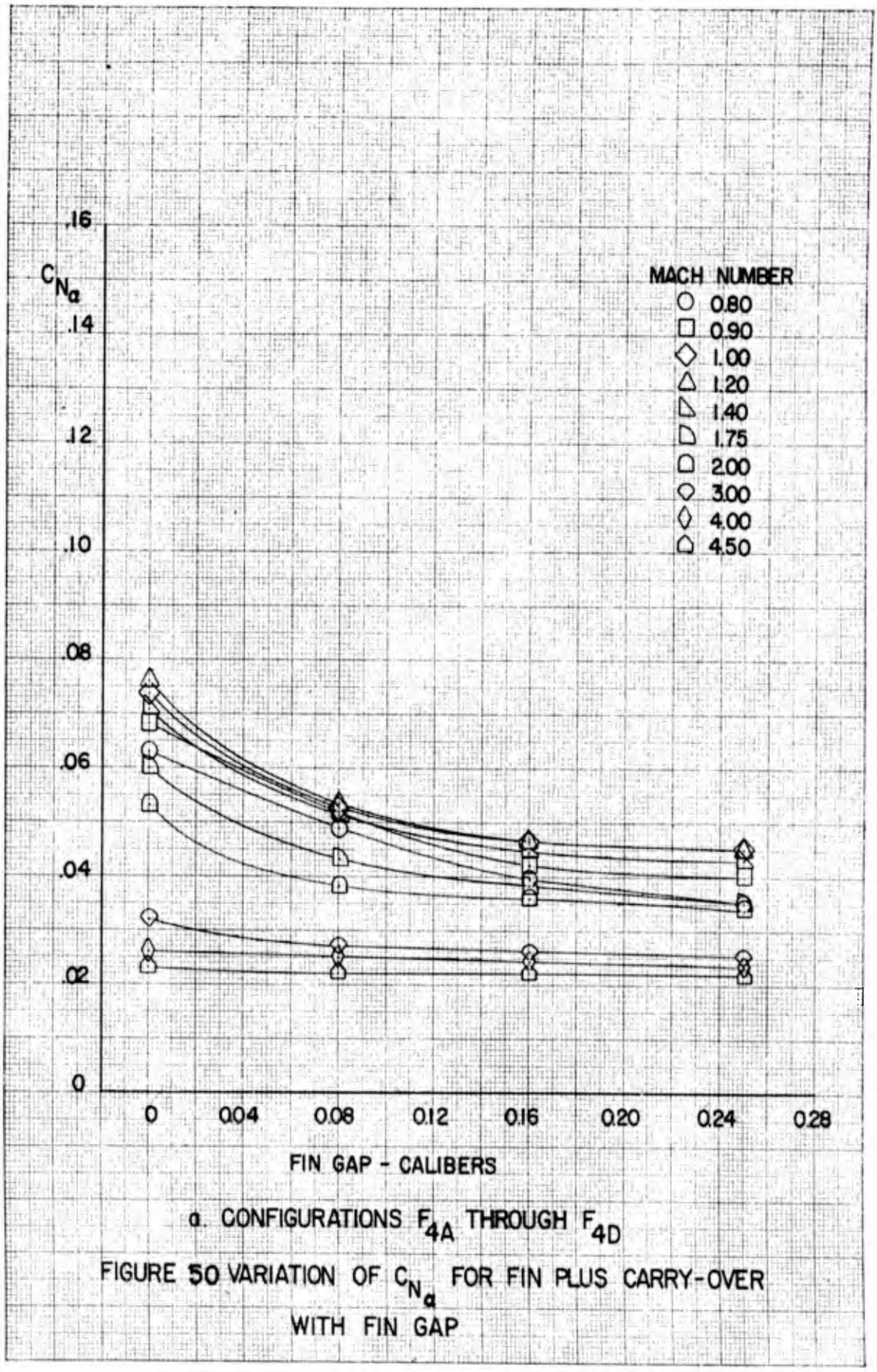

a. CONFIGURATIONS F_{4A} THROUGH F_{4D}

FIGURE 50 VARIATION OF C_{N_α} FOR FIN PLUS CARRY-OVER WITH FIN GAP

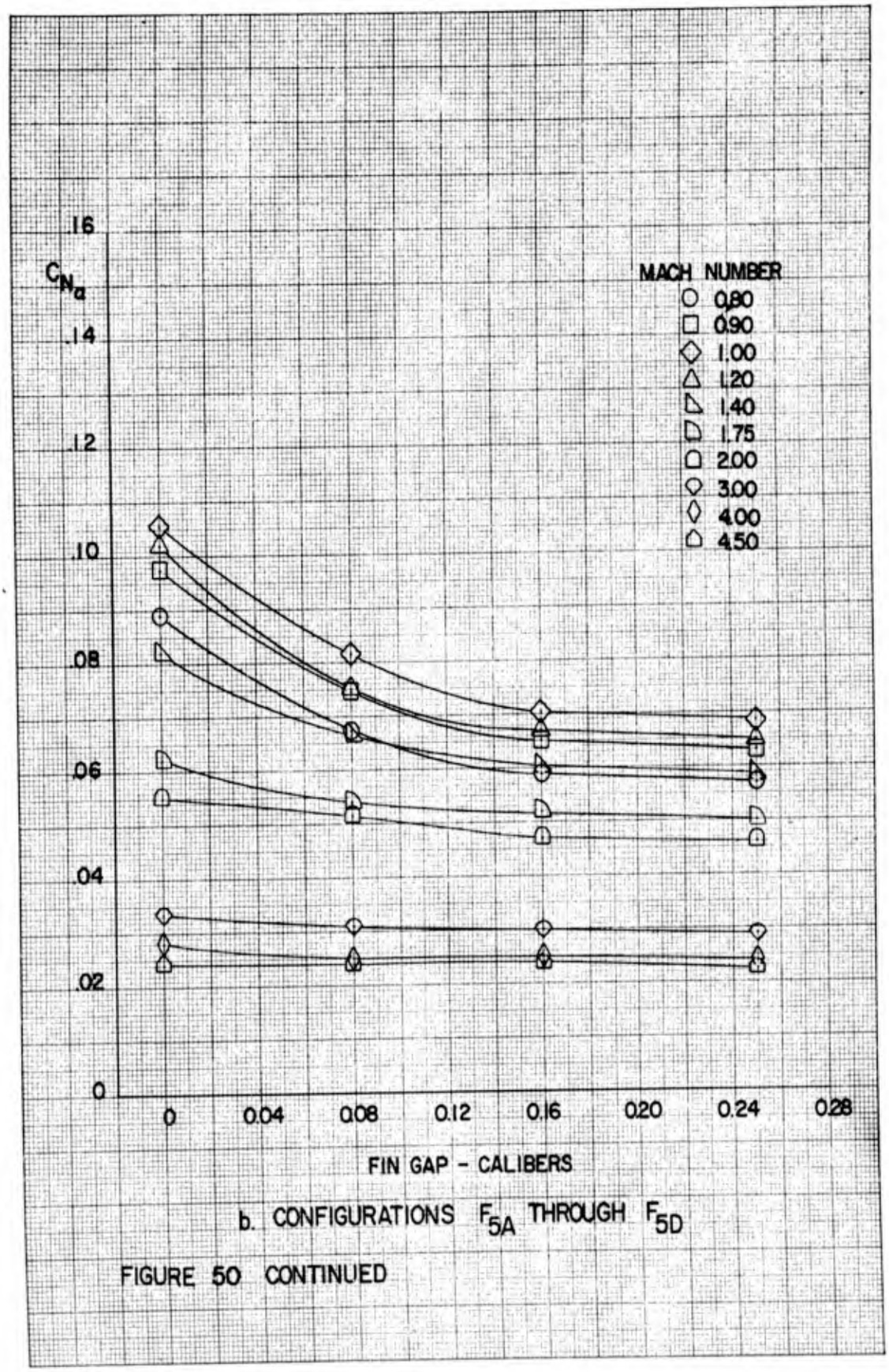

b. CONFIGURATIONS F_{5A} THROUGH F_{5D}

FIGURE 50 CONTINUED

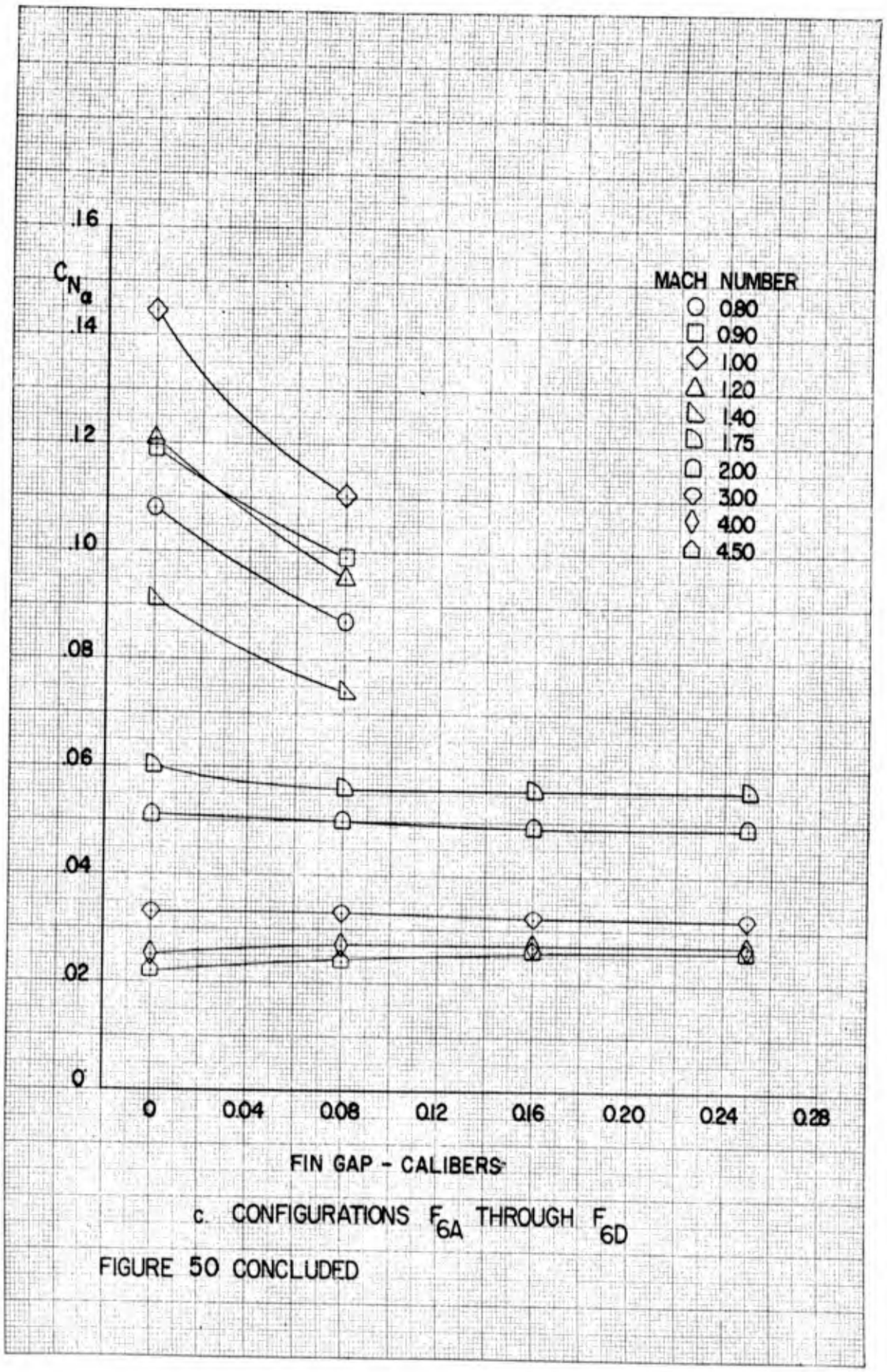

c. CONFIGURATIONS F_{6A} THROUGH F_{6D}

FIGURE 50 CONCLUDED

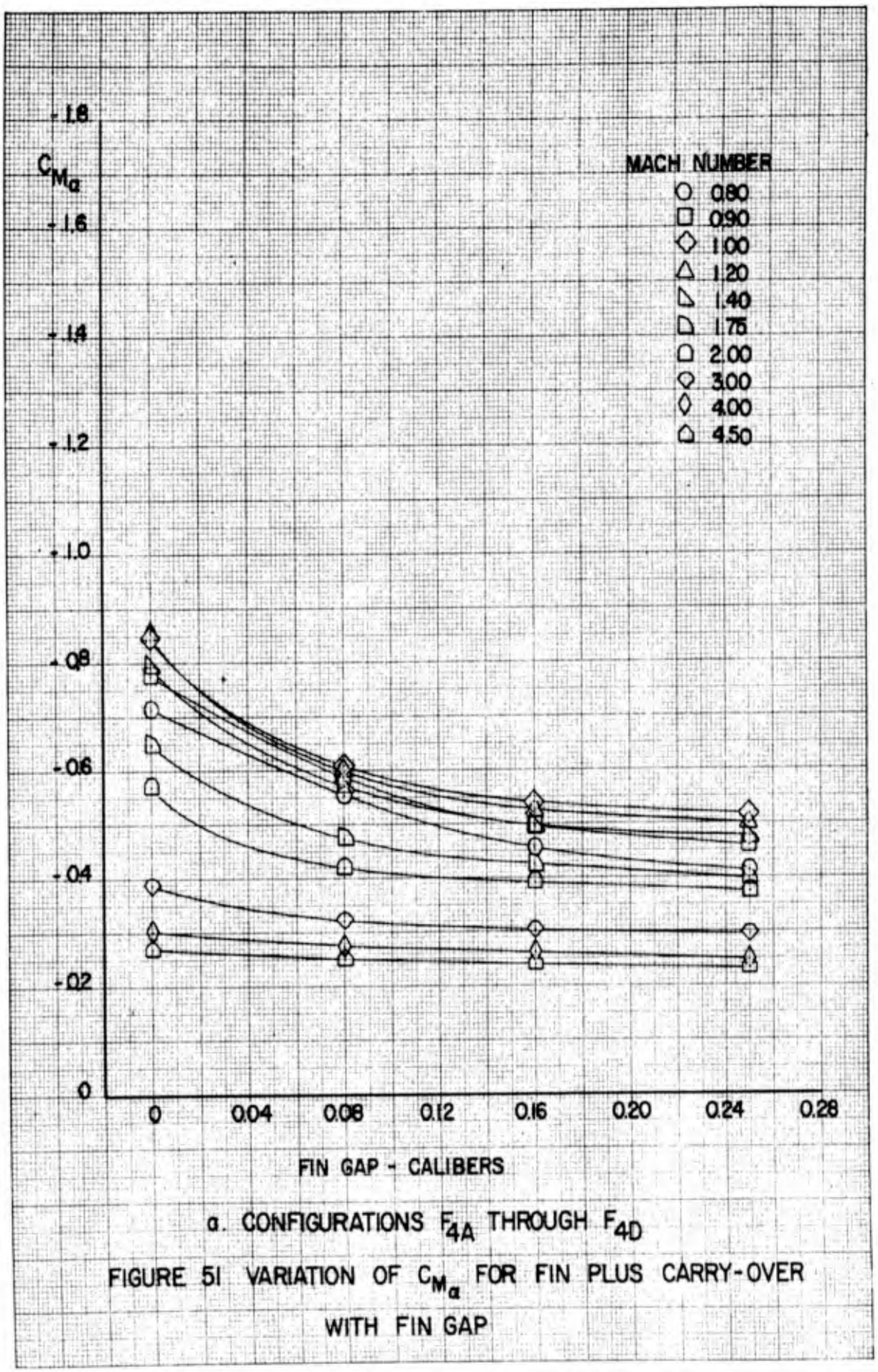

a. CONFIGURATIONS F_{4A} THROUGH F_{4D}

FIGURE 51 VARIATION OF C_{M_α} FOR FIN PLUS CARRY-OVER WITH FIN GAP

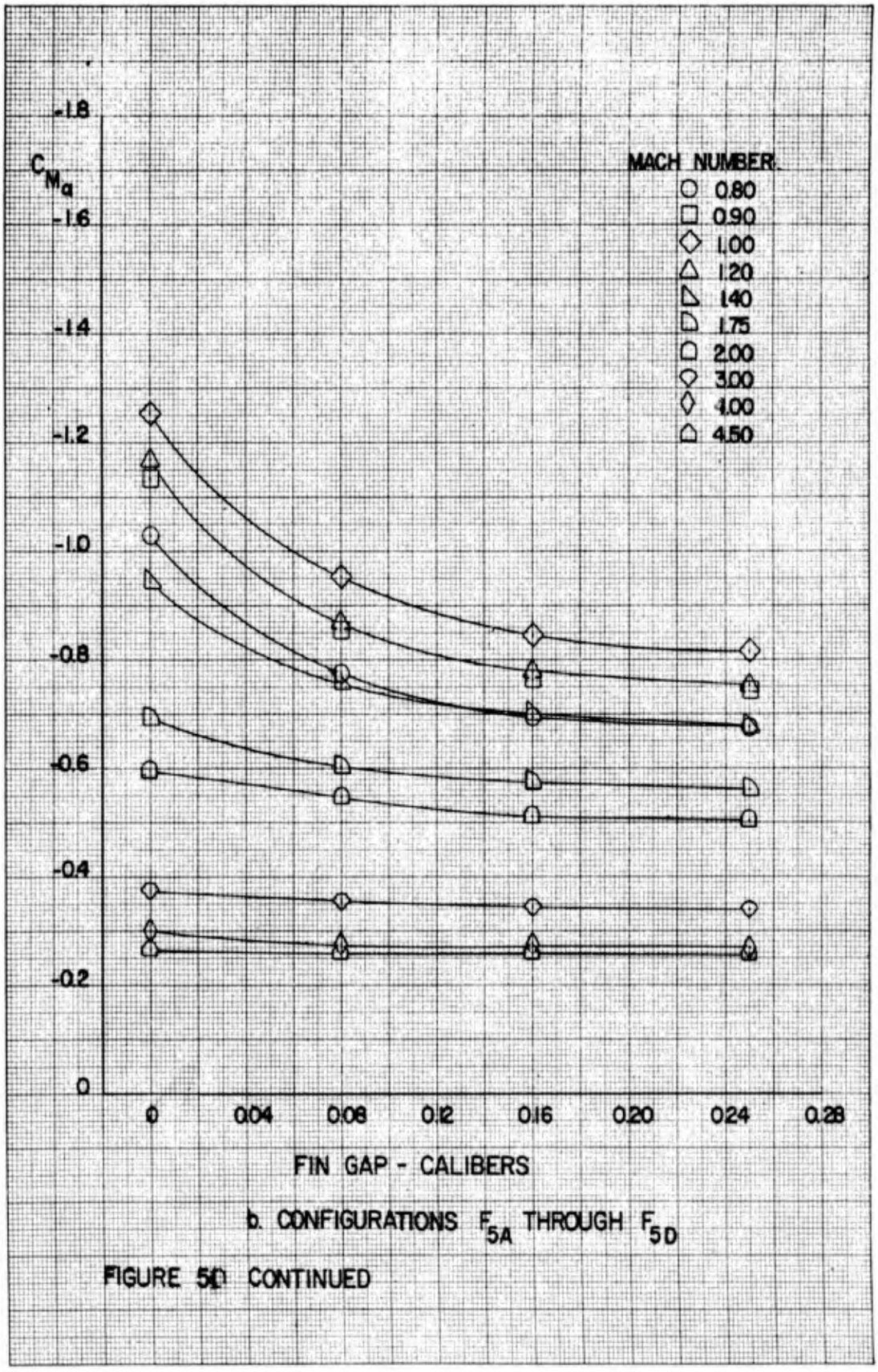

b. CONFIGURATIONS F_{5A} THROUGH F_{5D}

FIGURE 50 CONTINUED

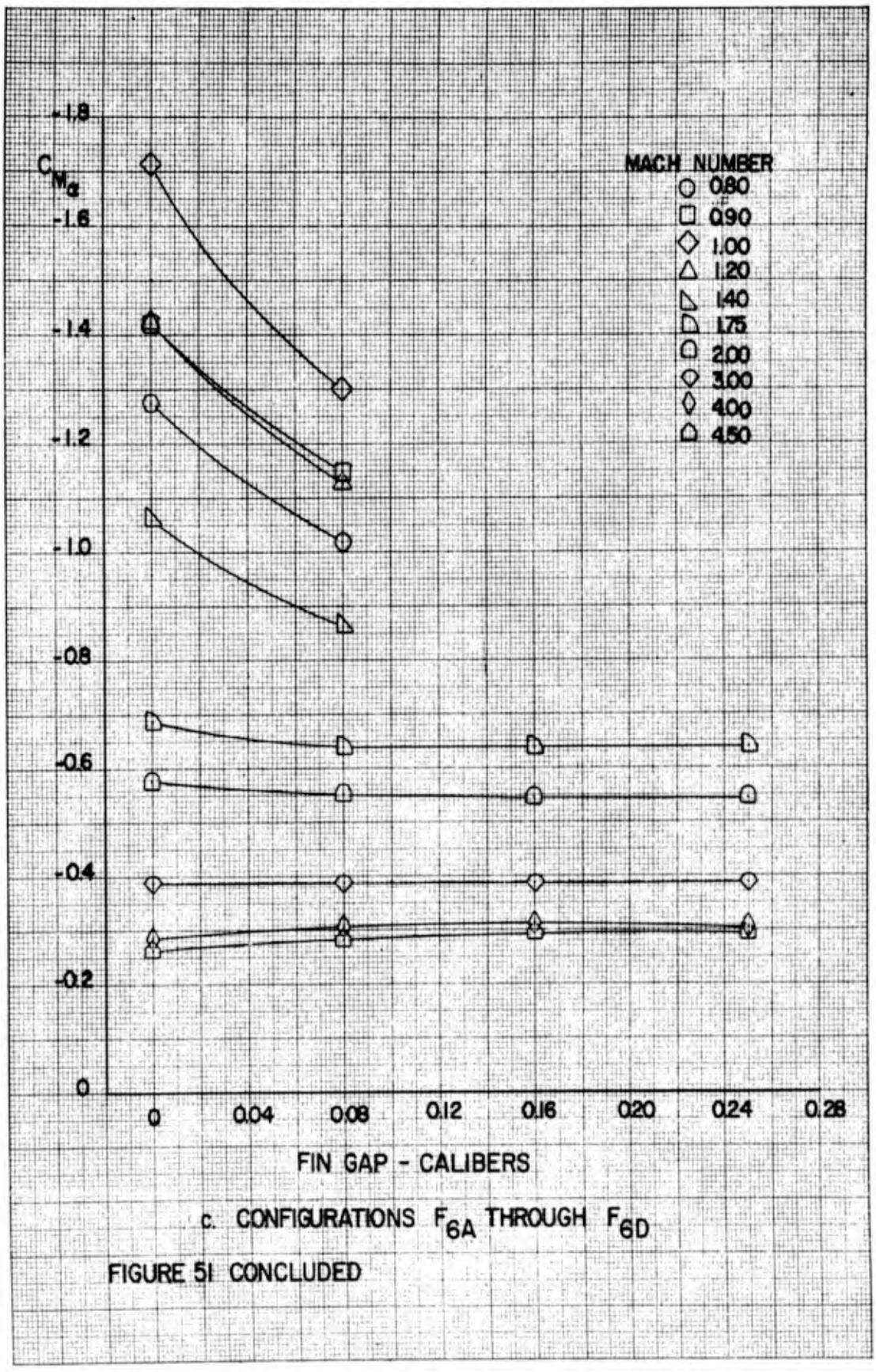

c. CONFIGURATIONS F_{6A} THROUGH F_{6D}

FIGURE 51 CONCLUDED

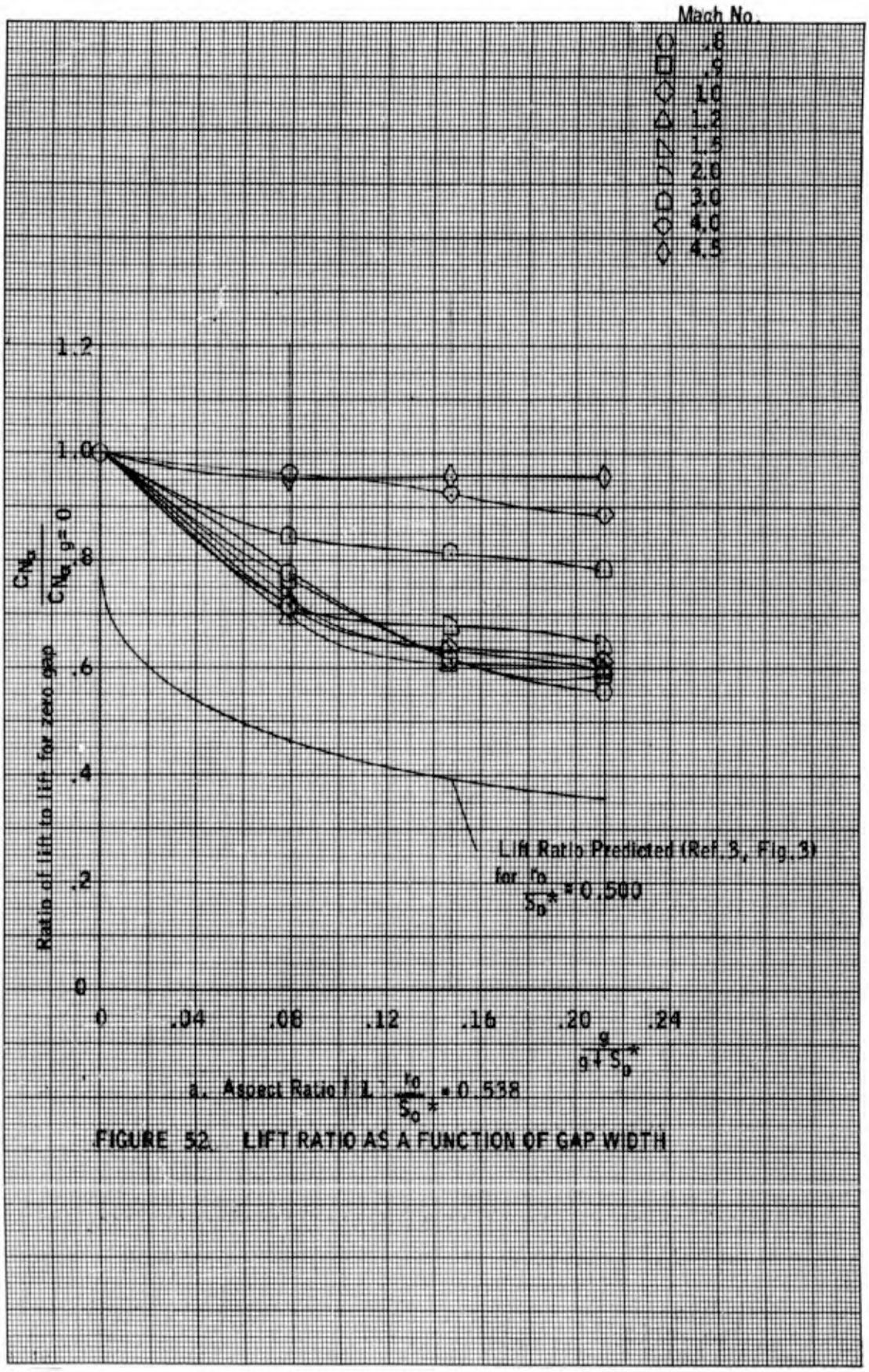

a. Aspect Ratio 1, $\frac{r_o}{S_o^*} = 0.538$

FIGURE 52. LIFT RATIO AS A FUNCTION OF GAP WIDTH

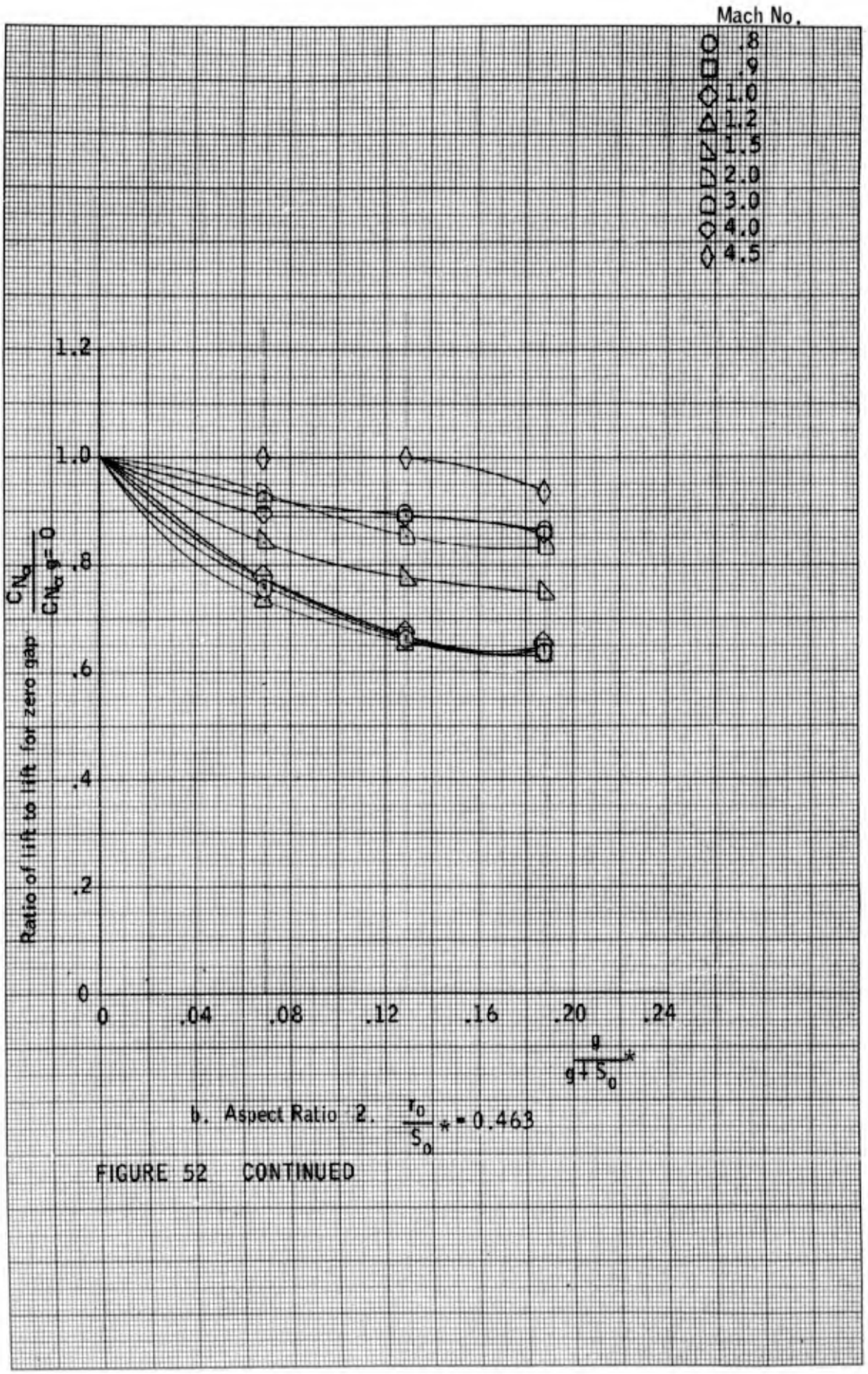

b. Aspect Ratio 2. $\frac{r_0}{S_0}^* = 0.463$

FIGURE 52 CONTINUED

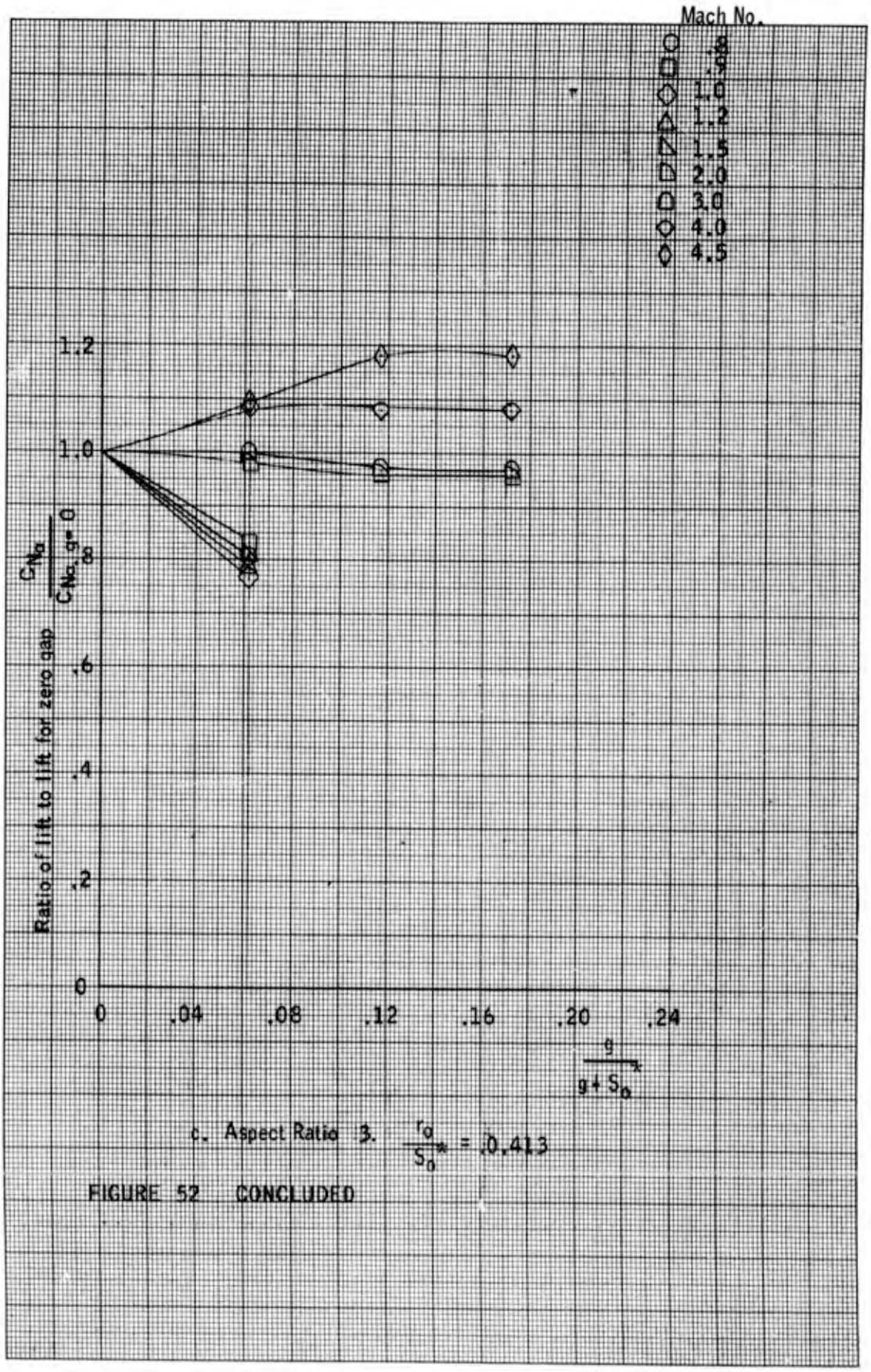

c. Aspect Ratio 3. $\frac{r_0}{S_0^*} = 0.413$

FIGURE 52 CONCLUDED

APPROVED:

ROBERT E. BECHT
Chief, Experimental Unit

RAYMOND A. DEEP
Chief, Aerodynamics Section

WILLIAM C. MCCORKLE, JR.
Director, Advanced Systems Laboratory
Future Missile Systems Division

DISTRIBUTION

	Copy No.
U. S. Army Missile Command Distribution List A for Technical Reports	1-103
Director of Defense Research and Engineering (OSD) Attn: Technical Library Room 3C128 The Pentagon Washington 25, D. C.	104
Commanding General U. S. Army Material Command Attn: AMCRD-RS-PE-Bal Research and Development Directorate Washington 25, D. C.	105
Commanding General Picatinny Arsenal Attn: ORDBB-VC 3, Mr. A. A. Loeb Dover, New Jersey	106
Commanding Officer Frankford Arsenal Attn: 0270 - Library Philadelphia 37, Pennsylvania	107
Commanding Officer Ballistic Research Labs Attn: AMXBR-E Aberdeen, Maryland	108-109
Chief, Bureau of Naval Weapons Attn: DIS-33 Department of the Navy Washington 25, D. C.	110-112
Naval Supersonic Laboratory Massachusetts Institute of Technology Attn: Mr. Frank Durgin 560 Memorial Drive Cambridge 39, Massachusetts	113

DISTRIBUTION (Continued)

	Copy No.
Chief of Naval Material Attn: Code M422 Department of the Navy Washington 25, D. C.	114
AFSWC (SWK, SWUND) Kirkland Air Force Base New Mexico	115
Commanding Officer and Director Attn: Aerodynamics Lab David W. Taylor Model Basin Washington 7, D. C.	116
Director, National Aeronautics and Space Administration Attn: Technical Library Ames Research Center Moffett Field, California	117-121
Director, National Aeronautics and Space Administration Attn: Technical Library Langley Research Center Langley Field, Virginia	122-126
Director, National Aeronautics and Space Administration Attn: Technical Library Lewis Research Center Cleveland, Ohio	127-131
Director, National Aeronautics and Space Administration Attn: W. Dahm E. Linsley J. Sims Marshall Space Flight Center Redstone Arsenal, Alabama	128-132
Director, National Bureau of Standards Attn: G. B. Schubauer 232 Dynamometer Bldg Washington 25, D. C.	133

DISTRIBUTION (Continued)

	Copy No.
U. S. Atomic Energy Commission Tech Info Service Extension P. O. Box 62 Oak Ridge, Tennessee	134
National Science Foundation Attn: Dr. R. Seeger Washington 25, D. C.	135
Applied Physics Laboratory The Johns Hopkins University Attn: Mr. G. L. Seielstad 8621 Georgia Avenue Silver Spring, Maryland	136
Autonetics, A division of North American Aviation, Inc. 9150 E. Imperial Highway Downey, California	137
AVCO Manufacturing Corp. Advance Developement Division Research Lab 2385 Revere Beach Parkway Everett 49, Massachusetts	138
Armour Research Foundation Illinois Institute of Technology Center Chicago, Illinois	139
Aerojet-General Corp. Attn: Technical Information Office Sacramento Plants (Liquid & Solid Rocket Motors) P. O. Box 1947 Sacramento, California	140
American Bosch Arma Corporation Attn: Technical Library Roosevelt Field Garden City, New York	141
Bell Aircraft Corporation P. O. Box 1 Attn: Librarian Buffalo 5, New York	142

DISTRIBUTION (Continued)

	Copy No.
Bell Telephone Labs, Inc. Attn: Director of Military Systems Development Whippany, New Jersey	143
Bendix Corporation Attn: Reports Library Research Labs Division P. O. Box 5115 Detroit 35, Michigan	144
Boeing Company Attn: Library Unit Chief P. O. Box 3707 Seattle 24, Washington	145-146
Bendix Mishawaka Division Attn: Tech Librarian Bendix Corporation 400 South Beiger Street Mishawaka, Indiana	147
Battelle Memorial Institute 505 King Avenue Columbus 1, Ohio	148
Bendix-Corporation Bendix Systems Division Ann Arbor, Michigan	149
Beech Aircraft Corporation Wichita 1, Kansas	150
CONVAIR, A Division of General Dynamics Corporation P. O. Box 1950 San Diego 12, California	151
Cornell Aeronautical Lab, Inc. Attn: Librarian Buffalo, New York	152
CONVAIR, A Division of General Dynamics Corporation Attn: Engineering Librarian Fort Worth 1, Texas	153

DISTRIBUTION (Continued)

	Copy No.
Chance Vought Aircraft, Inc. P. O. Box 5807 Dallas, Texas	154-155
CONVAIR, A Division of General Dynamics Corporation Attn: Division Library Pomona, California	156
Chrysler Corporation Attn: Technical Library Missile Operations P. O. Box 2628 Detroit 31, Michigan	157
Convair-Astronautics, Division of General Dynamics Corp. Attn: Chief Librarian San Diego 12, California	158
Douglas Aircraft Company Attn: Chief Engineer, Missiles & Space Systems 3000 Ocean Park Blvd Santa Monica, California	159
Douglas Aircraft Company Attn: R. L. Coleman, Aero Sec. 1820 Statesville, Avenue Charlotte, N. C.	160
Documentation Inc. Man-Machine Information Center 2521 Connecticut Avenue, N. W. Washington 8, D. C.	161
Electronics Defense Laboratory Sylvania Electric Products, Inc. P. O. Box 205 Mountain View, California	162
Fairchild Engine and Airplane Corporation Fairchild Astronics Division Wyandanch, Long Island New York	163

DISTRIBUTION (Continued)

	Copy No.
Fairchild Stratos Corporation Aircraft-Missiles Division Attn: Sarah M. Thomas Library Hagerstown, Maryland	164
Goodyear Aircraft Corporation Akron 15, Ohio	165
General Electric Company Aircraft Products Dept Lakeside Avenue Burlington, Vermont	166
Grumman Aircraft Engineering Corporation Attn: Director, Engineering Library, Plant 5 Bethpage, Long Island, N. Y.	167
General Electric Company Attn: Technical Information Services Technical Military Planning Operation Box 535 Santa Barbara, California	168
General Electric Company Missile & Ordnance Systems Department 3198 Chestnut Street Philadelphia, Pennsylvania	169
General Electric Company FPD Technical Information Center Mail Stop F-22 Cincinnati 15, Ohio	170
Hughes Aircraft Company Attn: Documents Group Tech Library Florence Avenue at Teale Street Culver City, California	171
Institute for Defense Analyses Research & Engineering Support Division 1825 Connecticut Avenue, N. W. Washington, D. C.	172

DISTRIBUTION (Continued)

	Copy No.
Lockheed Aircraft Corporation Attn: Technical Information Center Msls 1 Space Division P. O. Box 504 Sunnydale, California	173
Librascope, Inc. 808 Western Avenue Glendale 1, California	174
McDonnell Aircraft Corporation P. O. Box 516 St. Louis 3, Missouri	175
The Martin Company Attn: Librarian Orlando Division Orlando, Florida	176
The Martin Company Attn: Research Library Denver Division P. O. Box 179 Denver 1, Colorado	177
The Mitre Corporation 244 Wood Street Lexington 73, Massachusetts	178
Marquardt Aircraft Co 16555 Saticoy Street P. O. Box 2013 South Annex Van Nuys, California	179
Northrop Corporation Attn: Technical Information Norair Division 1001 East Broadway Hawthorne, California	180
North American Aviation, Inc. Attn: Missile Development Division 12214 Lakewood Blvd Downey, California	181

	Copy No.
Nortronics, A division of Northrop Aircraft, Inc. Attn: Technical Information Center 222 North Prairie Avenue Hawthorne, California	182
Raytheon Company Missiles Systems Division Bristol, Tennessee	183
Reeves Instrument Corporation East Gate Blvd Garden City, Long Island, N. W.	184
Raytheon Company Attn: Librarian Missile Systems Division Bedford, Massachusetts	185
Republic Aviation Corporation Attn: Manager, Contracts and Liaison Guided Missiles Division Mineola, Long Island, N. Y.	186
Radio Corporation of America Missile & Surface Radar Department Moorestown, New Jersey	187
Raytheon Company Attn: Librarian Andover Plant Haverhill Street Andover, Massachusetts	188
Radioplane, A division of Northrop Corporation P. O. Box 511 Van Nuys, California	189
Ryan Aeronautical Company Attn: Chief Librarian Lindbergh Field San Diego 12, California	190

DISTRIBUTION (Continued)

	Copy No.
Republic Aviation Corporation Military Contract Department Farmingdale, Long Island, New York	191
Sylvania Electric Products, Inc. Waltham Laboratory Library Attn: Librarian 100 First Avenue Waltham 54, Massachusetts	192
Sperry Utah Engineering Laboratory 322 North 21st Street, West Salt Lake City 16, Utah	193
System Development Corporation Attn: Librarian 2500 Colorado Avenue Santa Monica, California	194
Sanders Associates, Inc. Document Library 95 Canal Street Nashua, New Hampshire	195
TEMCO Aircraft Corporation Attn: Engineering Library P. O. Box 6191 Dallas, Texas	196
United Aircraft Corporation Missile and Space Division 400 Main Street East Hartford 8, Connecticut	197
United Aircraft Corporation Research Department Ease Hartford 8, Connecticut	198
Vitro Laboratories Division of Vitro Corporation of America Attn: Librarian 14000 Georgia Avenue Silver Springs, Maryland	199

DISTRIBUTION (Continued)

	Copy No.
Writht Aeronautical Division Attn: Sales Department (Fovt.) Curtiss-Wright Corporation Wood-Ridge, New Jersey	200
Brown University Attn: Dr. R. Probstein, Graduate Division of Applied Mathematics Attn: Prof. William Prager, Chairman, Physical Sciences Council Providence 12, Rhode Island	201-202
Catholic University of America Attn: Prof. K. F. Herzfeld Prof. M. Munk Department of Physics Washington 17, D. C.	203
Auburn University Attn: Department of Aerospace Engineering Auburn, Alabama	204
University of Alabama Attn: Department of Aerospace Engineering University, Alabama	205
Case Institute of Technology Attn: Dr. G. Kuerti Cleveland, Ohio	206
California Institute of Technology Guggenheim Aeronautical Laboratory Attn: Prof. H. W. Leipman Pasadena 4, California	207
University of California at Berkeley Attn: Prof. S. A. Schaaf Berkeley, California	208
University of California at Los Angeles Attn: Dr. L. M. Boelter Department of Engineering Los Angeles 24, California	209
University of Southern California Engineering Center Los Angeles 7, California	210

DISTRIBUTION (Continued)

	Copy No.
University of Chicago Attn: Librarian Labs for Applied Sciences Museum of Science & Industry Chicago 37, Illinois	211
Cornell University Attn: Dr. W. R. Sears Graduate School of Aeronautical Engineering Ithaca, New York	212-213
Harvard University Attn: Prof. H. W. Emmons Dr. A. Bryson Prof. G. E. Carrier Department of Applied Physics & Engineering Science Cambridge 38, Massachusetts	214-216
University of Illinois Attn: Prof. C. H. Fletcher Department of Aeronautical Engineering Attn: Dr. H. H. Korst Engineering Experimental Station Urbans, Illinois	217-218
American Institute of Aeronautics & Astronautics Attn: Library 2 East 64th Street New York 21, New York	219
The Johns Hopkins University Attn: Dr. L. Kosvasznay Prof. F. H. Clauser, Jr. Department of Aeronautical Engineering Attn: Dr. S. Corrsin Department of Mechanical Engineering Baltimore 17, Maryland	220-222
Kansas State University Attn: Prof. W. Tripp Department of Mechanical Engineering Manhattan, Kansas	223

	Copy No.
Lehigh University Attn: Dr. R. Emrich Physics Department Bethlehem, Pennsylvania	224
University of Maryland Attn: Director, Institute of Fluid Dynamics & Applied Mathematics Attn: S. F. Shen, Department of Aeronautical Engineering College Park, Maryland	225-226
University of Michigan Institute of Science & Technology Attn: Technical Documents Service Ann Arbor, Michigan	227
Massachusetts Institute of Technology Attn: Prof. J. R. Markham Department of Aeronautical Engineering Cambridge 39, Massachusetts	228
University of Michigan Attn: Dr. Arnold Kuethe Department of Aeronautical Engineering East Engineering Bldg Ann Arbor, Michigan	229
University of Minnesota Attn: Department of Aeronautical Engineering Department of Mechanical Engineering, Division of Thermodynamics Minneapolis 14, Minnesota	230-231
Midwest Research Institute Attn: M. Goland, Director for Engineering Sciences 4049 Pennsylvania Kansas City 11, Missouri	232
New York University Attn: Dr. R. W. Courant, Institute of Mathematics & Mechanics Attn: Dr. J. F. Ludloff, Department of Aeronautics 45 Fourth Street New York 53, N. Y.	233-234

DISTRIBUTION (Continued)

	Copy No.
North Carolina State College Attn: Prof. R. M. Pinkerton Department of Engineering Raleigh, North Carolina	235
Ohio State University Attn: Prof. G. L. von Eschen Aeronautical Engineering Department Columbus, Ohio	236
Pennsylvania State College Attn: Prof. M. Lessen Department of Aeronautical Engineering State College, Pennsylvania	237
Polytechnic Institute of Brooklyn Attn: Dr. A. Ferri Aerodynamic Laboratory 527 Atlantic Avenue Freeport, New York	238
Princeton University Attn: Prof. S. Bogdonoff Prof. W. Hayes Forrestal Research Center Princeton, New Jersey	239-240
Purdue University Lafayette, Indiana	241
Princeton University Forrestal Research Center Library Project SQUID Princeton, New Jersey	242
The Rice Institute Attn: Prof. A. J. Chapman Department of Mechanical Engineering Houston, Texas	243
Rensselaer Polytechnic Institute Attn: Dr. R. P. Harrington Aeronautics Department Troy, New York	244

DISTRIBUTION (Continued)

	Copy No.
Rutgers University Attn: Prof. R. H. Page Department of Mechanical Engineering New Brunswick, N. J.	245
Stanford Research Institute Attn: Acquisitions Documents Center Menlo Park, California	246
University of Virginia Ordnance Research Laboratory P. O. Box 3366 University Station Charlottesville, Virginia	247
University of Texas Defense Research Laboratory Attn: Mr. J. B. Oliphint P. O. Box 8029 University Station Austin 12, Texas	248-249
University of Washington Attn: Prof. R. E. Street Department of Aeronautical Engineering Attn: Prof. M. E. Childs Department of Mechanical Engineering Seattle 5, Washington	250-251
University of Virginia Attn: Prof. J. W. Beams Department of Physics Charlottesville, Virginia	252
University of Manchester, England Attn: Dr. E. R. Benton	253
Case Institute of Technology Attn: Dr. R. Bolz Cleveland, Ohio	254
General Electric Company Attn: Mr. Gerald Hieser Systems Engineering Department 21 South 12th Street Room 514 Philadelphia, Pennsylvania	255

DISTRIBUTION (Concluded)

	Copy No.
University of Wisconsin Attn: Prof. J. O. Hirschfelder Department of Chemistry Madison, Wisconsin	256
California Institute of Technology Attn: Prof. C. B. Millikan Director, Guggenheim Aeronautical Laboratory Pasadena 4, California	257
Tulane University Attn: Dr. Henry F. Hrubecky Department of Mechanical Engineering New Orleans 18, Louisiana	258
AMSMI-R Mr. McDaniel	259
-RF, Mr. Hussey	260
-RFS, Record Copies	261-263
-RFSK, Mr. Deep	264
Mr. Henderson	265
Mr. Killough	266-280
Mr. Johnson	281
Mr. Spring	282
Mr. Martin	283
Mr. Greene	284
Mr. Becht	285
File Copy	286
-RBL	287-291
-RG	292
-RK	293
-RE	294
-RFE, Mr. Garner	295
-RT	296
-RH	297
-RL	298
-RR	299
-RS	300
-RAP	301

UNCLASSIFIED